Eur. Phys. J. C (2025) 85:729
https://doi.org/10.1140/epjc/s10052-025-14178-x

THE EUROPEAN PHYSICAL JOURNAL C

Check for updates

Regular Article - Experimental Physics

Measurement of $W^{\pm}$-boson differential cross-sections in proton–proton collisions with low pile-up data at $\sqrt{s} = 5.02$ TeV and 13 TeV with the ATLAS detector

ATLAS Collaboration*

CERN,1211 Geneva 23, Switzerland

Received: 14 February 2025 / Accepted: 10 April 2025
© CERN for the benefit of the ATLAS Collaboration 2025

Abstract High precision single-differential $W^{\pm}$-boson production cross-sections as a function of electron or muon transverse momentum p_{T} or their pseudorapity η, as well as double-differential cross-sections as functions of these variables, are measured in proton–proton collisions at centre-of-mass energies $\sqrt{s} = 5.02$ TeV and 13 TeV. The W-boson charge asymmetry as a function of lepton η is also measured. The data, collected in dedicated runs at reduced instantaneous luminosity with the ATLAS detector at the Large Hadron Collider, correspond to integrated luminosities of 255 pb^{-1} at 5.02 TeV and 338 pb^{-1} at 13 TeV. The measurements are in agreement with Standard-Model predictions calculated at next-to-next-to-leading-order in the strong coupling constant α_s including transverse-momentum resummation at next-to-next-to-leading logarithmic accuracy using several parton distribution functions. The impact of the measured differential cross-sections as a function of lepton η on the determination of these functions is studied using a profiling technique.

Contents

* e-mail: atlas.publications@cern.ch

1 Introduction

Precise measurements of the differential cross-sections for $W^{\pm}$-boson production at hadron colliders provide a sensitive probe of perturbative quantum chromodynamics (QCD). Of particular interest is the ability of such measurements to discriminate between different parton distribution functions (PDFs) [1–7], since the W-boson rapidity is strongly correlated with the initial-state parton momentum fraction x. In high-energy proton–proton (pp) collisions at the Large Hadron Collider (LHC), the main production mechanism of single W bosons is a quark annihilating with a sea antiquark. The production at higher x is enhanced by the valence quark contribution which leads to an increase of W bosons boosted in the valence quark direction. Since the proton contains two valence u quarks and one valence d quark, there is a production asymmetry between W^+ and W^- bosons (referred to as the W-boson charge asymmetry), which also varies as a function of rapidity. The boson rapidity cannot be determined unambiguously in leptonic decays of the W boson ($W \to \ell\nu$) because the neutrino passes through the detector unobserved. The charge asymmetry can instead be measured as a function of pseudorapidity (η) of the charged lepton, which is strongly correlated with the rapidity of the W boson. In addition, the transverse momentum (p_{T}) distribution of the charged lepton is sensitive to the mass of the W boson.

High precision predictions with increasingly higher-order corrections are available to compare with data. These predictions incorporate the fixed-order corrections, known up to third order in the strong coupling constant α_s [8–10], and the resummation of logarithmic terms from soft and collinear emissions [11–13].

This paper presents a high precision measurement of single-differential cross-sections for $W^{\pm}$-boson production as a function of lepton $|\eta|$ ($d\sigma/d|\eta|$) and lepton transverse momentum p_{T} ($d\sigma/dp_{\mathrm{T}}$) in the electron and muon ($\ell = e, \mu$) final states. Double-differential cross-sections as functions

Published online: 02 July 2025

of lepton $|\eta|$ and p_{T} ($d^2\sigma/d|\eta|dp_{\mathrm{T}}$) are also measured. The measurements are based on dedicated data samples collected by the ATLAS experiment at the LHC with low instantaneous luminosity at centre-of-mass energies $\sqrt{s} = 5.02$ TeV and 13 TeV. These datasets correspond to about 255 pb^{-1} and 338 pb^{-1}, respectively, with on average two inelastic pp collisions taking place in the same bunch crossing (pile-up). These low pile-up datasets provide unique and excellent experimental conditions for high precision measurements. This analysis shares the same datasets, analysis techniques and systematic studies as Ref. [14], where further details of many aspects can be found. The measurements of the $d\sigma/d|\eta|$, $d\sigma/dp_{\mathrm{T}}$ and $d^2\sigma/d|\eta|dp_{\mathrm{T}}$ presented here complement the inclusive cross-sections and single-differential cross-sections as a function of the transverse momentum of the W^+, W^- and Z vector bosons ($V = W, Z$) from ATLAS in Ref. [14] and the inclusive cross-sections from the CMS experiment [15] using similar data samples. Single-differential cross-sections of W-boson production as a function of η have also been measured previously by ATLAS at 5.02 TeV using a much smaller data sample [16], 7 TeV [17] and 8 TeV [18], by CMS at 8 TeV [19], and by LHCb in the forward region at 7 TeV and 8 TeV [20–22]. The W-boson double-differential cross-section as functions of lepton η and p_{T} has been measured by CMS at $\sqrt{s} = 13$ TeV [23].

This paper also presents a measurement of the W-boson charge asymmetry (A_ℓ) as a function of lepton $|\eta|$. The W-boson charge asymmetry has been measured by ATLAS at 5.02 TeV, 7 TeV and 8 TeV [16–18], by CMS at 7 TeV [24,25], 8 TeV [19] and $\sqrt{s} = 13$ TeV [23], and by LHCb at 7 TeV and 8 TeV [20–22]. It has also been measured in proton–antiproton collisions by the CDF and D0 collaborations [26–29].

The measurements in the electron and muon channels are combined, and then compared with theoretical predictions at next-to-next-to-leading-order (NNLO) in α_s including transverse-momentum resummation at next-to-next-to-leading logarithmic (NNLL) accuracy with different PDF sets [1–7]. The impact of the measured $d\sigma/d|\eta|$ on the PDFs is further studied using a profiling technique [30,31].

2 ATLAS detector

The ATLAS detector [32] at the LHC covers nearly the entire solid angle around the collision point.[1] It consists of an inner tracking detector surrounded by a thin superconducting solenoid, electromagnetic and hadronic calorimeters, and a muon spectrometer incorporating three large superconducting air-core toroidal magnets.

The inner-detector system (ID) is immersed in a 2 T axial magnetic field and provides charged-particle tracking in the range $|\eta| < 2.5$. The high-granularity silicon pixel detector covers the vertex region and typically provides four measurements per track, the first hit generally being in the insertable B-layer (IBL) installed before Run 2 [33,34]. It is followed by the SemiConductor Tracker (SCT), which usually provides eight measurements per track. These silicon detectors are complemented by the transition radiation tracker (TRT), which enables radially extended track reconstruction up to $|\eta| = 2.0$. The TRT also provides electron identification information based on the fraction of hits (typically 30 in total) above a higher energy-deposit threshold corresponding to transition radiation.

The calorimeter system covers the pseudorapidity range $|\eta| < 4.9$. Within the region $|\eta| < 3.2$, electromagnetic calorimetry is provided by barrel and endcap high-granularity lead/liquid-argon (LAr) calorimeters, with an additional thin LAr presampler covering $|\eta| < 1.8$ to correct for energy loss in material upstream of the calorimeters. Hadronic calorimetry is provided by the steel/scintillator-tile calorimeter, segmented into three barrel structures within $|\eta| < 1.7$, and two copper/LAr hadronic endcap calorimeters. The solid angle coverage is completed with forward copper/LAr and tungsten/LAr calorimeter modules optimised for electromagnetic and hadronic energy measurements respectively.

The muon spectrometer (MS) comprises separate trigger and high-precision tracking chambers measuring the deflection of muons in a magnetic field generated by the superconducting air-core toroidal magnets. The field integral of the toroids ranges between 2.0 and 6.0 T m across most of the detector. Three layers of precision chambers, each consisting of layers of monitored drift tubes, cover the region $|\eta| < 2.7$, complemented by cathode-strip chambers in the forward region, where the background is highest. The muon trigger system covers the range $|\eta| < 2.4$ with resistive-plate chambers in the barrel, and thin-gap chambers in the endcap regions.

The luminosity is measured mainly by the LUCID–2 [35] detector that records Cherenkov light produced in the quartz windows of photomultipliers located close to the beampipe.

Events are selected by the first-level trigger system implemented in custom hardware, followed by selections made by algorithms implemented in software in the high-level

[1] ATLAS uses a right-handed coordinate system with its origin at the nominal interaction point (IP) in the centre of the detector and the z-axis along the beam pipe. The x-axis points from the IP to the centre of the LHC ring, and the y-axis points upwards. Polar coordinates (r, ϕ) are used in the transverse plane, ϕ being the azimuthal angle around the z-axis. The pseudorapidity is defined in terms of the polar angle θ

footnote 1 continued
as $\eta = -\ln\tan(\theta/2)$ and is equal to the rapidity $y = \frac{1}{2}\ln\left(\frac{E+p_z}{E-p_z}\right)$ in the relativistic limit. Angular distance is measured in units of $\Delta R \equiv \sqrt{(\Delta y)^2 + (\Delta\phi)^2}$.

trigger [36]. The first-level trigger accepts events from the 40 MHz bunch crossings at a rate close to 100 kHz, which the high-level trigger further reduces in order to record complete events to disk at about 1.25 kHz.

A software suite [37] is used in data simulation, in the reconstruction and analysis of real and simulated data, in detector operations, and in the trigger and data acquisition systems of the experiment.

3 Data and simulated event samples

This analysis is performed using datasets corresponding to integrated luminosities of $254.9 \pm 2.6\,\text{pb}^{-1}$ at 5.02 TeV and $338.1 \pm 3.1\,\text{pb}^{-1}$ at 13 TeV [38]. They were recorded in 2017 and 2018 during dedicated LHC low pile-up runs with an average number of pp interactions of about two, which is about a factor 20 smaller than that of the nominal LHC Run 2 operation between 2015 and 2018. The data was collected with triggers that require at least one muon or electron with transverse momentum thresholds of 14 GeV and 15 GeV, respectively [39–41].

Samples of Monte Carlo (MC) simulated events are used to model the signal and background processes, except multijet production that is modelled from data as discussed in Sect. 5. All MC samples were processed through the full ATLAS detector simulation [42] based on GEANT4 [43] using settings specific to the low pile-up run conditions. The effects of pile-up collisions in the same or neighbouring bunch crossings were included in the MC simulation by overlaying inelastic pp interactions produced using PYTHIA 8.1 [44] with the NNPDF2.3LO set of PDFs [45] and the A3 set of tuned parameters (tune) [46].

The event samples for signal W-boson and background Z-boson production were generated using the POWHEG event generator at next-to-leading-order (NLO) in QCD [47–50] using the CT10 PDF [51], interfaced to PYTHIA 8.2 [52] using the AZNLO tune [53]. These POWHEG+PYTHIA 8 samples were interfaced to PHOTOS++ [54] to simulate the effect of final-state QED radiation. Alternative samples were prepared with SHERPA 2.2.1 (for 13 TeV) and 2.2.5 (for 5.02 TeV) [55] using the NNPDF3.0 NNLO PDFs [56] and merging matrix element calculations from COMIX [57] and OPENLOOPS [58–60] for $V + 0, 1, 2$ partons at NLO accuracy with $V + 3, 4$ partons at leading-order (LO) accuracy in the MEPS@NLO scheme [61–65]. The W-boson signal samples are used to evaluate the uncertainty arising from the choice of MC generator. The W and Z-boson samples are normalised to NNLO calculations performed using the DYTURBO program [13,66–68], an optimised version of DYNNLO [69,70], using the MMHT2014 NNLO PDF set [71]. The contribution to the electron and muon final states from leptonically decaying τ-leptons in W-boson decays is treated as background [72].

Background processes from top-antitop-quark pair ($t\bar{t}$) production and single-top-quark production (Wt associated production, t-channel, s-channel) were generated with POWHEG+PYTHIA 8 [73] and normalised to the NNLO predictions with resummation at NNLL accuracy [74–76]. Diboson production VV was generated with SHERPA 2.2.1 in all decay channels with at least one real lepton in the final state and treated as background [72].

4 Event reconstruction and selection

Events are selected if they include exactly one electron or muon candidate that is matched to a corresponding trigger lepton candidate. Events are also required to have at least one reconstructed collision vertex with two or more charged-particle tracks [77]. The vertex with the largest sum of squared transverse momenta of its associated tracks is taken as the primary vertex.

Electron candidates are reconstructed from clusters of energy deposited in the electromagnetic calorimeter and associated with at least one track in the ID [78]. Electrons are required to be within the coverage of the ID and the precision region of the EM calorimeter, $|\eta| < 2.47$. Electrons in the transition region between the barrel and endcap calorimeters, $1.37 < |\eta| < 1.52$, are excluded. Electron candidates are required to have a transverse momentum of $p_{\text{T}} > 25$ GeV and pass the *Medium* likelihood identification requirements [78]. They are also required to be isolated from nearby activity, as measured by tracks in a cone of size $\Delta R < 0.2$ around the candidate. The scalar sum of the p_{T} of these tracks ($p_{\text{T}}^{\text{cone20}}$) is required to be less than 10% of the electron p_{T} and may not exceed 5 GeV for electrons with $p_{\text{T}} > 50$ GeV, i.e. $p_{\text{T}}^{\text{cone20}}/\min(p_{\text{T}}, 50\,\text{GeV}) < 0.1$.

The muon reconstruction is performed independently in the ID and in the MS, and a muon candidate is formed using the combined information from the MS and ID tracks [79]. The muon candidates are required to have an absolute pseudorapidity of $|\eta| < 2.4$, a transverse momentum of $p_{\text{T}} >$ 25 GeV and to satisfy the *Medium* identification criteria [79]. Muons are required to be isolated from nearby activity with the same criterion as electrons.

Lepton candidates are required to originate from the primary vertex. The track transverse impact parameter significance, $|d_0/\sigma_{d_0}|$, calculated relative to the beam line, must be smaller than three for muons and smaller than five for electrons. Furthermore, the longitudinal impact parameter, z_0 (the difference between the z-coordinate of the point on the track at which d_0 is defined and the longitudinal position of the primary vertex), is required to satisfy $|z_0 \sin(\theta)| <$ 0.5 mm. Dedicated lepton calibrations and efficiency corrections are applied to the reconstructed electron and muon candidates as described in Ref. [14].

The missing transverse momentum, $\vec{p}_{\mathrm{T}}^{\mathrm{miss}}$, with its magnitude $E_{\mathrm{T}}^{\mathrm{miss}}$, represents a measure of the transverse momentum of the neutrino. It is defined as $\vec{p}_{\mathrm{T}}^{\mathrm{miss}} = -(\vec{p}_{\mathrm{T}} + \vec{u}_{\mathrm{T}})$ using the lepton $\vec{p}_{\mathrm{T}}$ and hadronic recoil $\vec{u}_{\mathrm{T}}$. The hadronic recoil is reconstructed in the plane transverse to the beam using particle-flow objects (PFOs), that combine information from charged-particle tracks in the ID and energy deposits in the calorimeter [80,81]. The hadronic recoil is calibrated using $Z \rightarrow \ell^+\ell^-$ events by comparing u_{T} with $p_{\mathrm{T}}^{\ell\ell}$, the transverse momentum of the dilepton system [14]. The resolution of the u_{T} is mainly affected by the event activity variable ΣE_{T}, which represents the scalar sum of the transverse energies of all PFOs included in the recoil objects. The modified event activity $\Sigma \bar{E}_{\mathrm{T}}$, defined as $\Sigma \bar{E}_{\mathrm{T}} = \Sigma E_{\mathrm{T}} - u_{\mathrm{T}}$, primarily reflects contributions from the underlying event and pile-up, and is used to characterise the hadronic recoil resolution. The low pile-up datasets used in this analysis significantly improve the resolution of the recoil measurement.

The background from QCD multijet events is reduced by the requirement $E_{\mathrm{T}}^{\mathrm{miss}} > 25\,\mathrm{GeV}$. Furthermore, the W-boson transverse mass $m_{\mathrm{T}} = \sqrt{2 p_{\mathrm{T}} E_{\mathrm{T}}^{\mathrm{miss}} (1 - \cos \Delta\phi_{\ell\nu})}$ must exceed 50 GeV, where $\Delta\phi_{\ell\nu}$ is the azimuthal angle between the lepton $\vec{p}_{\mathrm{T}}$ and $\vec{p}_{\mathrm{T}}^{\mathrm{miss}}$. After all selections, the numbers of $W \rightarrow e\nu$ and $W \rightarrow \mu\nu$ candidates for the 5.02 TeV dataset are 7.1×10^5 and 7.5×10^5, respectively, and the corresponding number for the 13 TeV dataset is around 2.2×10^6 for both channels.

5 Background estimates and event yields

Electroweak backgrounds include $W \rightarrow \tau\nu$ decays where the τ-lepton decays leptonically, and $Z \rightarrow \ell^+\ell^-$ events where one lepton escapes detection. In the electron channel, the $W \rightarrow e\nu$ background also includes a contribution from signal $W \rightarrow e\nu$ events where the charge of the electron is misreconstructed, forming a background in the oppositely-charged signal sample. In the muon channel, such a charge misreconstruction is negligibly small. There are also background contributions from diboson production and from top quark events that mainly contribute at high lepton p_{T}.

Background from QCD multijet (MJ) production cannot be reliably simulated and has to be derived from data [14]. Depending on the lepton flavour, the MJ background has significant contributions from leptons produced in semileptonic decays of heavy quarks, pion and kaon decays, or photon conversions. The multijet yields in the electron and muon channels are estimated separately for positively and negatively charged W-boson samples, and also for different centre-of-mass energies.

Four selection regions are used for the multijet background estimate. The signal region (SR) is defined by events satisfying all selection criteria described in Sect. 4, including $E_{\mathrm{T}}^{\mathrm{miss}} > 25\,\mathrm{GeV}$ and $m_{\mathrm{T}} > 50\,\mathrm{GeV}$. As multijet production is concentrated at lower values of p_{T}, $E_{\mathrm{T}}^{\mathrm{miss}}$ and m_{T} as compared to the signal, a fit region (FR) is constructed with the requirements on $E_{\mathrm{T}}^{\mathrm{miss}}$ and m_{T} dropped, while other selections remain the same as in the SR. Two control regions, CR1 and CR2, are defined, corresponding to the FR and SR, respectively, except that the lepton in CR1 and CR2 fails the isolation condition.

The number of multijet events in the FR is derived from a template fit to the data distributions as a function of p_{T}, $E_{\mathrm{T}}^{\mathrm{miss}}$ or m_{T}, exploiting the different shapes of multijet events, $W \rightarrow \ell\nu$ signal, electroweak and top-quark background components in these variables. The multijet template used in the FR is derived from the data distributions in the CR1, after subtracting the small $W \rightarrow \ell\nu$ signal and non-multijet background components using simulation. The other components in the FR are taken from simulation. In a final step, the multijet yields in the SR are determined by multiplying the FR yields by a transfer factor that corrects for the acceptance of the $E_{\mathrm{T}}^{\mathrm{miss}}$ and m_{T} selections and the dependence on the isolation requirement. The transfer factor is determined by calculating the ratio of multijet event yields in the CR2 and the CR1. As the transfer factor depends on the isolation criterion, mutually exclusive intervals in the isolation variable are chosen to create statistically independent samples that are progressively closer to the signal-candidate selection. Figure 1 shows the dependence on the isolation variable interval of multijet yields derived using these transfer factors, taking the m_{T} variable as an example. A linear extrapolation to the signal region is performed, with the difference in normalisation with respect to a quadratic extrapolation included as an additional systematic uncertainty. The other dominant multijet yield uncertainties include the statistical uncertainty from the finite data and MC sample size in the fit regions, and those arising from the linear extrapolation to the average isolation value in the signal region and the possible mismodelling of the jet activity in those regions failing the isolation requirement [14]. In addition, a shape uncertainty is obtained by taking the difference between the extrapolated shape in the SR and the multijet shape in the isolation interval [0.1, 0.2] in the CR2. The multijet yields are estimated by using template fits performed as functions of p_{T}, $E_{\mathrm{T}}^{\mathrm{miss}}$ and m_{T} separately. The results are found to be consistent and their average is used for the final result.

The expected event yields for signal and background processes are shown in Table 1. The total background level ranges between 3% and 7% depending on the channel and the centre-of-mass energy. Figure 2 shows the detector-level $|\eta|$ and p_{T} distributions for two selected channels at 5.02 TeV and 13 TeV. The two-dimensional distributions of η and p_{T}

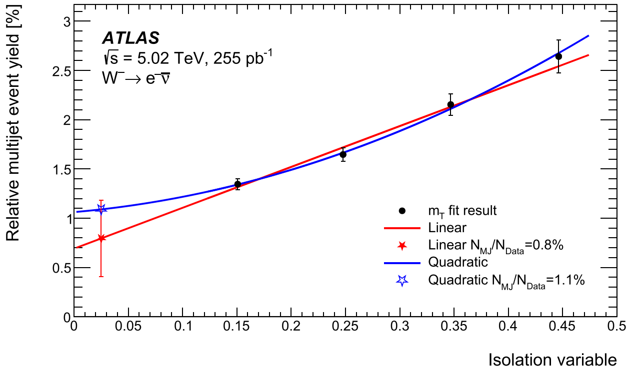

Fig. 1 Relative multijet event yield in data extrapolated in the signal region from its dependence as a function of isolation variable $p_{\mathrm{T}}^{\mathrm{cone20}}/\min(p_{\mathrm{T}}, 50\,\mathrm{GeV})$ is shown as an example for $W^- \rightarrow e^-\bar{\nu}$ at 5.02 TeV using the m_{T} distribution. The vertical error bar on the signal region point at 0.025 represents the total uncertainty including the difference between the linear and quadratic fits

are presented as consecutive distributions of $|\eta|$ for different ranges of p_{T}, as shown in Fig. 3. Overall, good agreement is observed between the data and the expectations in all the kinematic distributions. The choice of the bin boundaries for the $|\eta|$ distribution is different for the electron and muon channels, driven by details of the detector geometry. The bin boundaries for the p_{T} distribution are the same for electrons and muons, and correspond to those for the unfolded fiducial cross-section as discussed in Sect. 6. The hole in the $|\eta|$ distributions in the electron channel corresponds to the excluded barrel-endcap calorimeter transition region ($1.37 < |\eta| < 1.52$) in the selection. The differences between the electron and muon distributions reflect both the different efficiencies for reconstructing and selecting the two lepton flavours, and the intrinsic kinematic differences between W^+-boson events at 5.02 TeV and W^--boson events at 13 TeV.

6 Measurement procedure

The differential cross-sections at the particle level are measured in the same fiducial phase space as in Ref. [14], corresponding to Born-level leptons with $p_{\mathrm{T}} > 25\,\mathrm{GeV}$, $|\eta| < 2.5$, $m_{\mathrm{T}}^W > 50\,\mathrm{GeV}$ and $p_{\mathrm{T}}^{\nu} > 25\,\mathrm{GeV}$. The bins defined by particle-level kinematics for the single-differential cross-sections in lepton $|\eta|$ and p_{T} are:

- $|\eta|$: [0, 0.42, 0.84, 1.05, 1.37, 1.52, 1.95, 2.5],
- p_{T}: [25, 30, 35, 40, 45, 50, 60, 80, 100] GeV.

The bins are chosen by considering the sensitivity to the underlying physics, detector resolution effects, detector geometry, and the statistical precision in each bin. To simplify the combination process described below, a common binning scheme is chosen for the electron and muon channels. For the double-differential cross-section measurement, the $|\eta|$ bin boundaries from the single-differential measurement are used, while the last three p_{T} bins from 50 to 100 GeV are merged into a single bin due to the small number of events with high p_{T}.

To derive the differential cross-sections, the distributions observed at the detector level after analysis selection and background subtraction are corrected for detector effects using an iterative Bayesian unfolding method [82,83]. First, the data are corrected for events that pass the detector-level selection but not the particle-level selection, with purity correction factors derived from simulated samples. The iterative Bayesian unfolding technique is then used to correct for the finite detector acceptance, resolution and reconstruction efficiency in order to estimate the true underlying distribution. Simulated events are used to determine the response matrices needed to correct for the migration between bins in the detector-level distributions. The unfolding procedure follows Ref. [14] and determines the best estimate of the underlying distribution using:

$$\tilde{u}_j = \sum_i U_{ji}(d_i - b_i)p_i\,, \tag{1}$$

where the indices i and j refer to bin i and j in the detector-level and unfolded or true distributions, respectively, $\tilde{u}_j$ is the unfolded spectrum, and U symbolically represents the unfolding transformation, which in the simplest case is just the inverse of the response matrix. The background-subtracted data distribution $d_i - b_i$ is multiplied by the purity correction factors p_i. The purity correction factors p_i are defined by the number of generated and reconstructed events in bin i divided by the number of reconstructed events in the bin. The number of iterations in the unfolding procedure is optimised to minimise the total measurement uncertainty, and specifically the uncertainty related to possible biases induced by the unfolding. Finally, the differential cross-section in bin j is derived by dividing $\tilde{u}_j$ by the product of the luminosity, bin width and efficiency correction factors. The latter are defined by the number of generated and reconstructed events in bin j divided by the number of generated events in the bin.

The W-boson production differential cross-sections are measured separately in the electron and muon channels. The measured cross-sections in the two channels are compared and are found to be consistent within the uncorrelated uncertainties. They are then combined as in Ref. [14] by using an iterative implementation [84] of the best linear unbiased estimator (BLUE) method [85,86]. The iterative procedure reduces the bias resulting from non-Gaussian uncertainty sources.

Table 1 Observed and expected event yields for the W-boson selections in the 5.02 TeV and 13 TeV datasets for the electron and muon channels split by the charge of the reconstructed lepton. Fractions in percent for the signal and background processes relative to the total expected event yield are also shown, where the uncertainties for the multijet background correspond to the total uncertainties. The uncertainty in the expected event yield includes the simulation statistical uncertainty and that of the multijet background. The category $W \to \ell\nu$ BG refers to background from $W \to \tau\nu$ as well as charge misidentification in the electron channels

Channel	Observed	Expected	Signal [%]	$W \to \ell\nu$ BG [%]	$Z \to \ell\ell$ [%]	Top [%]	Diboson [%]	Multijet [%]
$\sqrt{s} = 5.02$ TeV $W \to \ell\nu$								
$W^- \to e^-\bar{\nu}$	274,375	276,000 ± 1000	95.8	2.6	0.4	0.3	0.1	0.8 ± 0.4
$W^+ \to e^+\nu$	430,662	431,000 ± 1000	96.8	2.1	0.3	0.2	0.1	0.5 ± 0.2
$W^- \to \mu^-\bar{\nu}$	288,026	289,000 ± 1000	94.8	1.8	2.9	0.3	0.1	0.1 ± 0.3
$W^+ \to \mu^+\nu$	457,223	457,000 ± 1000	95.8	1.7	2.1	0.2	0.1	0.1 ± 0.2
$\sqrt{s} = 13$ TeV $W \to \ell\nu$								
$W^- \to e^-\bar{\nu}$	949,297	947,000 ± 6000	92.6	2.4	0.7	1.3	0.2	2.9 ± 0.6
$W^+ \to e^+\nu$	1,207,652	1,192,000 ± 7000	93.7	2.1	0.6	1.1	0.1	2.4 ± 0.6
$W^- \to \mu^-\bar{\nu}$	964,514	966,000 ± 4000	92.9	1.5	3.5	1.2	0.2	0.6 ± 0.4
$W^+ \to \mu^+\nu$	1,245,755	1,230,000 ± 4000	93.8	1.5	3.1	1.0	0.1	0.5 ± 0.3

The W-boson charge asymmetry A_ℓ is extracted using the formula:

$$A_\ell(|\eta|) = \frac{\frac{d\sigma_{W+}}{d|\eta|} - \frac{d\sigma_{W-}}{d|\eta|}}{\frac{d\sigma_{W+}}{d|\eta|} + \frac{d\sigma_{W-}}{d|\eta|}}, \tag{2}$$

where the differential cross-sections as a function of lepton $|\eta|$ are obtained from the combination of the electron and muon channels.

7 Systematic uncertainties

The uncertainties in the integrated luminosities are 1.0% and 0.92% for the 5.02 TeV and 13 TeV datasets, respectively, following the methodology discussed in Ref. [38], using the LUCID-2 detector [35] for the primary luminosity measurements, complemented by measurements using the inner detector and calorimeters. These are the leading systematic uncertainties for the single-differential cross-section measurements except at the high lepton p_T tails.

The electron efficiency corrections and corresponding uncertainties as functions of lepton p_T and $|\eta|$ are determined following the strategies outlined in Ref. [78]. The reconstruction efficiency is extrapolated from corrections derived using datasets with high pile-up conditions [14]. The remaining efficiency corrections and their corresponding uncertainties are obtained using $Z \to e^+e^-$ events in the low pile-up datasets. The electron energy calibration uncertainty is also determined using the low pile-up datasets and the methods described in Ref. [78]. These uncertainties are typically below 0.3% for the single-differential cross-section measurements except at the low and high lepton p_T regions, where they reach up to 1%. The charge misidentification probability and the corresponding uncertainties are evaluated as a function of lepton η. The impact of charge misidentification is very small for the cross-section measurement but contributes up to 0.4% when determining the charge asymmetry.

The muon efficiency corrections and corresponding uncertainties follow a similar approach to those for electrons. Most of the efficiencies are measured using $Z \to \mu^+\mu^-$ events in the low pile-up dataset following Ref. [79], while the reconstruction efficiency is extrapolated from datasets with high pile-up conditions [14]. The muon energy calibration uncertainty is derived using the Run 2 dataset with high pile-up conditions [87] and then extrapolated to the low pile-up conditions. These uncertainties are typically at up to a few permille level.

The uncertainties arising from the hadronic recoil calibration are grouped into several categories [14]. The primary uncertainty arises from the corrections derived from Z-boson events. The corrections to the simulation to account for mismodelling of the data $\Sigma\bar{E}_T$ distribution give rise to subdominant uncertainty sources in the single-differential lepton p_T cross-section measurements in the high lepton p_T regions.

Uncertainties due to the unfolding procedure are determined following Ref. [88], based on the regularisation and differences in shape between the data and MC simulations. The particle-level spectra in simulation are reweighted using a smooth function so that the reconstructed-level spectra match the data distributions. The reweighted MC spectra are then treated as pseudodata and unfolded back to the particle-level. The differences between the unfolded and reweighted particle-level spectra are considered as the unfolding bias, which has only a negligible effect on the results.

The uncertainties originating from the finite size of the MC simulation samples are treated as systematic uncertainties, and they are estimated by using the bootstrap method [89].

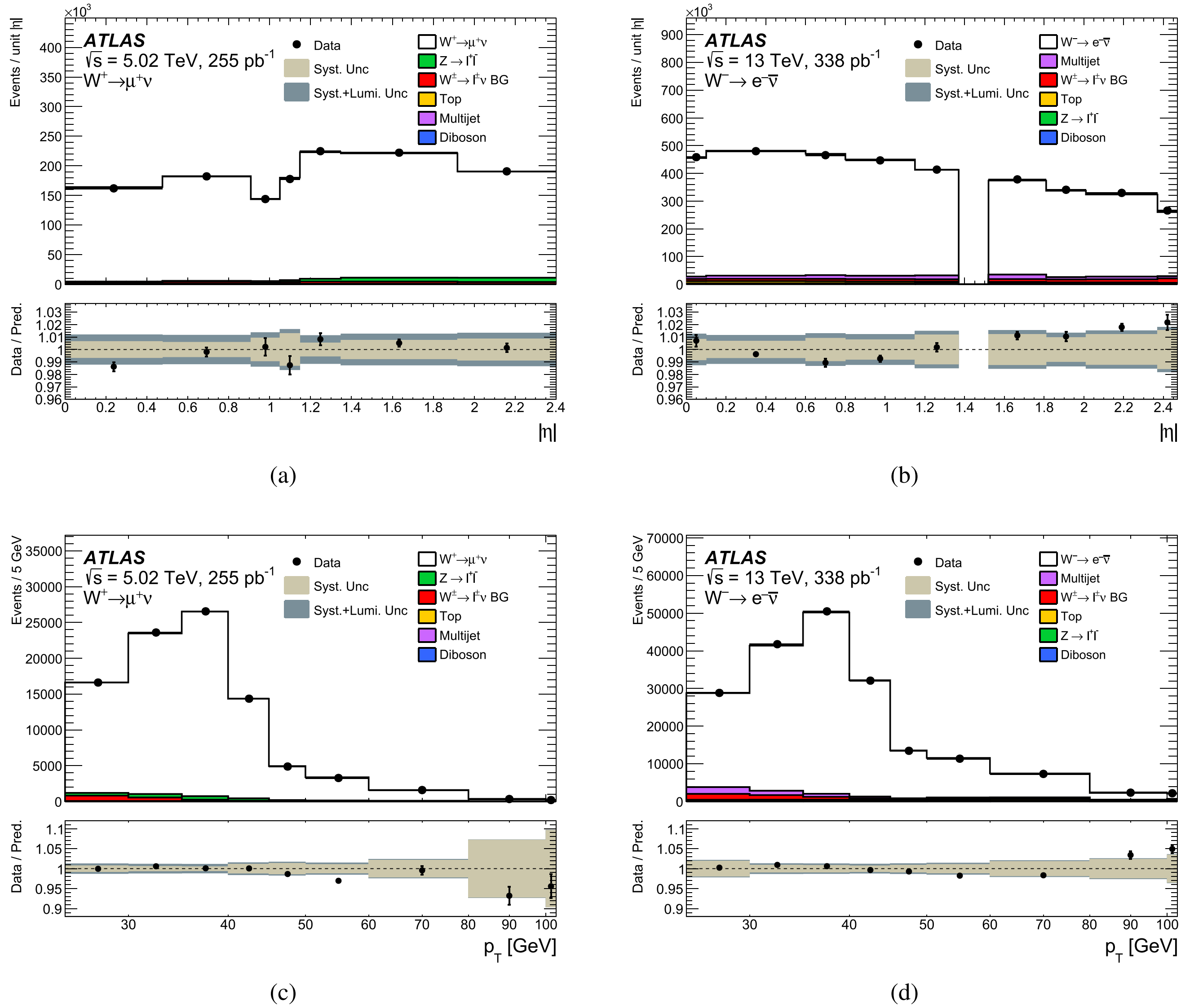

Fig. 2 Detector-level distributions of lepton $|\eta|$ in the (**a**) 5.02 TeV $W^+ \rightarrow \mu^+\nu$ and (**b**) 13 TeV $W^- \rightarrow e^-\bar{\nu}$ channels for data, and expected signal and various background contributions normalised to the integrated luminosity of the data sample. Similar detector-level distributions of lepton p_{T} in the (**c**) 5.02 TeV $W^+ \rightarrow \mu^+\nu$ and (**d**) 13 TeV $W^- \rightarrow e^-\bar{\nu}$ channels. The last p_{T} bin has a width of 5 GeV but includes all events with $p_{\mathrm{T}} > 100$ GeV. The bottom panel displays the ratio of data over expectation, with the data statistical error shown by the error bar on the points. The dark shaded band represents the total systematic uncertainty, while the light shaded band shows the total systematic uncertainty excluding the luminosity uncertainty

They only have a sizeable impact in the highest lepton p_{T} bin of the single-differential lepton p_{T} distributions. They have also a contribution around 0.5% for the W-boson charge asymmetry measurement.

The uncertainties arising from the choice of the generator for the $W^{\pm}$ signal samples are estimated by using alternative Sherpa $W^{\pm}$ samples, which are reweighted to have the same PDFs and calibrated to the default Powheg+Pythia $W^{\pm}$ samples for modelling the hadronic recoil and primary vertex reconstruction efficiency [14]. They are the dominant or next-most-dominant systematic uncertainty affecting the cross-section results by up to 5% at the highest p_{T} bin at 5.02 TeV and the charge asymmetry results by up to 1.5%.

The uncertainties related to the background modelling of the electroweak and top-quark background processes are estimated from simulated samples by varying the PDF input, α_{s}, and QCD renormalisation and factorisation scales to cover for missing higher-order contributions. They are 5% for the electroweak backgrounds involving W and Z bosons, 7% for $t\bar{t}$ processes, and 10% for diboson and single-top processes. They have negligible impact on the cross-section measurements given the small background contributions. On the other

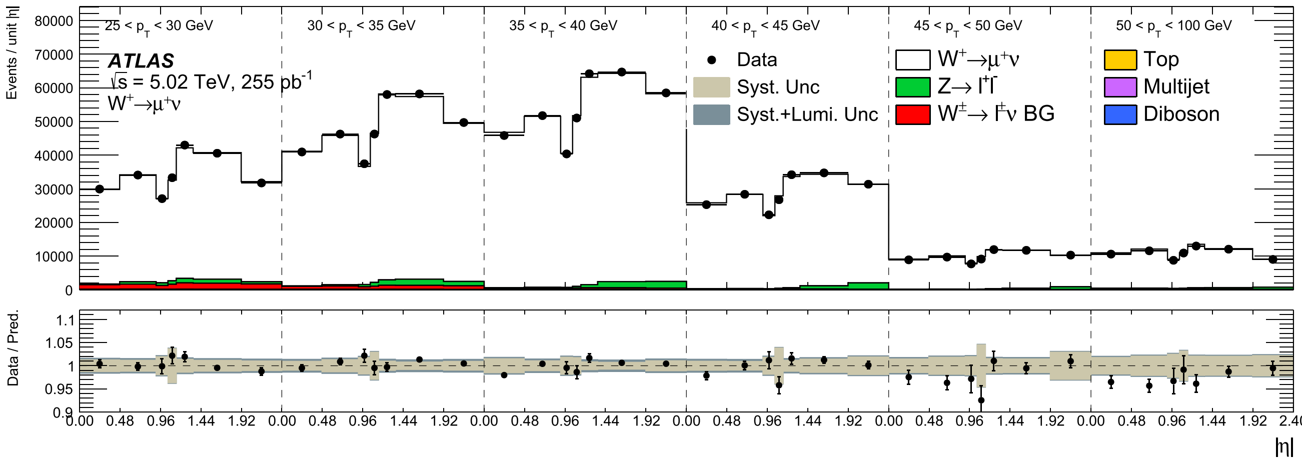

(a)

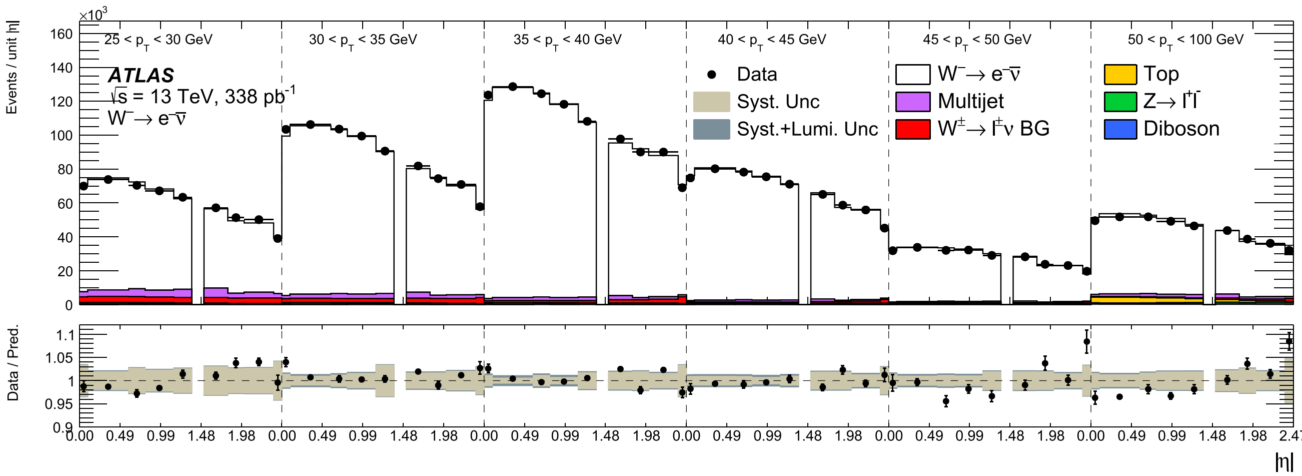

(b)

Fig. 3 Detector-level distributions of lepton $|\eta|$ for various ranges of lepton p_{T} in the (**a**) 5.02 TeV $W^+ \to \mu^+\nu$ and (**b**) 13 TeV $W^- \to e^-\bar{\nu}$ channels for data, and expected signal and various background contributions normalised to the integrated luminosity of the data sample. The bottom panel displays the ratio of data over expectation, with the data statistical error shown by the error bar on the points. The dark shaded band represents the total systematic uncertainty, while the light shaded band shows the total systematic uncertainty excluding the luminosity uncertainty

hand, the multijet background uncertainty is dominant at 13 TeV in particular in the low lepton p_{T} region.

The combination of the electron and muon decay channel results, and the determination of the W-boson charge asymmetry, require a model for the correlation of systematic uncertainties between decay channels and W-boson charges. The PDF profiling study described in Sect. 8.3 also requires the correlations between centre-of-mass energies. The following correlation model of the uncertainties is applied across the various lepton decay channels, W-boson charges and centre-of-mass energies [14]. The lepton efficiency corrections, trigger efficiency, and energy calibrations are considered fully correlated for the measurements at the same centre-of-mass energy, but uncorrelated between different energies. The latter choice has, however, a negligible impact on the results related to the PDF study. The recoil calibration uncertainty, determined using Z-boson events, is treated as fully correlated across the W^+ and W^- measurements and between lepton flavours. However, the recoil calibration remains independent between the 5.02 TeV and 13 TeV datasets. The subdominant component, which accounts for discrepancies between data and MC in $\sum \bar{E}_{\mathrm{T}}$ distributions, is treated as uncorrelated. Uncertainties in electroweak and top-quark backgrounds, are assumed to be fully correlated across all measurements. For the multijet background uncertainty, the statistical component is considered uncorrelated between different lepton decay channels, W-boson charges and beam energies, while methodological variations are assumed to be fully correlated among all measurements. The unfolding bias uncertainty is treated as uncorrelated between different measurements. Generator uncertainties are fully correlated between all measurements.

8 Results

In this section, the single- and double-differential cross-section results are presented first, followed by the W-boson charge asymmetry results. The impact of the new single-differential cross-sections as a function of lepton $|\eta|$ on PDFs is then presented. When integrating the differential cross-sections over all the full fiducial phase space defined in Sect. 6, the inclusive cross-section values are compatible with those reported in Ref. [14].

8.1 Differential cross-sections

The combined single-differential cross-sections are shown as a function of lepton $|\eta|$ in Fig. 4 and lepton p_{T} in Fig. 5.[2] The total uncertainty for the former is around 1.2% with little variation as a function of lepton $|\eta|$ and is dominated by the luminosity uncertainty, while the latter has a similar precision around the Jacobian peak and increases slightly up to 2% at low lepton p_{T} and up to 6% for 5.02 TeV and 3% for 13 TeV at the highest lepton p_{T} bin, where the dominant uncertainties are from the choice of generator and the hadronic recoil measurement. The combined two-dimensional cross-sections as functions of $|\eta|$ and p_{T} are presented in Fig. 6. The total uncertainty of the combined double-differential cross-sections is typically around 2% and is dominated at low p_{T} by the lepton-related uncertainty for 5.02 TeV and the multi-jet background uncertainty for 13 TeV and at high p_{T} by the data statistical and generator uncertainties.

The measured cross-sections are compared with the theoretical predictions calculated using DYTURBO [13,66–68] with recent NNLO PDF sets: CT18 [1], MSHT20 [2–4], NNPDF3.1 [5], NNPDF4.0 [6] and ATLASpdf21 [7]. The corresponding uncertainties of the predictions include the statistical and systematic ones accounting for variations in the PDF input, α_{s}, and QCD renormalisation and factorisation scales to cover for missing higher-order contributions. The calculation precision is NNLO in QCD with NNLL terms in the fiducial phase space. The prediction with NNPDF4.0 has the highest precision, followed by NNPDF3.1, MSHT20, CT18 and ATLASpdf2.1 due to different input datasets and tolerance values used in the definition of 1σ error. The predictions with NNPDF3.1 and NNPDF4.0 provide the best description of the $d\sigma/d|\eta|$ measurements over the full range and of $d\sigma/dp_{\mathrm{T}}$ for lepton p_{T} up to 45 GeV. Good agreement is also observed between the measurements and the predictions with the other PDF sets in all the channels and at both energies except in the high p_{T} tail where all the predictions are somewhat lower than the measurement in particular for the 5.02 TeV W^--boson channel.

[2] Unlike the previous ATLAS W-boson differential cross-section publications (e.g. Ref. [17]), the differential cross-sections as a function of lepton $|\eta|$ presented here are the sum of contributions from leptons with negative and positive η, rather than the average contributions.

8.2 W-boson charge asymmetry

Using Eq. (2) in Sect. 6, the W-boson charge asymmetry A_ℓ as a function of lepton $|\eta|$ is derived from the corresponding W^+ and W^--boson single-differential cross-sections. The correlations in uncertainties between the two measurements are taken into account, which significantly reduce the experimental uncertainties which are dominated by the statistical and generator uncertainties. The total uncertainty is below 1.8% and 3% for 5.02 TeV and 13 TeV, respectively. Figure 7 presents the comparison between measured and predicted $W^{\pm}$-boson charge asymmetry. Good agreement is observed in the full $|\eta|$ range and the measurements are more precise than the predictions, demonstrating the potential for additional constraints on the PDFs.

8.3 PDF profiling

Before investigating the impact of the cross-sections $d\sigma/d|\eta|$ on PDFs, it is possible to quantitatively compare the agreement between these cross-sections and the predictions using the recent NNLO PDF sets in terms of χ^2 defined as

$$\chi^2(\vec{\beta}^{\mathrm{exp}}, \vec{\beta}^{\mathrm{th}}) = \sum_i^{N_{\mathrm{data}}} \left(\frac{\sigma_i^{\mathrm{exp}} - \sigma_i^{\mathrm{th}} \left(1 - \sum_j \beta_j^{\mathrm{exp}} \gamma_{ij}^{\mathrm{exp}} - \sum_k \beta_k^{\mathrm{th}} \gamma_{ik}^{\mathrm{th}}\right)}{\Delta_i} \right)^2 + \sum_j^{N_{\mathrm{exp,sys}}} \left(\beta_j^{\mathrm{exp}}\right)^2 + \sum_k^{N_{\mathrm{th,sys}}} \left(\beta_k^{\mathrm{th}}\right)^2, \quad (3)$$

where the index i runs over all N_{data} data points [17]. The measurements and the theory predictions are given by σ_i^{exp} and σ_i^{th}, respectively. The correlated experimental and theoretical uncertainties are included using the corresponding vectors $\vec{\beta}^{\mathrm{exp}}$ and $\vec{\beta}^{\mathrm{th}}$. Their influence on the data and theory predictions is described by the matrices $\gamma_{ij}^{\mathrm{exp}}$ and $\gamma_{ik}^{\mathrm{th}}$, where the indices j and k correspond to the experimental ($N_{\mathrm{exp,sys}}$) and theoretical ($N_{\mathrm{th,sys}}$) uncertainty sources. The statistical and uncorrelated experimental uncertainties are included in Δ_i. For the experimental uncertainties, the correlation model described in Sect. 7 is employed.

The PDF sets considered are CT18, MSHT20, NNPDF4.0 and ATLASpdf21. These PDF sets are determined using datasets that include the LHC data from W-boson production at $\sqrt{s} = 7$ and 8 TeV but not at $\sqrt{s} = 5.02$ TeV and

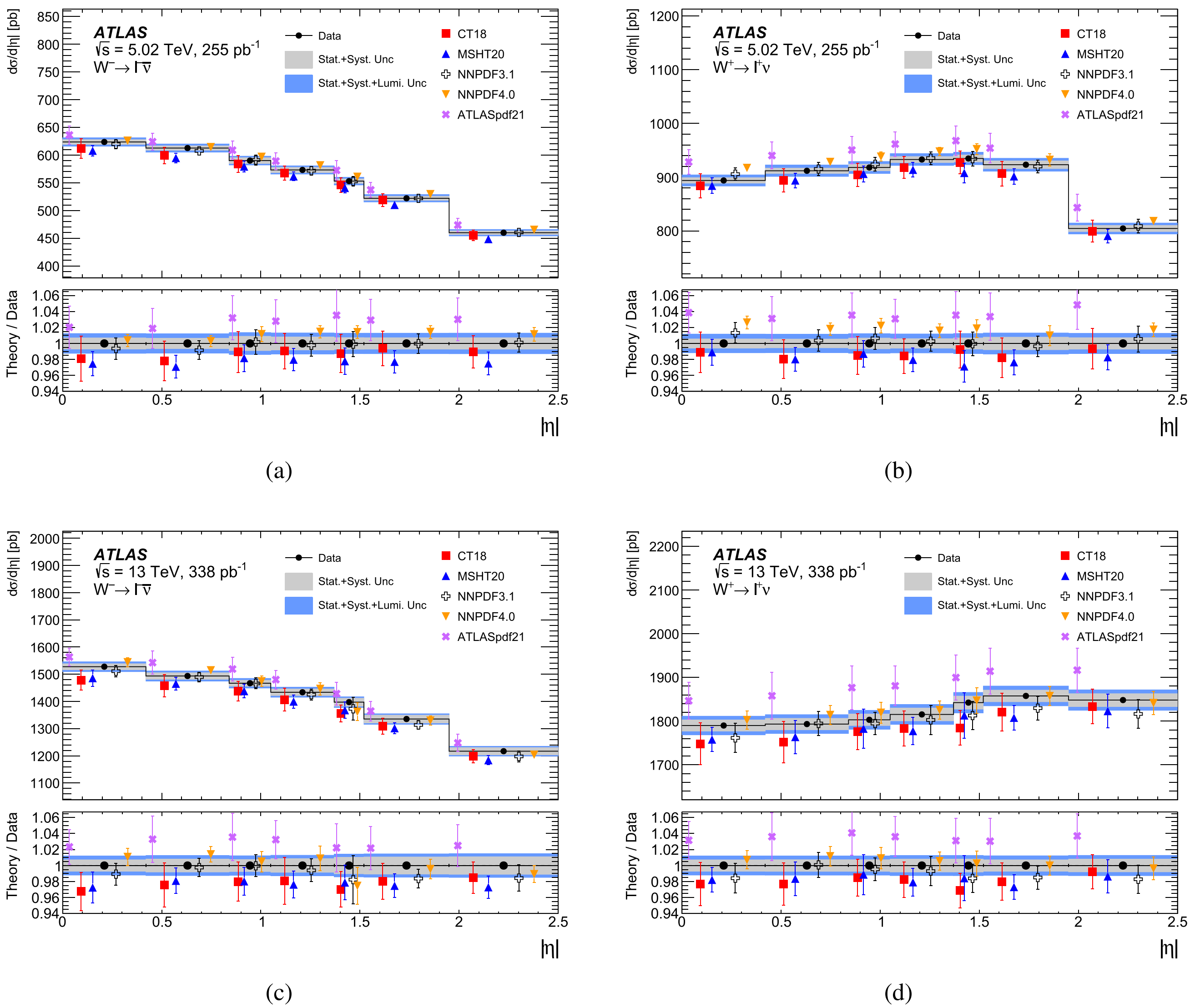

Fig. 4 Differential (**a**, **c**) W^- and (**b**, **d**) W^+-boson cross-section as a function of $|\eta|$ for the combination between the electron and muon channels at (**a**, **b**) 5.02 TeV and (**c**, **d**) 13 TeV. The data are presented with systematic (excluding luminosity) and total uncertainties and compared with the theory predictions with the corresponding uncertainties calculated with DYTURBO with different PDF sets. The ratios of the predictions to the data are shown in the lower panels

13 TeV. The theoretical prediction is calculated using MADGRAPH5_AMC@NLO [90] at NLO level, which is interfaced to APPLGRID [91] using AMCFAST [92]. In a further step, the bin-by-bin NNLO corrections are applied by comparing NLO predictions with NNLO+NNLO predictions calculated using DYTURBO for the same PDF, in terms of K-factors, $K^{\text{NLO}\to\ \text{NNLO QCD}}$:

$$K_i^{\text{NLO}\to\text{NNLO QCD}} = \left(d\sigma_{\text{PDF}}^{\text{NNLO+NNLL QCD}}/d|\eta|\right)_i / \left(d\sigma_{\text{PDF}}^{\text{NLO QCD}}/d|\eta|\right)_i , \quad (4)$$

where i denotes the bin number. The resulting χ^2 values per number of degrees of freedom (ndof) comparing the measured cross-sections and predictions for each of the PDF sets are shown in Table 2. The partial χ^2 value for each dataset corresponds to that of the first term on the right-hand side of Eq. (3), while the correlated χ^2 value is from the other two terms. The measurements are well described by these PDFs in particular for CT18 and MSHT20 given their large tolerance values used in the uncertainty definition, while they exhibit slight tension with ATLASpdf21 and NNPDF4.0.

The impact of new data on these PDF sets can be estimated in a quantitative way with a profiling technique [17,30]. The profiling is performed in the XFITTER framework [93–95]

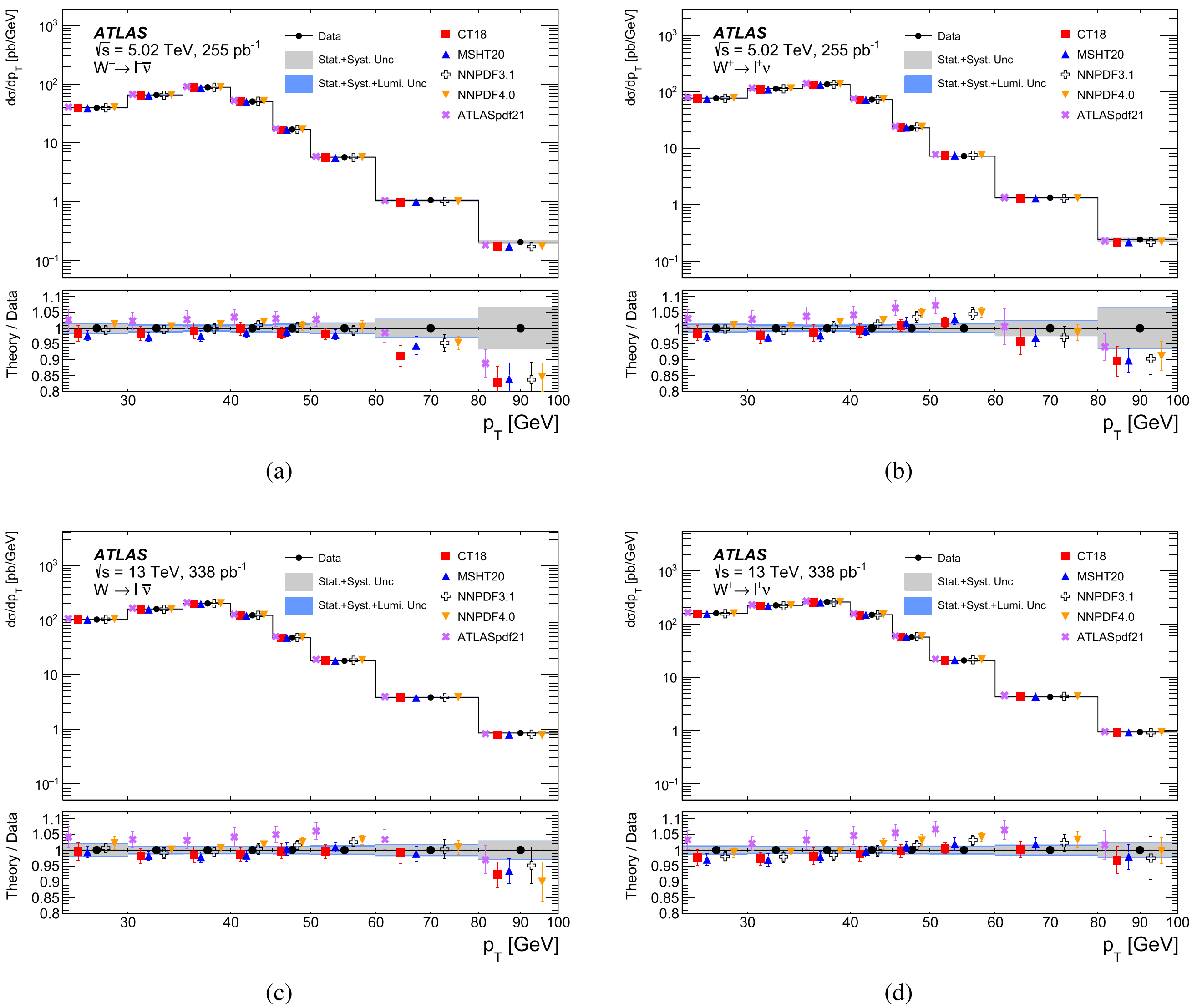

Fig. 5 Differential (**a**, **c**) W^- and (**b**, **d**) W^+-boson cross-section as a function of p_T for the combination between the electron and muon channels at (**a**, **b**) 5.02 TeV and (**c**, **d**) 13 TeV. The data are presented with systematic (excluding luminosity) and total uncertainties and compared with the theory predictions with the corresponding uncertainties calculated with DYTurbo with different PDF sets. The ratios of the predictions to the data are shown in the lower panels

using the above χ^2 formula, except that the correlated experimental and theory uncertainties are now treated as nuisance parameters. When the χ^2 function is minimised, the values of the nuisance parameters at the minimum can be interpreted as an optimisation ('profiling') of PDFs to describe the data [30].

Taking NNPDF4.0 as an example, the profiled parton distributions with reduced uncertainties incorporating the new measurements in comparison with the original ones are shown in Fig. 8 for up- and down-valence quarks (xu_v and xd_v) as well as the ratio of strange quark to light sea quark distributions ($R_s = (s + \bar{s})/(\bar{u} + \bar{d})$). The latter was chosen since it has been observed [96,97] to be higher in some PDF fits than previously expected. Figure 9 displays the corresponding change on the relative uncertainties of the parton distributions. Most of the constraining power arises from the $\sqrt{s} = 13$ TeV measurement. Sizeable improvements in the uncertainties in the quark distributions are observed. The largest reduction of about a factor two is achieved around $x = 0.004$ for the valence quarks. Similar improvement is also observed for the CT18, MSHT20 and ATLASpdf21 PDF sets.

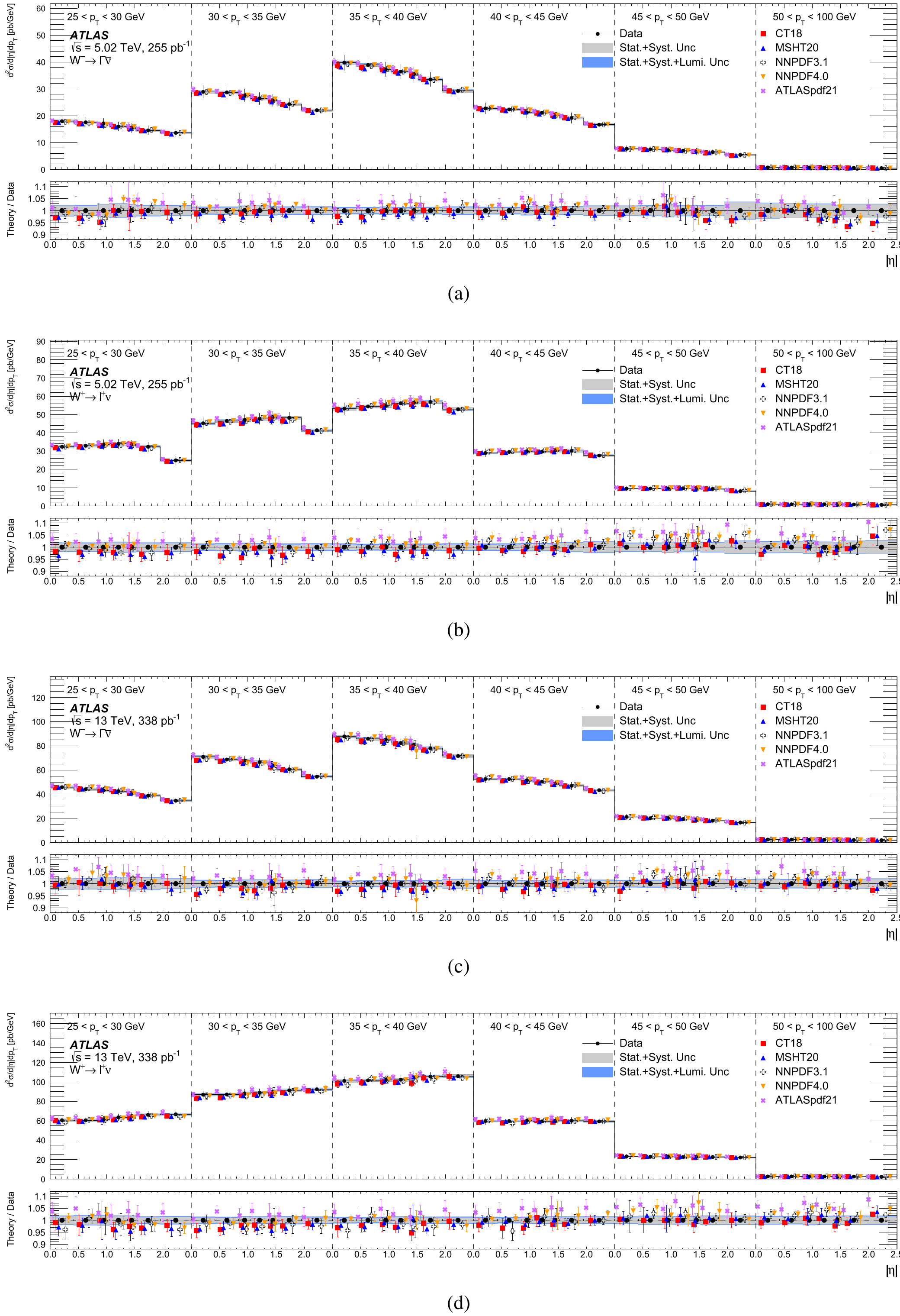

Fig. 6 Differential (**a**, **c**) W^- and (**b**, **d**) W^+-boson cross-section as functions of $|\eta|$ and p_T for the combination between the electron and muon channels at (**a**, **b**) 5.02 TeV and (**c**, **d**) 13 TeV. The data are presented with systematic (excluding luminosity) and total uncertainties and compared with the theory predictions with the corresponding uncertainties calculated with DYTurbo with different PDF sets. The ratios of the predictions to the data are shown in the lower panels

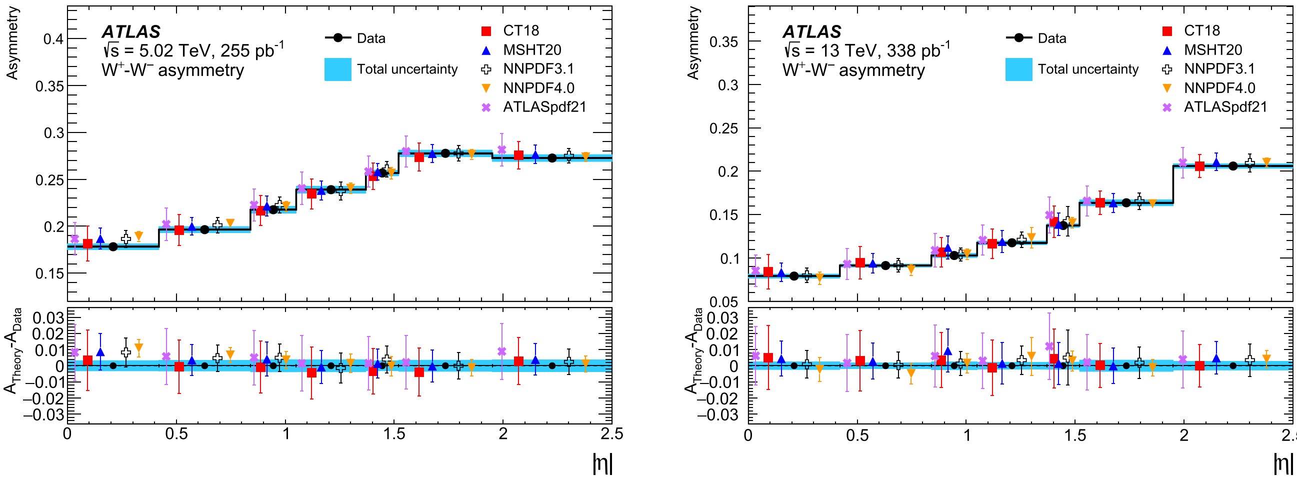

(a) (b)

Fig. 7 The measured W-boson charge asymmetry as a function of $|\eta|$ for the combined electron and muon channels at (**a**) 5.02 TeV and (**b**) 13 TeV. The data are presented with total uncertainties and compared with the theory predictions with the corresponding uncertainties using different PDF sets. The differences between the predictions and the measurement are shown in the lower panels

Table 2 Values of χ^2 with the corresponding numbers of degree of freedom (ndof) comparing the data and unprofiled predictions with various PDF sets. The χ^2 values are split by dataset, providing a detailed breakdown of the agreement between the data and predictions. Additionally, the contribution of the correlated terms arising from the experimental and theoretical correlated uncertainties is also listed

Dataset	Ndof	CT18	MSHT20	ATLASpdf21	NNPDF4.0
$W^- \to \ell^-\bar{\nu}$ 5.02 TeV	7	1.7	2.0	6.0	6.7
$W^+ \to \ell^+\nu$ 5.02 TeV	7	3.7	5.1	6.8	6.1
$W^- \to \ell^-\bar{\nu}$ 13 TeV	7	7.0	7.6	7.5	9.2
$W^+ \to \ell^+\nu$ 13 TeV	7	4.0	3.9	5.6	3.5
Correlated χ^2		11	16	30	25
Total χ^2	28	28	35	56	50

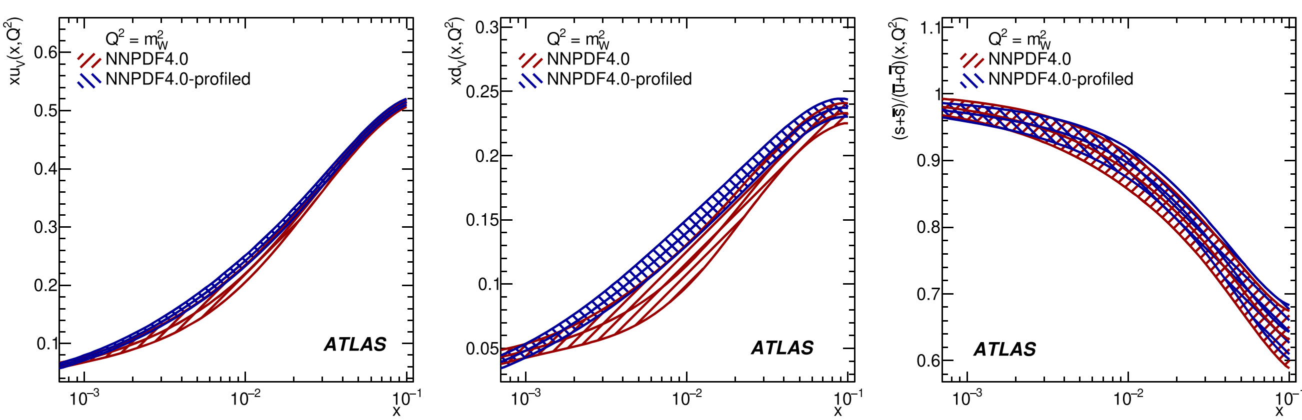

(a) (b) (c)

Fig. 8 Original (red) and profiled (blue) PDF distributions of the NNPDF4.0 PDF set at $Q^2 = m_W^2$ using the measured differential cross-sections in $|\eta|$ at 5.02 TeV and 13 TeV. The distributions of (**a**) xu_v, (**b**) xd_v, and (**c**) $(s+\bar{s})/(\bar{u}+\bar{d})$ PDFs are presented

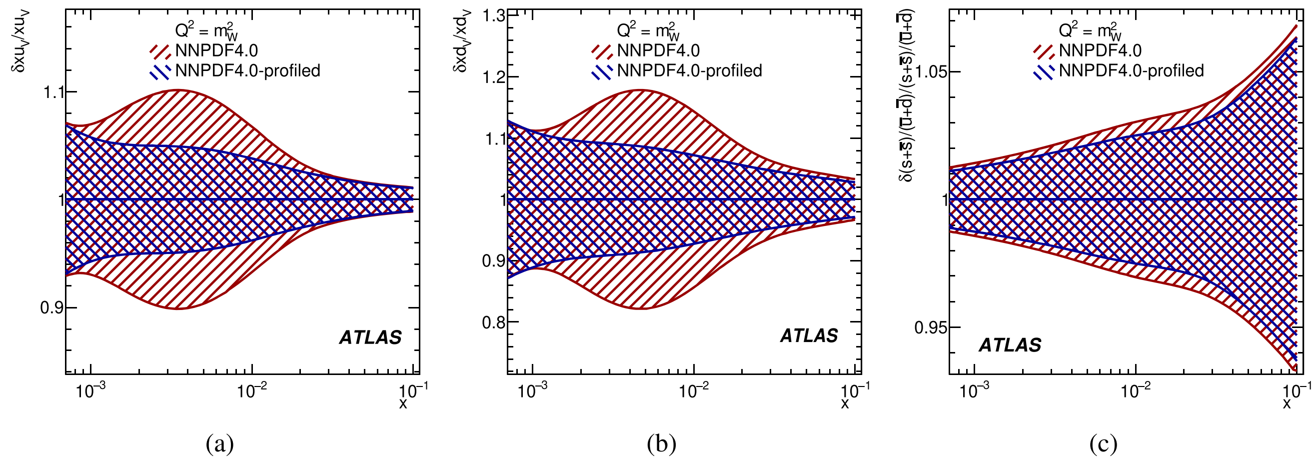

Fig. 9 The relative uncertainties of original (red) and profiled (blue) PDF distributions of the NNPDF4.0 PDF set at $Q^2 = m_W^2$ using the measured differential cross-sections in $|\eta|$ at 5.02 TeV and 13 TeV for (**a**) xu_v, (**b**) xd_v, and (**c**) $(s + \bar{s})/(\bar{u} + \bar{d})$

9 Conclusions

High precision single-differential cross-sections as a function of lepton transverse momentum p_T or lepton pseudorapidity $|\eta|$ in the electron and muon channels of the $W^{\pm}$-boson decays, as well as double-differential cross-sections of these variables, are measured in proton–proton collisions at $\sqrt{s} = 5.02$ TeV and 13 TeV. The single-differential cross-sections in p_T and the double-differential cross-sections are the first such measurements from ATLAS. They are based on data samples collected in dedicated low pile-up runs with the ATLAS detector at the LHC, corresponding to integrated luminosities of 255 pb^{-1} and 338 pb^{-1}, respectively. The cross-sections are measured to an experimental precision better than 0.5% in the bulk phase space, apart from the normalisation uncertainty of the luminosity determination, which is 1% and 0.92% for the 5.02 TeV and 13 TeV datasets, respectively. The combined cross-sections of the electron and muon channels are compared with predictions at NNLO including transverse momentum resummation at NNLL accuracy in QCD using different PDF sets and overall good agreement is observed. The W-boson charge asymmetry as a function of lepton $|\eta|$ is also measured at both centre-of-mass energies and the measurements are in good agreement with the corresponding predictions. In addition, the expected impact of the measured single-differential cross-sections as a function of lepton $|\eta|$ on several recent PDF sets is estimated, showing their constraining power on various quark PDFs.

Acknowledgements We thank CERN for the very successful operation of the LHC and its injectors, as well as the support staff at CERN and at our institutions worldwide without whom ATLAS could not be operated efficiently. The crucial computing support from all WLCG partners is acknowledged gratefully, in particular from CERN, the ATLAS Tier-1 facilities at TRIUMF/SFU (Canada), NDGF (Denmark, Norway, Sweden), CC-IN2P3 (France), KIT/GridKA (Germany), INFN-CNAF (Italy), NL-T1 (Netherlands), PIC (Spain), RAL (UK) and BNL (USA), the Tier-2 facilities worldwide and large non-WLCG resource providers. Major contributors of computing resources are listed in Ref. [98]. We gratefully acknowledge the support of ANPCyT, Argentina; YerPhI, Armenia; ARC, Australia; BMWFW and FWF, Austria; ANAS, Azerbaijan; CNPq and FAPESP, Brazil; NSERC, NRC and CFI, Canada; CERN; ANID, Chile; CAS, MOST and NSFC, China; Minciencias, Colombia; MEYS CR, Czech Republic; DNRF and DNSRC, Denmark; IN2P3-CNRS and CEA-DRF/IRFU, France; SRNSFG, Georgia; BMBF, HGF and MPG, Germany; GSRI, Greece; RGC and Hong Kong SAR, China; ICHEP and Academy of Sciences and Humanities, Israel; INFN, Italy; MEXT and JSPS, Japan; CNRST, Morocco; NWO, Netherlands; RCN, Norway; MNiSW, Poland; FCT, Portugal; MNE/IFA, Romania; MSTDI, Serbia; MSSR, Slovakia; ARIS and MVZI, Slovenia; DSI/NRF, South Africa; MICIU/AEI, Spain; SRC and Wallenberg Foundation, Sweden; SERI, SNSF and Cantons of Bern and Geneva, Switzerland; NSTC, Taipei; TENMAK, Türkiye; STFC/UKRI, United Kingdom; DOE and NSF, United States of America. Individual groups and members have received support from BCKDF, CANARIE, CRC and DRAC, Canada; CERN-CZ, FORTE and PRIMUS, Czech Republic; COST, ERC, ERDF, Horizon 2020, ICSC-NextGenerationEU and Marie Skłodowska-Curie Actions, European Union; Investissements d'Avenir Labex, Investissements d'Avenir Idex and ANR, France; DFG and AvH Foundation, Germany; Herakleitos, Thales and Aristeia programmes co-financed by EU-ESF and the Greek NSRF, Greece; BSF-NSF and MINERVA, Israel; NCN and NAWA, Poland; La Caixa Banking Foundation, CERCA Programme Generalitat de Catalunya and PROMETEO and GenT Programmes Generalitat Valenciana, Spain; Göran Gustafssons Stiftelse, Sweden; The Royal Society and Leverhulme Trust, United Kingdom. In addition, individual members wish to acknowledge support from Armenia: Yerevan Physics Institute (FAPERJ); CERN: European Organization for Nuclear Research (CERN DOCT); Chile: Agencia Nacional de Investigación y Desarrollo (FONDECYT 1230812, FONDECYT 1230987, FONDECYT 1240864); China: Chinese Ministry of Science and Technology (MOST-2023YFA1605700, MOST-2023YFA1609300), National Natural Science Foundation of China (NSFC - 12175119, NSFC 12275265, NSFC-12075060); Czech Republic: Czech Science Foundation (GACR - 24-11373S), Ministry of Education Youth and Sports (ERC-CZ-LL2327, FORTE CZ.02.01.01/00/22_008/0004632), PRIMUS Research Programme (PRIMUS/21/SCI/017); EU: H2020 European Research Council (ERC - 101002463); European Union: European Research Council (ERC - 948254, ERC 101089007, ERC, BARD, 101116429), Horizon 2020 Framework Programme (MUCCA - CHIST-ERA-19-XAI-00), European Union, Future Artificial Intelligence Research

(FAIR-NextGenerationEU PE00000013), Italian Center for High Performance Computing, Big Data and Quantum Computing (ICSC, NextGenerationEU); France: Agence Nationale de la Recherche (ANR-20-CE31-0013, ANR-21-CE31-0013, ANR-21-CE31-0022, ANR-22-EDIR-0002); Germany: Baden-Württemberg Stiftung (BW Stiftung-Postdoc Eliteprogramme), Deutsche Forschungsgemeinschaft (DFG - 469666862, DFG - CR 312/5-2); Italy: Istituto Nazionale di Fisica Nucleare (ICSC, NextGenerationEU), Ministero dell'Università e della Ricerca (NextGenEU PRIN20223N7F8K M4C2.1.1); Japan: Japan Society for the Promotion of Science (JSPS KAKENHI JP22H01227, JSPS KAKENHI JP22H04944, JSPS KAKENHI JP22KK0227, JSPS KAKENHI JP23KK0245); Norway: Research Council of Norway (RCN-314472); Poland: Ministry of Science and Higher Education (IDUB AGH, POB8, D4 no 9722), Polish National Science Centre (NCN 2021/42/E/ST2/00350, NCN OPUS 2023/51/B/ST2/02507, NCN OPUS nr 2022/47/B/ST2/03059, NCN UMO-2019/34/E/ST2/00393, UMO-2020/37/B/ST2/01043, UMO-2022/47/O/ST2/00148, UMO-2023/49/B/ST2/04085, UMO-2023/51/B/ST2/00920); Portugal: Foundation for Science and Technology (FCT); Spain: Generalitat Valenciana (Artemisa, FEDER, IDIFEDER/2018/048), Ministry of Science and Innovation (MCIN & NextGenEU PCI2022-135018-2, MICIN & FEDER PID2021-125273NB, RYC2019-028510-I, RYC2020-030254-I, RYC2021-031273-I, RYC2022-038164-I); Sweden: Carl Trygger Foundation (Carl Trygger Foundation CTS 22:2312), Swedish Research Council (Swedish Research Council 2023-04654, VR 2018-00482, VR 2021-03651, VR 2022-03845, VR 2022-04683, VR 2023-03403), Knut and Alice Wallenberg Foundation (KAW 2018.0458, KAW 2019.0447, KAW 2022.0358); Switzerland: Swiss National Science Foundation (SNSF - PCEFP2_194658); United Kingdom: Leverhulme Trust (Leverhulme Trust RPG-2020-004), Royal Society (NIF-R1-231091); United States of America: U.S. Department of Energy (ECA DE-AC02-76SF00515), Neubauer Family Foundation.

Data Availability Statement This manuscript has no associated data or the data will not be deposited. [Authors' comment: "All ATLAS scientific output is published in journals, and preliminary results are made available in Conference Notes. All are openly available, without restriction on use by external parties beyond copyright law and the standard conditions agreed by CERN. Data associated with journal publications are also made available: tables and data from plots (e.g. cross section values, likelihood profiles, selection efficiencies, cross section limits, ...) are stored in appropriate repositories such as HEPDATA (for this paper, https://www.hepdata.net/record/158064). ATLAS also strives to make additional material related to the paper available that allows a reinterpretation of the data in the context of new theoretical models. For example, an extended encapsulation of the analysis is often provided for measurements in the framework of RIVET (http://rivet.hepforge.org/)." This information is taken from the ATLAS Data Access Policy, which is a public document that can be downloaded from http://opendata.cern.ch/record/413.]

Code Availability Statement This manuscript has no associated code/software. [Author's comment: ATLAS collaboration software is open source, and all code necessary to recreate an analysis is publicly available. The Athena (http://gitlab.cern.ch/atlas/athena) software repository provides all code needed for calibration and uncertainty application, with configuration files that are also publicly available via Docker containers and cvmfs. The specific code and configurations written in support of this analysis are not public; however, these are internally preserved.]

Open Access This article is licensed under a Creative Commons Attribution 4.0 International License, which permits use, sharing, adaptation, distribution and reproduction in any medium or format, as long as you give appropriate credit to the original author(s) and the source, provide a link to the Creative Commons licence, and indicate if changes were made. The images or other third party material in this article are included in the article's Creative Commons licence, unless indicated otherwise in a credit line to the material. If material is not included in the article's Creative Commons licence and your intended use is not permitted by statutory regulation or exceeds the permitted use, you will need to obtain permission directly from the copyright holder. To view a copy of this licence, visit http://creativecommons.org/licenses/by/4.0/.
Funded by SCOAP^3.

References

1. T.-J. Hou et al., New CTEQ global analysis of quantum chromodynamics with high-precision data from the LHC. Phys. Rev. D **103**, 014013 (2021). https://doi.org/10.1103/PhysRevD.103.014013. arXiv:1912.10053 [hep-ph]
2. T. Cridge, L.A. Harland-Lang, A.D. Martin, R.S. Thorne, An investigation of the α_S and heavy quark mass dependence in the MSHT20 global PDF analysis. Eur. Phys. J. C **81**, 744 (2021). https://doi.org/10.1140/epjc/s10052-021-09533-7. arXiv:2106.10289 [hep-ph]
3. S. Bailey, T. Cridge, L.A. Harland-Lang, A.D. Martin, R.S. Thorne, Parton distributions from LHC, HERA, Tevatron and fixed target data: MSHT20 PDFs. Eur. Phys. J. C **81**, 341 (2021). https://doi.org/10.1140/epjc/s10052-021-09057-0. arXiv:2012.04684 [hep-ph]
4. T. Cridge, L.A. Harland-Lang, A.D. Martin, R.S. Thorne, QED parton distribution functions in the MSHT20 fit. Eur. Phys. J. C **82**, 90 (2022). https://doi.org/10.1140/epjc/s10052-022-10028-2. arXiv:2111.05357 [hep-ph]
5. NNPDF Collaboration, R.D. Ball et al., Parton distributions from high-precision collider data. Eur. Phys. J. C **77**, 663 (2017). https://doi.org/10.1140/epjc/s10052-017-5199-5. arXiv:1706.00428 [hep-ph]
6. NNPDF Collaboration, R.D. Ball et al., The path to proton structure at 1% accuracy. Eur. Phys. J. C **82**, 428 (2022). https://doi.org/10.1140/epjc/s10052-022-10328-7. arXiv:2109.02653 [hep-ph]
7. ATLAS Collaboration, Determination of the parton distribution functions of the proton using diverse ATLAS data from pp collisions at $\sqrt{s} = 7, 8$ and 13TeV. Eur. Phys. J. C **82**, 438 (2022). https://doi.org/10.1140/epjc/s10052-022-10217-z. arXiv:2112.11266 [hep-ex]
8. C. Duhr, F. Dulat, B. Mistlberger, Charged current Drell–Yan production at N^{3}LO. JHEP **11**, 143 (2020). https://doi.org/10.1007/JHEP11(2020)143. arXiv:2007.13313 [hep-ph]
9. X. Chen et al., Transverse mass distribution and charge asymmetry in W boson production to third order in QCD. Phys. Lett. B **840**, 137876 (2023). https://doi.org/10.1016/j.physletb.2023.137876. arXiv:2205.11426 [hep-ph]
10. J. Campbell, T. Neumann, Third order QCD predictions for fiducial W-boson production. JHEP **11**, 127 (2023). https://doi.org/10.1007/JHEP11(2023)127. arXiv:2308.15382 [hep-ph]
11. W. Bizoń et al., The transverse momentum spectrum of weak gauge bosons at N^{3}LL + NNLO. Eur. Phys. J. C **79**, 868 (2019). https://doi.org/10.1140/epjc/s10052-019-7324-0. arXiv:1905.05171 [hep-ph]
12. T. Neumann, J. Campbell, Fiducial Drell–Yan production at the LHC improved by transverse-momentum resummation at N^{4}LL$_\mathrm{p}$+N^{3}LO. Phys. Rev. D **107**, L011506 (2023). https://doi.org/10.1103/PhysRevD.107.L011506. arXiv:2207.07056 [hep-ph]
13. S. Camarda, L. Cieri, G. Ferrera, Drell-Yan lepton-pair production: q_T resummation at N^{4}LL+N^{4}LO accuracy. Phys. Lett. B **845**, 138125 (2023). https://doi.org/10.1016/j.physletb.2023.138125. arXiv:2303.12781 [hep-ph]

14. ATLAS Collaboration, Precise measurements of W- and Z-boson transverse momentum spectra with the ATLAS detector using pp collisions at $\sqrt{s} = 5.02$TeV and 13TeV. Eur. Phys. J. C **84**, 1126 (2024). https://doi.org/10.1140/epjc/s10052-024-13414-0. arXiv:2404.06204 [hep-ex]
15. CMS Collaboration, Measurement of the inclusive cross sections for W and Z boson production in proton–proton collisions at $\sqrt{s} =$ 5.02 and 13TeV. JHEP **04**, 162 (2025). https://doi.org/10.1007/JHEP04(2025)162
16. ATLAS Collaboration, Measurements of W and Z boson production in pp collisions at $\sqrt{s} = 5.02$TeV with the ATLAS detector. Eur. Phys. J. C **79**, 128 (2019). https://doi.org/10.1140/epjc/s10052-019-6622-x. arXiv:1810.08424 [hep-ex]. Erratum: Eur. Phys. J. C **79**, 374 (2019). https://doi.org/10.1140/epjc/s10052-019-6870-9
17. ATLAS Collaboration, Precision measurement and interpretation of inclusive W^+, W^- and Z/γ^* production cross sections with the ATLAS detector. Eur. Phys. J. C **77**, 367 (2017). https://doi.org/10.1140/epjc/s10052-017-4911-9. arXiv:1612.03016 [hep-ex]
18. ATLAS Collaboration, Measurement of the cross-section and charge asymmetry of W bosons produced in proton–proton collisions at $\sqrt{s} = 8$TeV with the ATLAS detector, Eur. Phys. J. C **79**, 760 (2019). https://doi.org/10.1140/epjc/s10052-019-7199-0. arXiv:1904.05631 [hep-ex]
19. C. Collaboration, Measurement of the differential cross section and charge asymmetry for inclusive $pp \to W^{\pm} + X$ production at $\sqrt{s} = 8$TeV. Eur. Phys. J. C **76**, 469 (2016). https://doi.org/10.1140/epjc/s10052-016-4293-4. arXiv:1603.01803 [hep-ex]
20. LHCb Collaboration, Measurement of the forward W boson cross-section in pp collisions at $\sqrt{s} = 7$ TeV. JHEP **12**, 079 (2014). https://doi.org/10.1007/JHEP12(2014)079. arXiv:1408.4354 [hep-ex]
21. LHCb Collaboration, Measurement of forward W and Z boson production in pp collisions at $\sqrt{s} = 8$ TeV. JHEP **01**, 155 (2016). https://doi.org/10.1007/JHEP01(2016)155. arXiv:1511.08039 [hep-ex]
22. LHCb Collaboration, Measurement of forward $W \to e\nu$ production in pp collisions at $\sqrt{s} = 8$ TeV. JHEP **10**, 030 (2016). https://doi.org/10.1007/JHEP10(2016)030. arXiv:1608.01484 [hep-ex]
23. C. Collaboration, Measurements of the W boson rapidity, helicity, double-differential cross sections, and charge asymmetry in pp collisions at $\sqrt{s} = 13$TeV. Phys. Rev. D **102**, 092012 (2020). https://doi.org/10.1103/PhysRevD.102.092012. arXiv:2008.04174 [hep-ex]
24. CMS Collaboration, Measurement of the electron charge asymmetry in inclusive W production in pp collisions at $\sqrt{s} = 7$TeV. Phys. Rev. Lett. **109**, 111806 (2012). https://doi.org/10.1103/PhysRevLett.109.111806. arXiv:1206.2598 [hep-ex]
25. C. Collaboration, Measurement of the muon charge asymmetry in inclusive $pp \to W+X$ production at $\sqrt{s} = 7$TeV and an improved determination of light parton distribution functions. Phys. Rev. D **90**, 032004 (2014). https://doi.org/10.1103/PhysRevD.90.032004. arXiv:1312.6283 [hep-ex]
26. CDF Collaboration, Direct Measurement of the W Production Charge Asymmetry in $p\bar{p}$ Collisions at $\sqrt{s} = 1.96$ TeV. Phys. Rev. Lett. **102**, 181801 (2009). https://doi.org/10.1103/PhysRevLett.102.181801. arXiv:0901.2169 [hep-ex]
27. D0 Collaboration, Measurement of the muon charge asymmetry in $p\bar{p} \to$ W+X $\to \mu\nu$ + X events at $\sqrt{s}$=1.96 TeV. Phys. Rev. D **88**, 091102 (2013). https://doi.org/10.1103/PhysRevD.88.091102. arXiv:1309.2591 [hep-ex]
28. D0 Collaboration, Measurement of the electron charge asymmetry in $p\bar{p} \to W + X \to e\nu + X$ decays in $p\bar{p}$ collisions at $\sqrt{s} =$ 1.96 TeV. Phys. Rev. D **91**, 032007 (2015). https://doi.org/10.1103/PhysRevD.91.032007. arXiv:1412.2862 [hep-ex]. [Erratum: Phys. Rev. D **91**, 079901 (2015)]
29. CDF Collaboration, Measurement of the charge asymmetry of electrons from the decays of W bosons produced in $p\bar{p}$ collisions at $\sqrt{s} = 1.96$ TeV. Phys. Rev. D **104**, 092002 (2021). https://doi.org/10.1103/PhysRevD.104.092002. arXiv:2107.04678 [hep-ex]
30. H. Paukkunen, P. Zurita, PDF reweighting in the Hessian matrix approach. JHEP **12**, 100 (2014). https://doi.org/10.1007/JHEP12(2014)100. arXiv:1402.6623 [hep-ph]
31. HERAFitter developers' team, S. Camarda et al., QCD analysis of W- and Z-boson production at Tevatron. Eur. Phys. J. C **75**, 458 (2015). https://doi.org/10.1140/epjc/s10052-015-3655-7. arXiv:1503.05221 [hep-ph]
32. ATLAS Collaboration, The ATLAS Experiment at the CERN Large Hadron Collider. JINST **3**, S08003 (2008). https://doi.org/10.1088/1748-0221/3/08/S08003
33. ATLAS Collaboration, ATLAS Insertable B-Layer: Technical Design Report, ATLAS-TDR-19; CERN-LHCC-2010-013 (2010). https://cds.cern.ch/record/1291633. Addendum: ATLAS-TDR-19-ADD-1; CERN-LHCC-2012-009 (2012). https://cds.cern.ch/record/1451888
34. B. Abbott et al., Production and integration of the ATLAS Insertable B-Layer. JINST **13**, T05008 (2018). https://doi.org/10.1088/1748-0221/13/05/T05008. arXiv:1803.00844 [physics.ins-det]
35. G. Avoni et al., The new LUCID-2 detector for luminosity measurement and monitoring in ATLAS. JINST **13**, P07017 (2018). https://doi.org/10.1088/1748-0221/13/07/P07017
36. ATLAS Collaboration, Performance of the ATLAS trigger system in 2015. Eur. Phys. J. C **77**, 317 (2017). https://doi.org/10.1140/epjc/s10052-017-4852-3. arXiv:1611.09661 [hep-ex]
37. ATLAS Collaboration, Software and computing for Run 3 of the ATLAS experiment at the LHC (2024). arXiv:2404.06335 [hep-ex]
38. ATLAS Collaboration, Luminosity determination in pp collisions at $\sqrt{s} = 13$TeV using the ATLAS detector at the LHC. Eur. Phys. J. C **83**, 982 (2023). https://doi.org/10.1140/epjc/s10052-023-11747-w. arXiv:2212.09379 [hep-ex]
39. ATLAS Collaboration, Performance of electron and photon triggers in ATLAS during LHC Run 2. Eur. Phys. J. C **80**, 47 (2020). https://doi.org/10.1140/epjc/s10052-019-7500-2. arXiv:1909.00761 [hep-ex]
40. ATLAS Collaboration, Performance of the ATLAS muon triggers in Run 2. JINST **15**, P09015 (2020). https://doi.org/10.1088/1748-0221/15/09/p09015. arXiv:2004.13447 [physics.ins-det]
41. ATLAS Collaboration, The ATLAS inner detector trigger performance in pp collisions at 13TeV during LHC Run 2. Eur. Phys. J. C **82**, 206 (2022). https://doi.org/10.1140/epjc/s10052-021-09920-0. arXiv:2107.02485 [hep-ex]
42. ATLAS Collaboration, The ATLAS simulation infrastructure. Eur. Phys. J. C **70**, 823 (2010). https://doi.org/10.1140/epjc/s10052-010-1429-9. arXiv:1005.4568 [physics.ins-det]
43. S. Agostinelli et al., Geant4—a simulation toolkit. Nucl. Instrum. Methods A **506**, 250 (2003). https://doi.org/10.1016/S0168-9002(03)01368-8
44. T. Sjöstrand, S. Mrenna, P. Skands, A brief introduction to PYTHIA 8.1. Comput. Phys. Commun. **178**, 852 (2008). https://doi.org/10.1016/j.cpc.2008.01.036. arXiv:0710.3820 [hep-ph]
45. NNPDF Collaboration, R.D. Ball et al., Parton distributions with LHC data. Nucl. Phys. B **867**, 244 (2013). https://doi.org/10.1016/j.nuclphysb.2012.10.003. arXiv:1207.1303 [hep-ph]
46. ATLAS Collaboration, The Pythia 8 A3 tune description of ATLAS minimum bias and inelastic measurements incorporating the Donnachie–Landshoff diffractive model. ATL-PHYS-PUB-2016-017 (2016). https://cds.cern.ch/record/2206965
47. P. Nason, A new method for combining NLO QCD with shower Monte Carlo algorithms. JHEP **11**, 040 (2004). https://doi.org/10.1088/1126-6708/2004/11/040. arXiv:hep-ph/0409146

48. S. Frixione, P. Nason, C. Oleari, Matching NLO QCD computations with parton shower simulations: the POWHEG method. JHEP **11**, 070 (2007). https://doi.org/10.1088/1126-6708/2007/11/070. arXiv:0709.2092 [hep-ph]
49. S. Alioli, P. Nason, C. Oleari, E. Re, NLO vector-boson production matched with shower in POWHEG. JHEP **07**, 060 (2008). https://doi.org/10.1088/1126-6708/2008/07/060. arXiv:0805.4802 [hep-ph]
50. S. Alioli, P. Nason, C. Oleari, E. Re, A general framework for implementing NLO calculations in shower Monte Carlo programs: the POWHEG BOX. JHEP **06**, 043 (2010). https://doi.org/10.1007/JHEP06(2010)043. arXiv:1002.2581 [hep-ph]
51. H.-L. Lai et al., New parton distributions for collider physics. Phys. Rev. D **82**, 074024 (2010). https://doi.org/10.1103/PhysRevD.82.074024. arXiv:1007.2241 [hep-ph]
52. T. Sjöstrand et al., An introduction to PYTHIA 8.2. Comput. Phys. Commun. **191**, 159 (2015). https://doi.org/10.1016/j.cpc.2015.01.024. arXiv:1410.3012 [hep-ph]
53. ATLAS Collaboration, Measurement of the Z/γ^* boson transverse momentum distribution in pp collisions at $\sqrt{s}$ = 7TeV with the ATLAS detector. JHEP **09**, 145 (2014). https://doi.org/10.1007/JHEP09(2014)145. arXiv:1406.3660 [hep-ex]
54. P. Golonka, Z. Was, PHOTOS Monte Carlo: a precision tool for QED corrections in Z and W decays. Eur. Phys. J. C **45**, 97 (2006). https://doi.org/10.1140/epjc/s2005-02396-4. arXiv:hep-ph/0506026
55. E. Bothmann et al., Event generation with Sherpa 2.2. SciPost Phys. **7**, 034 (2019). https://doi.org/10.21468/SciPostPhys.7.3.034. arXiv:1905.09127 [hep-ph]
56. NNPDF Collaboration, R.D. Ball et al., Parton distributions for the LHC run II. JHEP **04**, 040 (2015). https://doi.org/10.1007/JHEP04(2015)040. arXiv:1410.8849 [hep-ph]
57. T. Gleisberg, S. Höche, Comix, a new matrix element generator. JHEP **12**, 039 (2008). https://doi.org/10.1088/1126-6708/2008/12/039. arXiv:0808.3674 [hep-ph]
58. F. Buccioni et al., OpenLoops 2. Eur. Phys. J. C **79**, 866 (2019). https://doi.org/10.1140/epjc/s10052-019-7306-2. arXiv:1907.13071 [hep-ph]
59. F. Cascioli, P. Maierhöfer, S. Pozzorini, Scattering amplitudes with open loops. Phys. Rev. Lett. **108**, 111601 (2012). https://doi.org/10.1103/PhysRevLett.108.111601. arXiv:1111.5206 [hep-ph]
60. A. Denner, S. Dittmaier, L. Hofer, Collier: a fortran-based complex one-loop library in extended regularizations. Comput. Phys. Commun. **212**, 220 (2017). https://doi.org/10.1016/j.cpc.2016.10.013. arXiv:1604.06792 [hep-ph]
61. S. Schumann, F. Krauss, A parton shower algorithm based on Catani–Seymour dipole factorisation. JHEP **03**, 038 (2008). https://doi.org/10.1088/1126-6708/2008/03/038. arXiv:0709.1027 [hep-ph]
62. S. Höche, F. Krauss, M. Schönherr, F. Siegert, A critical appraisal of NLO+PS matching methods. JHEP **09**, 049 (2012). https://doi.org/10.1007/JHEP09(2012)049. arXiv:1111.1220 [hep-ph]
63. S. Höche, F. Krauss, M. Schönherr, F. Siegert, QCD matrix elements + parton showers. The NLO case. JHEP **04**, 027 (2013). https://doi.org/10.1007/JHEP04(2013)027. arXiv:1207.5030 [hep-ph]
64. S. Catani, F. Krauss, B.R. Webber, R. Kuhn, QCD matrix elements + parton showers. JHEP **11**, 063 (2001). https://doi.org/10.1088/1126-6708/2001/11/063. arXiv:hep-ph/0109231
65. S. Höche, F. Krauss, S. Schumann, F. Siegert, QCD matrix elements and truncated showers. JHEP **05**, 053 (2009). https://doi.org/10.1088/1126-6708/2009/05/053. arXiv:0903.1219 [hep-ph]
66. S. Camarda et al., DYTurbo: fast predictions for Drell–Yan processes. Eur. Phys. J. C **80**, 251 (2020). https://doi.org/10.1140/epjc/s10052-020-7757-5. arXiv:1910.07049 [hep-ph]. [Erratum: Eur. Phys. J. C **80**, 440 (2020)]
67. S. Camarda, L. Cieri, G. Ferrera, Drell–Yan lepton-pair production: q_T resummation at N^{3}LL accuracy and fiducial cross sections at N^{3}LO. Phys. Rev. D **104**, L111503 (2021). https://doi.org/10.1103/PhysRevD.104.L111503. arXiv:2103.04974 [hep-ph]
68. S. Camarda, L. Cieri, G. Ferrera, Fiducial perturbative power corrections within the $\mathbf{q}_T$ subtraction formalism. Eur. Phys. J. C **82**, 575 (2022). https://doi.org/10.1140/epjc/s10052-022-10510-x. arXiv:2111.14509 [hep-ph]
69. S. Catani, M. Grazzini, Next-to-next-to-leading-order subtraction formalism in hadron collisions and its application to Higgs-boson production at the large hadron collider. Phys. Rev. Lett. **98**, 222002 (2007). https://doi.org/10.1103/PhysRevLett.98.222002. arXiv:hep-ph/0703012 [hep-ph]
70. S. Catani, L. Cieri, G. Ferrera, D. de Florian, M. Grazzini, Vector boson production at hadron colliders: a fully exclusive QCD calculation at next-to-next-to-leading order. Phys. Rev. Lett. **103**, 082001 (2009). https://doi.org/10.1103/PhysRevLett.103.082001. arXiv:0903.2120 [hep-ph]
71. L.A. Harland-Lang, A.D. Martin, P. Motylinski, R.S. Thorne, Parton distributions in the LHC era: MMHT 2014 PDFs. Eur. Phys. J. C **75**, 204 (2015). https://doi.org/10.1140/epjc/s10052-015-3397-6. arXiv:1412.3989 [hep-ph]
72. ATLAS Collaboration, Multi-Boson Simulation for 13 TeV ATLAS Analyses, ATL-PHYS-PUB-2017-005 (2017). https://cds.cern.ch/record/2261933
73. ATLAS Collaboration, Study of top-quark pair modelling and uncertainties using ATLAS measurements at $\sqrt{s}$ = 13TeV, ATL-PHYS-PUB-2020-023 (2020). https://cds.cern.ch/record/2730443
74. M. Beneke, P. Falgari, S. Klein, C. Schwinn, Hadronic top-quark pair production with NNLL threshold resummation. Nucl. Phys. B **855**, 695 (2012). https://doi.org/10.1016/j.nuclphysb.2011.10.021. arXiv:1109.1536 [hep-ph]
75. M. Czakon, P. Fiedler, A. Mitov, Total top-quark pair-production cross section at hadron colliders through $\mathcal{O}(\alpha_S^4)$. Phys. Rev. Lett. **110**, 252004 (2013). https://doi.org/10.1103/PhysRevLett.110.252004. arXiv:1303.6254 [hep-ph]
76. M. Czakon, A. Mitov, Top++: a program for the calculation of the top-pair cross-section at hadron colliders. Comput. Phys. Commun. **185**, 2930 (2014). https://doi.org/10.1016/j.cpc.2014.06.021. arXiv:1112.5675 [hep-ph]
77. ATLAS Collaboration, Vertex Reconstruction Performance of the ATLAS Detector at $\sqrt{s}$ = 13TeV, ATL-PHYS-PUB-2015-026 (2015). https://cds.cern.ch/record/2037717
78. ATLAS Collaboration, Electron and photon performance measurements with the ATLAS detector using the 2015–2017 LHC proton–proton collision data. JINST **14**, P12006 (2019). https://doi.org/10.1088/1748-0221/14/12/P12006. arXiv:1908.00005 [hep-ex]
79. ATLAS Collaboration, Muon reconstruction and identification efficiency in ATLAS using the full Run 2 pp collision data set at $\sqrt{s}$ = 13TeV. Eur. Phys. J. C **81**, 578 (2021). https://doi.org/10.1140/epjc/s10052-021-09233-2. arXiv:2012.00578 [hep-ex]
80. ATLAS Collaboration, Jet reconstruction and performance using particle flow with the ATLAS Detector. Eur. Phys. J. C **77**, 466 (2017). https://doi.org/10.1140/epjc/s10052-017-5031-2. arXiv:1703.10485 [hep-ex]
81. ATLAS Collaboration, Jet energy scale and resolution measured in proton–proton collisions at $\sqrt{s}$ = 13TeV with the ATLAS detector. Eur. Phys. J. C **81**, 689 (2021). https://doi.org/10.1140/epjc/s10052-021-09402-3. arXiv:2007.02645 [hep-ex]
82. G. D'Agostini, A multidimensional unfolding method based on Bayes' theorem. Nucl. Instrum. Methods A **362**, 487 (1995). https://doi.org/10.1016/0168-9002(95)00274-X
83. G. D'Agostini, Improved iterative Bayesian unfolding (2010). arXiv:1010.0632 [physics.data-an]

84. H. Dembinski, M. Schmelling, R. Waldi, Application of the iterated weighted least-squares fit to counting experiments. Nucl. Instrum. Methods A **940**, 135 (2019). https://doi.org/10.1016/j.nima.2019.05.086. arXiv:1807.07911 [physics.data-an]
85. L. Lyons, D. Gibaut, P. Clifford, How to combine correlated estimates of a single physical quantity. Nucl. Instrum. Methods A **270**, 110 (1988). https://doi.org/10.1016/0168-9002(88)90018-6
86. A. Valassi, Combining correlated measurements of several different physical quantities. Nucl. Instrum. Methods A **500**, 391 (2003). https://doi.org/10.1016/S0168-9002(03)00329-2
87. ATLAS Collaboration, Studies of the muon momentum calibration and performance of the ATLAS detector with pp collisions at $\sqrt{s}$ = 13TeV. Eur. Phys. J. C **83**, 686 (2023). https://doi.org/10.1140/epjc/s10052-023-11584-x. arXiv:2212.07338 [hep-ex]
88. ATLAS Collaboration, Measurement of inclusive jet and dijet cross-sections in proton–proton collisions at $\sqrt{s}$ = 13TeV with the ATLAS detector. JHEP **05**, 195 (2018). https://doi.org/10.1007/JHEP05(2018)195. arXiv:1711.02692 [hep-ex]
89. ATLAS Collaboration, Evaluating statistical uncertainties and correlations using the bootstrap method, ATL-PHYS-PUB-2021-011 (2021). https://cds.cern.ch/record/2759945
90. J. Alwall et al., The automated computation of tree-level and next-to-leading order differential cross sections, and their matching to parton shower simulations. JHEP **07**, 079 (2014). https://doi.org/10.1007/JHEP07(2014)079. arXiv:1405.0301 [hep-ph]
91. T. Carli et al., A posteriori inclusion of parton density functions in NLO QCD final-state calculations at hadron colliders: the APPLGRID Project. Eur. Phys. J. C **66**, 503 (2010). https://doi.org/10.1140/epjc/s10052-010-1255-0. arXiv:0911.2985 [hep-ph]
92. V. Bertone, R. Frederix, S. Frixione, J. Rojo, M. Sutton, aMCfast: automation of fast NLO computations for PDF fits. JHEP **08**, 166 (2014). https://doi.org/10.1007/JHEP08(2014)166. arXiv:1406.7693 [hep-ph]
93. H1 Collaboration, A precision measurement of the inclusive ep scattering cross section at HERA. Eur. Phys. J. C **64**, 561 (2009). https://doi.org/10.1140/epjc/s10052-009-1169-x. arXiv:0904.3513 [hep-ex]
94. H1 and ZEUS collaborations, Combination and QCD analysis of charm and beauty production cross-section measurements in deep inelastic ep scattering at HERA. Eur. Phys. J. C **78**, 473 (2018). https://doi.org/10.1140/epjc/s10052-018-5848-3. arXiv:1804.01019 [hep-ex]
95. S. Alekhin et al., HERAFitter, Open Source QCD Fit Project (2015). arXiv:1410.4412 [hep-ph]
96. ATLAS Collaboration, Measurement of the production of a W boson in association with a charm quark in pp collisions at $\sqrt{s}$ = 7 TeV with the ATLAS detector. JHEP **05**, 068 (2014). https://doi.org/10.1007/JHEP05(2014)068. arXiv:1402.6263 [hep-ex]
97. ATLAS Collaboration, Determination of the parton distribution functions of the proton from ATLAS measurements of differential $W^{\pm}$ and Z boson production in association with jets. JHEP **07**, 223 (2021). https://doi.org/10.1007/JHEP07(2021)223. arXiv:2101.05095 [hep-ex]
98. ATLAS Collaboration, ATLAS Computing Acknowledgements, ATL-SOFT-PUB-2025-001 (2025). https://cds.cern.ch/record/2922210

ATLAS Collaboration*

G. Aad[104], E. Aakvaag[17], B. Abbott[123], S. Abdelhameed[119a], K. Abeling[55], N. J. Abicht[49], S. H. Abidi[30], M. Aboelela[45], A. Aboulhorma[36e], H. Abramowicz[157], Y. Abulaiti[120], B. S. Acharya[69a,69b,p], A. Ackermann[63a], C. Adam Bourdarios[4], L. Adamczyk[86a], S. V. Addepalli[149], M. J. Addison[103], J. Adelman[118], A. Adiguzel[22c], T. Adye[137], A. A. Affolder[139], Y. Afik[40], M. N. Agaras[13], A. Aggarwal[102], C. Agheorghiesei[28c], F. Ahmadov[39,af], S. Ahuja[97], X. Ai[143b], G. Aielli[76a,76b], A. Aikot[169], M. Ait Tamlihat[36e], B. Aitbenchikh[36a], M. Akbiyik[102], T. P. A. Åkesson[100], A. V. Akimov[151], D. Akiyama[174], N. N. Akolkar[25], S. Aktas[22a], G. L. Alberghi[24b], J. Albert[171], P. Albicocco[53], G. L. Albouy[60], S. Alderweireldt[52], Z. L. Alegria[124], M. Aleksa[37], I. N. Aleksandrov[39], C. Alexa[28b], T. Alexopoulos[10], F. Alfonsi[24b], M. Algren[56], M. Alhroob[173], B. Ali[135], H. M. J. Ali[93,y], S. Ali[32], S. W. Alibocus[94], M. Aliev[34c], G. Alimonti[71a], W. Alkakhi[55], C. Allaire[66], B. M. M. Allbrooke[152], J. S. Allen[103], J. F. Allen[52], P. P. Allport[21], A. Aloisio[72a,72b], F. Alonso[92], C. Alpigiani[142], Z. M. K. Alsolami[93], A. Alvarez Fernandez[102], M. Alves Cardoso[56], M. G. Alviggi[72a,72b], M. Aly[103], Y. Amaral Coutinho[83b], A. Ambler[106], C. Amelung[37], M. Amerl[103], C. G. Ames[111], D. Amidei[108], B. Amini[54], K. Amirie[161], A. Amirkhanov[39], S. P. Amor Dos Santos[133a], K. R. Amos[169], D. Amperiadou[158], S. An[84], V. Ananiev[128], C. Anastopoulos[145], T. Andeen[11], J. K. Anders[94], A. C. Anderson[59], A. Andreazza[71a,71b], S. Angelidakis[9], A. Angerami[42], A. V. Anisenkov[39], A. Annovi[74a], C. Antel[56], E. Antipov[151], M. Antonelli[53], F. Anulli[75a], M. Aoki[84], T. Aoki[159], M. A. Aparo[152], L. Aperio Bella[48], C. Appelt[157], A. Apyan[27], S. J. Arbiol Val[87], C. Arcangeletti[53], A. T. H. Arce[51], J-F. Arguin[110], S. Argyropoulos[158], J.-H. Arling[48], O. Arnaez[4], H. Arnold[151], G. Artoni[75a,75b], H. Asada[113], K. Asai[121], S. Asai[159], N. A. Asbah[37], R. A. Ashby Pickering[173], A. M. Aslam[97], K. Assamagan[30], R. Astalos[29a], K. S. V. Astrand[100], S. Atashi[165], R. J. Atkin[34a], H. Atmani[36f], P. A. Atmasiddha[131], K. Augsten[135], A. D. Auriol[41], V. A. Austrup[103], G. Avolio[37], K. Axiotis[56], G. Azuelos[110,ak], D. Babal[29b], H. Bachacou[138], K. Bachas[158,t], A. Bachiu[35], E. Bachmann[50], M. J. Backes[63a], A. Badea[40], T. M. Baer[108], P. Bagnaia[75a,75b], M. Bahmani[19], D. Bahner[54], K. Bai[126], J. T. Baines[137], L. Baines[96], O. K. Baker[178], E. Bakos[16], D. Bakshi Gupta[8], L. E. Balabram Filho[83b], V. Balakrishnan[123], R. Balasubramanian[4], E. M. Baldin[38], P. Balek[86a],

E. Ballabene[24a,24b], F. Balli[138], L. M. Baltes[63a], W. K. Balunas[33], J. Balz[102], I. Bamwidhi[119b], E. Banas[87], M. Bandieramonte[132], A. Bandyopadhyay[25], S. Bansal[25], L. Barak[157], M. Barakat[48], E. L. Barberio[107], D. Barberis[18b], M. Barbero[104], M. Z. Barel[117], T. Barillari[112], M-S. Barisits[37], T. Barklow[149], P. Baron[125], D. A. Baron Moreno[103], A. Baroncelli[62], A. J. Barr[129], J. D. Barr[98], F. Barreiro[101], J. Barreiro Guimarães da Costa[14], M. G. Barros Teixeira[133a], S. Barsov[38], F. Bartels[63a], R. Bartoldus[149], A. E. Barton[93], P. Bartos[29a], A. Basan[102], M. Baselga[49], S. Bashiri[87], A. Bassalat[66,b], M. J. Basso[162a], S. Bataju[45], R. Bate[170], R. L. Bates[59], S. Batlamous[101], M. Battaglia[139], D. Battulga[19], M. Bauce[75a,75b], M. Bauer[79], P. Bauer[25], L. T. Bayer[48], L. T. Bazzano Hurrell[31], J. B. Beacham[112], T. Beau[130], J. Y. Beaucamp[92], P. H. Beauchemin[164], P. Bechtle[25], H. P. Beck[20,s], K. Becker[173], A. J. Beddall[82], V. A. Bednyakov[39], C. P. Bee[151], L. J. Beemster[16], M. Begalli[83d], M. Begel[30], J. K. Behr[48], J. F. Beirer[37], F. Beisiegel[25], M. Belfkir[119b], G. Bella[157], L. Bellagamba[24b], A. Bellerive[35], P. Bellos[21], K. Beloborodov[38], D. Benchekroun[36a], F. Bendebba[36a], Y. Benhammou[157], K. C. Benkendorfer[61], L. Beresford[48], M. Beretta[53], E. Bergeaas Kuutmann[167], N. Berger[4], B. Bergmann[135], J. Beringer[18a], G. Bernardi[5], C. Bernius[149], F. U. Bernlochner[25], F. Bernon[37], A. Berrocal Guardia[13], T. Berry[97], P. Berta[136], A. Berthold[50], R. Bertrand[104], S. Bethke[112], A. Betti[75a,75b], A. J. Bevan[96], L. Bezio[56], N. K. Bhalla[54], S. Bharthuar[112], S. Bhatta[151], P. Bhattarai[149], Z. M. Bhatti[120], K. D. Bhide[54], V. S. Bhopatkar[124], R. M. Bianchi[132], G. Bianco[24a,24b], O. Biebel[111], M. Biglietti[77a], C. S. Billingsley[45], Y. Bimgdi[36f], M. Bindi[55], A. Bingham[177], A. Bingul[22b], C. Bini[75a,75b], G. A. Bird[33], M. Birman[175], M. Biros[136], S. Biryukov[152], T. Bisanz[49], E. Bisceglie[24a,24b], J. P. Biswal[137], D. Biswas[147], I. Bloch[48], A. Blue[59], U. Blumenschein[96], J. Blumenthal[102], V. S. Bobrovnikov[39], M. Boehler[54], B. Boehm[172], D. Bogavac[37], A. G. Bogdanchikov[38], L. S. Boggia[130], V. Boisvert[97], P. Bokan[37], T. Bold[86a], M. Bomben[5], M. Bona[96], M. Boonekamp[138], A. G. Borbély[59], I. S. Bordulev[38], G. Borissov[93], D. Bortoletto[129], D. Boscherini[24b], M. Bosman[13], K. Bouaouda[36a], N. Bouchhar[169], L. Boudet[4], J. Boudreau[132], E. V. Bouhova-Thacker[93], D. Boumediene[41], R. Bouquet[57a,57b], A. Boveia[122], J. Boyd[37], D. Boye[30], I. R. Boyko[39], L. Bozianu[56], J. Bracinik[21], N. Brahimi[4], G. Brandt[177], O. Brandt[33], B. Brau[105], J. E. Brau[126], R. Brener[175], L. Brenner[117], R. Brenner[167], S. Bressler[175], G. Brianti[78a,78b], D. Britton[59], D. Britzger[112], I. Brock[25], R. Brock[109], G. Brooijmans[42], A. J. Brooks[68], E. M. Brooks[162b], E. Brost[30], L. M. Brown[162a,171], L. E. Bruce[61], T. L. Bruckler[129], P. A. Bruckman de Renstrom[87], B. Brüers[48], A. Bruni[24b], G. Bruni[24b], D. Brunner[47a,47b], M. Bruschi[24b], N. Bruscino[75a,75b], T. Buanes[17], Q. Buat[142], D. Buchin[112], A. G. Buckley[59], O. Bulekov[82], B. A. Bullard[149], S. Burdin[94], C. D. Burgard[49], A. M. Burger[37], B. Burghgrave[8], O. Burlayenko[54], J. Burleson[168], J. T. P. Burr[33], J. C. Burzynski[148], E. L. Busch[42], V. Büscher[102], P. J. Bussey[59], J. M. Butler[26], C. M. Buttar[59], J. M. Butterworth[98], W. Buttinger[137], C. J. Buxo Vazquez[109], A. R. Buzykaev[39], S. Cabrera Urbán[169], L. Cadamuro[66], D. Caforio[58], H. Cai[132], Y. Cai[24a,24b,114c], Y. Cai[114a], V. M. M. Cairo[37], O. Cakir[3a], N. Calace[37], P. Calafiura[18a], G. Calderini[130], P. Calfayan[35], G. Callea[59], L. P. Caloba[83b], D. Calvet[41], S. Calvet[41], R. Camacho Toro[130], S. Camarda[37], D. Camarero Munoz[27], P. Camarri[76a,76b], M. T. Camerlingo[72a,72b], C. Camincher[171], M. Campanelli[98], A. Camplani[43], V. Canale[72a,72b], A. C. Canbay[3a], E. Canonero[97], J. Cantero[169], Y. Cao[168], F. Capocasa[27], M. Capua[44a,44b], A. Carbone[71a,71b], R. Cardarelli[76a], J. C. J. Cardenas[8], M. P. Cardiff[27], G. Carducci[44a,44b], T. Carli[37], G. Carlino[72a], J. I. Carlotto[13], B. T. Carlson[132,u], E. M. Carlson[171], J. Carmignani[94], L. Carminati[71a,71b], A. Carnelli[4], M. Carnesale[37], S. Caron[116], E. Carquin[140f], I. B. Carr[107], S. Carrá[71a], G. Carratta[24a,24b], A. M. Carroll[126], M. P. Casado[13,j], M. Caspar[48], F. L. Castillo[4], L. Castillo Garcia[13], V. Castillo Gimenez[169], N. F. Castro[133a,133e], A. Catinaccio[37], J. R. Catmore[128], T. Cavaliere[4], V. Cavaliere[30], L. J. Caviedes Betancourt[23b], Y. C. Cekmecelioglu[48], E. Celebi[82], S. Cella[37], V. Cepaitis[56], K. Cerny[125], A. S. Cerqueira[83a], A. Cerri[74a,74b,an], L. Cerrito[76a,76b], F. Cerutti[18a], B. Cervato[71a,71b], A. Cervelli[24b], G. Cesarini[53], S. A. Cetin[82], P. M. Chabrillat[130], J. Chan[18a], W. Y. Chan[159], J. D. Chapman[33], E. Chapon[138], B. Chargeishvili[155b], D. G. Charlton[21], C. Chauhan[136], Y. Che[114a], S. Chekanov[6], S. V. Chekulaev[162a], G. A. Chelkov[39,a], B. Chen[157], B. Chen[171], H. Chen[114a], H. Chen[30], J. Chen[144a], J. Chen[148], M. Chen[129], S. Chen[89], S. J. Chen[114a], X. Chen[144a], X. Chen[15,aj], Z. Chen[62], C. L. Cheng[176], H. C. Cheng[64a], S. Cheong[149], A. Cheplakov[39], E. Cheremushkina[48], E. Cherepanova[117], R. Cherkaoui El Moursli[36e], E. Cheu[7], K. Cheung[65], L. Chevalier[138], V. Chiarella[53], G. Chiarelli[74a], N. Chiedde[104], G. Chiodini[70a], A. S. Chisholm[21], A. Chitan[28b], M. Chitishvili[169], M. V. Chizhov[39,v], K. Choi[11], Y. Chou[142], E. Y. S. Chow[116], K. L. Chu[175], M. C. Chu[64a], X. Chu[14,114c], Z. Chubinidze[53], J. Chudoba[134], J. J. Chwastowski[87], D. Cieri[112], K. M. Ciesla[86a], V. Cindro[95],

A. Ciocio[18a], F. Cirotto[72a,72b], Z. H. Citron[175], M. Citterio[71a], D. A. Ciubotaru[28b], A. Clark[56], P. J. Clark[52], N. Clarke Hall[98], C. Clarry[161], S. E. Clawson[48], C. Clement[47a,47b], Y. Coadou[104], M. Cobal[69a,69c], A. Coccaro[57b], R. F. Coelho Barrue[133a], R. Coelho Lopes De Sa[105], S. Coelli[71a], L. S. Colangeli[161], B. Cole[42], P. Collado Soto[101], J. Collot[60], P. Conde Muiño[133a,133g], M. P. Connell[34c], S. H. Connell[34c], E. I. Conroy[129], F. Conventi[72a,al], H. G. Cooke[21], A. M. Cooper-Sarkar[129], L. Corazzina[75a,75b], F. A. Corchia[24a,24b], A. Cordeiro Oudot Choi[142], L. D. Corpe[41], M. Corradi[75a,75b], F. Corriveau[106,ad], A. Cortes-Gonzalez[19], M. J. Costa[169], F. Costanza[4], D. Costanzo[145], B. M. Cote[122], J. Couthures[4], G. Cowan[97], K. Cranmer[176], L. Cremer[49], D. Cremonini[24a,24b], S. Crépé-Renaudin[60], F. Crescioli[130], T. Cresta[73a,73b], M. Cristinziani[147], M. Cristoforetti[78a,78b], V. Croft[117], J. E. Crosby[124], G. Crosetti[44a,44b], A. Cueto[101], H. Cui[98], Z. Cui[7], W. R. Cunningham[59], F. Curcio[169], J. R. Curran[52], P. Czodrowski[37], M. J. Da Cunha Sargedas De Sousa[57a,57b], J. V. Da Fonseca Pinto[83b], C. Da Via[103], W. Dabrowski[86a], T. Dado[37], S. Dahbi[154], T. Dai[108], D. Dal Santo[20], C. Dallapiccola[105], M. Dam[43], G. D'amen[30], V. D'Amico[111], J. Damp[102], J. R. Dandoy[35], D. Dannheim[37], G. D'anniballe[74a,74b], M. Danninger[148], V. Dao[151], G. Darbo[57b], S. J. Das[30], F. Dattola[48], S. D'Auria[71a,71b], A. D'Avanzo[72a,72b], T. Davidek[136], J. Davidson[173], I. Dawson[96], H. A. Day-hall[135], K. De[8], C. De Almeida Rossi[161], R. De Asmundis[72a], N. De Biase[48], S. De Castro[24a,24b], N. De Groot[116], P. de Jong[117], H. De la Torre[118], A. De Maria[114a], A. De Salvo[75a], U. De Sanctis[76a,76b], F. De Santis[70a,70b], A. De Santo[152], J. B. De Vivie De Regie[60], J. Debevc[95], D. V. Dedovich[39], J. Degens[94], A. M. Deiana[45], J. Del Peso[101], L. Delagrange[130], F. Deliot[138], C. M. Delitzsch[49], M. Della Pietra[72a,72b], D. Della Volpe[56], A. Dell'Acqua[37], L. Dell'Asta[71a,71b], M. Delmastro[4], C. C. Delogu[102], P. A. Delsart[60], S. Demers[178], M. Demichev[39], S. P. Denisov[38], H. Denizli[22a,n], L. D'Eramo[41], D. Derendarz[87], F. Derue[130], P. Dervan[94], K. Desch[25], F. A. Di Bello[57a,57b], A. Di Ciaccio[76a,76b], L. Di Ciaccio[4], A. Di Domenico[75a,75b], C. Di Donato[72a,72b], A. Di Girolamo[37], G. Di Gregorio[37], A. Di Luca[78a,78b], B. Di Micco[77a,77b], R. Di Nardo[77a,77b], K. F. Di Petrillo[40], M. Diamantopoulou[35], F. A. Dias[117], M. A. Diaz[140a,140b], A. R. Didenko[39], M. Didenko[169], E. B. Diehl[108], S. Díez Cornell[48], C. Diez Pardos[147], C. Dimitriadi[150], A. Dimitrievska[21], A. Dimri[151], J. Dingfelder[25], T. Dingley[129], I-M. Dinu[28b], S. J. Dittmeier[63b], F. Dittus[37], M. Divisek[136], B. Dixit[94], F. Djama[104], T. Djobava[155b], C. Doglioni[100,103], A. Dohnalova[29a], Z. Dolezal[136], K. Domijan[86a], K. M. Dona[40], M. Donadelli[83d], B. Dong[109], J. Donini[41], A. D'Onofrio[72a,72b], M. D'Onofrio[94], J. Dopke[137], A. Doria[72a], N. Dos Santos Fernandes[133a], P. Dougan[103], M. T. Dova[92], A. T. Doyle[59], M. A. Draguet[129], M. P. Drescher[55], E. Dreyer[175], I. Drivas-koulouris[10], M. Drnevich[120], M. Drozdova[56], D. Du[62], T. A. du Pree[117], F. Dubinin[39], M. Dubovsky[29a], E. Duchovni[175], G. Duckeck[111], P. K. Duckett[98], O. A. Ducu[28b], D. Duda[52], A. Dudarev[37], E. R. Duden[27], M. D'uffizi[103], L. Duflot[66], M. Dührssen[37], I. Duminica[28g], A. E. Dumitriu[28b], M. Dunford[63a], S. Dungs[49], K. Dunne[47a,47b], A. Duperrin[104], H. Duran Yildiz[3a], M. Düren[58], A. Durglishvili[155b], D. Duvnjak[35], B. L. Dwyer[118], G. I. Dyckes[18a], M. Dyndal[86a], B. S. Dziedzic[37], Z. O. Earnshaw[152], G. H. Eberwein[129], B. Eckerova[29a], S. Eggebrecht[55], E. Egidio Purcino De Souza[83e], G. Eigen[17], K. Einsweiler[18a], T. Ekelof[167], P. A. Ekman[100], S. El Farkh[36b], Y. El Ghazali[62], H. El Jarrari[37], A. El Moussaouy[36a], V. Ellajosyula[167], M. Ellert[167], F. Ellinghaus[177], N. Ellis[37], J. Elmsheuser[30], M. Elsawy[119a], M. Elsing[37], D. Emeliyanov[137], Y. Enari[84], I. Ene[18a], S. Epari[110], D. Ernani Martins Neto[87], F. Ernst[37], M. Errenst[177], M. Escalier[66], C. Escobar[169], E. Etzion[157], G. Evans[133a,133b], H. Evans[68], L. S. Evans[97], A. Ezhilov[38], S. Ezzarqtouni[36a], F. Fabbri[24a,24b], L. Fabbri[24a,24b], G. Facini[98], V. Fadeyev[139], R. M. Fakhrutdinov[38], D. Fakoudis[102], S. Falciano[75a], L. F. Falda Ulhoa Coelho[133a], F. Fallavollita[112], G. Falsetti[44a,44b], J. Faltova[136], C. Fan[168], K. Y. Fan[64b], Y. Fan[14], Y. Fang[14,114c], M. Fanti[71a,71b], M. Faraj[69a,69b], Z. Farazpay[99], A. Farbin[8], A. Farilla[77a], T. Farooque[109], J. N. Farr[178], S. M. Farrington[52,137], F. Fassi[36e], D. Fassouliotis[9], L. Fayard[66], P. Federic[136], P. Federicova[134], O. L. Fedin[38,a], M. Feickert[176], L. Feligioni[104], D. E. Fellers[18a], C. Feng[143a], Z. Feng[117], M. J. Fenton[165], L. Ferencz[48], B. Fernandez Barbadillo[93], P. Fernandez Martinez[67], M. J. V. Fernoux[104], J. Ferrando[93], A. Ferrari[167], P. Ferrari[116,117], R. Ferrari[73a], D. Ferrere[56], C. Ferretti[108], M. P. Fewell[1], D. Fiacco[75a,75b], F. Fiedler[102], P. Fiedler[135], S. Filimonov[39], A. Filipčič[95], E. K. Filmer[162a], F. Filthaut[116], M. C. N. Fiolhais[133a,133c,c], L. Fiorini[169], W. C. Fisher[109], T. Fitschen[103], P. M. Fitzhugh[138], I. Fleck[147], P. Fleischmann[108], T. Flick[177], M. Flores[34d,ah], L. R. Flores Castillo[64a], L. Flores Sanz De Acedo[37], F. M. Follega[78a,78b], N. Fomin[33], J. H. Foo[161], A. Formica[138], A. C. Forti[103], E. Fortin[37], A. W. Fortman[18a], L. Foster[18a], L. Fountas[9,k], D. Fournier[66], H. Fox[93], P. Francavilla[74a,74b], S. Francescato[61], S. Franchellucci[56], M. Franchini[24a,24b], S. Franchino[63a], D. Francis[37], L. Franco[116], V. Franco Lima[37], L. Franconi[48], M. Franklin[61], G. Frattari[27], Y. Y. Frid[157], J. Friend[59], N. Fritzsche[37],

A. Froch[56], D. Froidevaux[37], J. A. Frost[129], Y. Fu[109], S. Fuenzalida Garrido[140f], M. Fujimoto[104], K. Y. Fung[64a], E. Furtado De Simas Filho[83e], M. Furukawa[159], J. Fuster[169], A. Gaa[55], A. Gabrielli[24a,24b], A. Gabrielli[161], P. Gadow[37], G. Gagliardi[57a,57b], L. G. Gagnon[18a], S. Gaid[88b], S. Galantzan[157], J. Gallagher[1], E. J. Gallas[129], A. L. Gallen[167], B. J. Gallop[137], K. K. Gan[122], S. Ganguly[159], Y. Gao[52], A. Garabaglu[142], F. M. Garay Walls[140a,140b], C. García[169], A. Garcia Alonso[117], A. G. Garcia Caffaro[178], J. E. García Navarro[169], M. Garcia-Sciveres[18a], G. L. Gardner[131], R. W. Gardner[40], N. Garelli[164], R. B. Garg[149], J. M. Gargan[52], C. A. Garner[161], C. M. Garvey[34a], V. K. Gassmann[164], G. Gaudio[73a], V. Gautam[13], P. Gauzzi[75a,75b], J. Gavranovic[95], I. L. Gavrilenko[133a], A. Gavrilyuk[38], C. Gay[170], G. Gaycken[126], E. N. Gazis[10], A. Gekow[122], C. Gemme[57b], M. H. Genest[60], A. D. Gentry[115], S. George[97], W. F. George[21], T. Geralis[46], A. A. Gerwin[123], P. Gessinger-Befurt[37], M. E. Geyik[177], M. Ghani[173], K. Ghorbanian[96], A. Ghosal[147], A. Ghosh[165], A. Ghosh[7], B. Giacobbe[24b], S. Giagu[75a,75b], T. Giani[117], A. Giannini[62], S. M. Gibson[97], M. Gignac[139], D. T. Gil[86b], A. K. Gilbert[86a], B. J. Gilbert[42], D. Gillberg[35], G. Gilles[117], D. M. Gingrich[2,ak], M. P. Giordani[69a,69c], P. F. Giraud[138], G. Giugliarelli[69a,69c], D. Giugni[71a], F. Giuli[76a,76b], I. Gkialas[9,k], L. K. Gladilin[38], C. Glasman[101], G. Glemža[48], M. Glisic[126], I. Gnesi[44b], Y. Go[30], M. Goblirsch-Kolb[37], B. Gocke[49], D. Godin[110], B. Gokturk[22a], S. Goldfarb[107], T. Golling[56], M. G. D. Gololo[34c], D. Golubkov[38], J. P. Gombas[109], A. Gomes[133a,133b], G. Gomes Da Silva[147], A. J. Gomez Delegido[169], R. Gonçalo[133a], L. Gonella[21], A. Gongadze[155c], F. Gonnella[21], J. L. Gonski[149], R. Y. González Andana[52], S. González de la Hoz[169], C. Gonzalez Renteria[18a], M. V. Gonzalez Rodrigues[48], R. Gonzalez Suarez[167], S. Gonzalez-Sevilla[56], L. Goossens[37], B. Gorini[37], E. Gorini[70a,70b], A. Gorišek[95], T. C. Gosart[131], A. T. Goshaw[51], M. I. Gostkin[39], S. Goswami[124], C. A. Gottardo[37], S. A. Gotz[111], M. Gouighri[36b], A. G. Goussiou[142], N. Govender[34c], R. P. Grabarczyk[129], I. Grabowska-Bold[86a], K. Graham[35], E. Gramstad[128], S. Grancagnolo[70a,70b], C. M. Grant[1,138], P. M. Gravila[28f], F. G. Gravili[70a,70b], H. M. Gray[18a], M. Greco[112], M. J. Green[1], C. Grefe[25], A. S. Grefsrud[17], I. M. Gregor[48], K. T. Greif[165], P. Grenier[149], S. G. Grewe[112], A. A. Grillo[139], K. Grimm[32], S. Grinstein[13,z], J.-F. Grivaz[66], E. Gross[175], J. Grosse-Knetter[55], L. Guan[108], G. Guerrieri[37], R. Guevara[128], R. Gugel[102], J. A. M. Guhit[108], A. Guida[19], E. Guilloton[173], S. Guindon[37], F. Guo[14,114c], J. Guo[144a], L. Guo[48], L. Guo[114b,x], Y. Guo[108], A. Gupta[49], R. Gupta[132], S. Gupta[27], S. Gurbuz[25], S. S. Gurdasani[48], G. Gustavino[75a,75b], P. Gutierrez[123], L. F. Gutierrez Zagazeta[131], M. Gutsche[50], C. Gutschow[98], C. Gwenlan[129], C. B. Gwilliam[94], E. S. Haaland[128], A. Haas[120], M. Habedank[59], C. Haber[18a], H. K. Hadavand[8], A. Haddad[41], A. Hadef[50], A. I. Hagan[93], J. J. Hahn[147], E. H. Haines[98], M. Haleem[172], J. Haley[124], G. D. Hallewell[104], L. Halser[20], K. Hamano[171], M. Hamer[25], S. E. D. Hammoud[66], E. J. Hampshire[97], J. Han[143a], L. Han[114a], L. Han[62], S. Han[18a], K. Hanagaki[84], M. Hance[139], D. A. Hangal[42], H. Hanif[148], M. D. Hank[131], J. B. Hansen[43], P. H. Hansen[43], D. Harada[56], T. Harenberg[177], S. Harkusha[179], M. L. Harris[105], Y. T. Harris[25], J. Harrison[13], N. M. Harrison[122], P. F. Harrison[173], M. L. E. Hart[98], N. M. Hartman[112], N. M. Hartmann[111], R. Z. Hasan[97,137], Y. Hasegawa[146], F. Haslbeck[129], S. Hassan[17], R. Hauser[109], M. Haviernik[136], C. M. Hawkes[21], R. J. Hawkings[37], Y. Hayashi[159], D. Hayden[109], C. Hayes[108], R. L. Hayes[117], C. P. Hays[129], J. M. Hays[96], H. S. Hayward[94], F. He[62], M. He[14,114c], Y. He[48], Y. He[98], N. B. Heatley[96], V. Hedberg[100], A. L. Heggelund[128], C. Heidegger[54], K. K. Heidegger[54], J. Heilman[35], S. Heim[48], T. Heim[18a], J. G. Heinlein[131], J. J. Heinrich[126], L. Heinrich[112,ai], J. Hejbal[134], A. Held[176], S. Hellesund[17], C. M. Helling[170], S. Hellman[47a,47b], L. Henkelmann[33], A. M. Henriques Correia[37], H. Herde[100], Y. Hernández Jiménez[151], L. M. Herrmann[25], T. Herrmann[50], G. Herten[54], R. Hertenberger[111], L. Hervas[37], M. E. Hesping[102], N. P. Hessey[162a], J. Hessler[112], M. Hidaoui[36b], N. Hidic[136], E. Hill[161], S. J. Hillier[21], J. R. Hinds[109], F. Hinterkeuser[25], M. Hirose[127], S. Hirose[163], D. Hirschbuehl[177], T. G. Hitchings[103], B. Hiti[95], J. Hobbs[151], R. Hobincu[28e], N. Hod[175], M. C. Hodgkinson[145], B. H. Hodkinson[129], A. Hoecker[37], D. D. Hofer[108], J. Hofer[169], M. Holzbock[37], L. B. A. H. Hommels[33], V. Homsak[129], B. P. Honan[103], J. J. Hong[68], J. Hong[144a], T. M. Hong[132], B. H. Hooberman[168], W. H. Hopkins[6], M. C. Hoppesch[168], Y. Horii[113], M. E. Horstmann[112], S. Hou[154], M. R. Housenga[168], A. S. Howard[95], J. Howarth[59], J. Hoya[6], M. Hrabovsky[125], T. Hryn'ova[4], P. J. Hsu[65], S.-C. Hsu[142], T. Hsu[66], M. Hu[18a], Q. Hu[62], S. Huang[33], X. Huang[14,114c], Y. Huang[136], Y. Huang[114b], Y. Huang[102], Y. Huang[14], Z. Huang[66], Z. Hubacek[135], M. Huebner[25], F. Huegging[25], T. B. Huffman[129], M. Hufnagel Maranha De Faria[83a], C. A. Hugli[48], M. Huhtinen[37], S. K. Huiberts[17], R. Hulsken[106], C. E. Hultquist[18a], N. Huseynov[12,h], J. Huston[109], J. Huth[61], R. Hyneman[7], G. Iacobucci[56], G. Iakovidis[30], L. Iconomidou-Fayard[66], J. P. Iddon[37], P. Iengo[72a,72b], R. Iguchi[159], Y. Iiyama[159], T. Iizawa[129], Y. Ikegami[84], D. Iliadis[158], N. Ilic[161],

H. Imam[83c], G. Inacio Goncalves[83d], S. A. Infante Cabanas[140c], T. Ingebretsen Carlson[47a,47b], J. M. Inglis[96], G. Introzzi[73a,73b], M. Iodice[77a], V. Ippolito[75a,75b], R. K. Irwin[94], M. Ishino[159], W. Islam[176], C. Issever[19], S. Istin[22a,aq], K. Itabashi[84], H. Ito[174], R. Iuppa[78a,78b], A. Ivina[175], V. Izzo[72a], P. Jacka[134], P. Jackson[1], P. Jain[48], K. Jakobs[54], T. Jakoubek[175], J. Jamieson[59], W. Jang[159], S. Jankovych[136], M. Javurkova[105], P. Jawahar[103], L. Jeanty[126], J. Jejelava[155a,ag], P. Jenni[54,g], C. E. Jessiman[35], C. Jia[143a], H. Jia[170], J. Jia[151], X. Jia[14,114c], Z. Jia[114a], C. Jiang[52], Q. Jiang[64b], S. Jiggins[48], M. Jimenez Ortega[169], J. Jimenez Pena[13], S. Jin[114a], A. Jinaru[28b], O. Jinnouchi[141], P. Johansson[145], K. A. Johns[7], J. W. Johnson[139], F. A. Jolly[48], D. M. Jones[152], E. Jones[48], K. S. Jones[8], P. Jones[33], R. W. L. Jones[93], T. J. Jones[94], H. L. Joos[37,55], R. Joshi[122], J. Jovicevic[16], X. Ju[18a], J. J. Junggeburth[37], T. Junkermann[63a], A. Juste Rozas[13,z], M. K. Juzek[87], S. Kabana[140e], A. Kaczmarska[87], M. Kado[112], H. Kagan[122], M. Kagan[149], A. Kahn[131], C. Kahra[102], T. Kaji[159], E. Kajomovitz[156], N. Kakati[175], N. Kakoty[13], I. Kalaitzidou[54], S. Kandel[8], N. J. Kang[139], D. Kar[34g], K. Karava[129], E. Karentzos[25], O. Karkout[117], S. N. Karpov[39], Z. M. Karpova[39], V. Kartvelishvili[93], A. N. Karyukhin[38], E. Kasimi[158], J. Katzy[48], S. Kaur[35], K. Kawade[146], M. P. Kawale[123], C. Kawamoto[89], T. Kawamoto[62], E. F. Kay[37], F. I. Kaya[164], S. Kazakos[109], V. F. Kazanin[38], Y. Ke[151], J. M. Keaveney[34a], R. Keeler[171], G. V. Kehris[61], J. S. Keller[35], J. J. Kempster[152], O. Kepka[134], J. Kerr[162b], B. P. Kerridge[137], B. P. Kerševan[95], L. Keszeghova[29a], R. A. Khan[132], A. Khanov[124], A. G. Kharlamov[38], T. Kharlamova[38], E. E. Khoda[142], M. Kholodenko[133a], T. J. Khoo[19], G. Khoriauli[172], Y. Khoulaki[36a], J. Khubua[155b,*], Y. A. R. Khwaira[130], B. Kibirige[34g], D. Kim[6], D. W. Kim[47a,47b], Y. K. Kim[40], N. Kimura[98], M. K. Kingston[55], A. Kirchhoff[55], C. Kirfel[25], F. Kirfel[25], J. Kirk[137], A. E. Kiryunin[112], S. Kita[163], C. Kitsaki[10], O. Kivernyk[25], M. Klassen[164], C. Klein[35], L. Klein[172], M. H. Klein[45], S. B. Klein[56], U. Klein[94], A. Klimentov[30], T. Klioutchnikova[37], P. Kluit[117], S. Kluth[112], E. Kneringer[79], T. M. Knight[161], A. Knue[49], M. Kobel[50], D. Kobylianskii[175], S. F. Koch[129], M. Kocian[149], P. Kodyš[136], D. M. Koeck[126], P. T. Koenig[25], T. Koffas[35], O. Kolay[50], I. Koletsou[4], T. Komarek[87], K. Köneke[55], A. X. Y. Kong[1], T. Kono[121], N. Konstantinidis[98], P. Kontaxakis[56], B. Konya[100], R. Kopeliansky[42], S. Koperny[86a], K. Korcyl[87], K. Kordas[158,e], A. Korn[98], S. Korn[55], I. Korolkov[13], N. Korotkova[38], B. Kortman[117], O. Kortner[112], S. Kortner[112], W. H. Kostecka[118], M. Kostov[29a], V. V. Kostyukhin[147], A. Kotsokechagia[37], A. Kotwal[51], A. Koulouris[37], A. Kourkoumeli-Charalampidi[73a,73b], C. Kourkoumelis[9], E. Kourlitis[112], O. Kovanda[126], R. Kowalewski[171], W. Kozanecki[126], A. S. Kozhin[38], V. A. Kramarenko[38], G. Kramberger[95], P. Kramer[25], M. W. Krasny[130], A. Krasznahorkay[105], A. C. Kraus[118], J. W. Kraus[177], J. A. Kremer[48], N. B. Krengel[147], T. Kresse[50], L. Kretschmann[177], J. Kretzschmar[94], K. Kreul[19], P. Krieger[161], K. Krizka[21], K. Kroeninger[49], H. Kroha[112], J. Kroll[134], J. Kroll[131], K. S. Krowpman[109], U. Kruchonak[39], H. Krüger[25], N. Krumnack[81], M. C. Kruse[51], O. Kuchinskaia[39], S. Kuday[3a], S. Kuehn[37], R. Kuesters[54], T. Kuhl[48], V. Kukhtin[39], Y. Kulchitsky[39], S. Kuleshov[140b,140d], J. Kull[1], M. Kumar[34g], N. Kumari[48], P. Kumari[162b], A. Kupco[134], T. Kupfer[49], A. Kupich[38], O. Kuprash[54], H. Kurashige[85], L. L. Kurchaninov[162a], O. Kurdysh[4], Y. A. Kurochkin[38], A. Kurova[38], M. Kuze[141], A. K. Kvam[105], J. Kvita[125], N. G. Kyriacou[108], L. A. O. Laatu[104], C. Lacasta[169], F. Lacava[75a,75b], H. Lacker[19], D. Lacour[130], N. N. Lad[98], E. Ladygin[39], A. Lafarge[41], B. Laforge[130], T. Lagouri[178], F. Z. Lahbabi[36a], S. Lai[55], J. E. Lambert[171], S. Lammers[68], W. Lampl[7], C. Lampoudis[158,e], G. Lamprinoudis[102], A. N. Lancaster[118], E. Lançon[30], U. Landgraf[54], M. P. J. Landon[96], V. S. Lang[54], O. K. B. Langrekken[128], A. J. Lankford[165], F. Lanni[37], K. Lantzsch[25], A. Lanza[73a], M. Lanzac Berrocal[169], J. F. Laporte[138], T. Lari[71a], D. Larsen[17], L. Larson[11], F. Lasagni Manghi[24b], M. Lassnig[37], V. Latonova[134], S. D. Lawlor[145], Z. Lawrence[103], R. Lazaridou[173], M. Lazzaroni[71a,71b], H. D. M. Le[109], E. M. Le Boulicaut[178], L. T. Le Pottier[18a], B. Leban[24a,24b], M. LeBlanc[103], F. Ledroit-Guillon[60], S. C. Lee[154], T. F. Lee[94], L. L. Leeuw[34c,ao], M. Lefebvre[171], C. Leggett[18a], G. Lehmann Miotto[37], M. Leigh[56], W. A. Leight[105], W. Leinonen[116], A. Leisos[158,w], M. A. L. Leite[83c], C. E. Leitgeb[19], R. Leitner[136], K. J. C. Leney[45], T. Lenz[25], S. Leone[74a], C. Leonidopoulos[52], A. Leopold[150], J. H. Lepage Bourbonnais[35], R. Les[109], C. G. Lester[33], M. Levchenko[38], J. Levêque[4], L. J. Levinson[175], G. Levrini[24a,24b], M. P. Lewicki[87], C. Lewis[142], D. J. Lewis[4], L. Lewitt[145], A. Li[30], B. Li[143a], C. Li[108], C-Q. Li[112], H. Li[62], H. Li[143a], H. Li[103], H. Li[15], H. Li[62], H. Li[143a], J. Li[144a], K. Li[14], L. Li[144a], R. Li[178], S. Li[14,114c], S. Li[144a,144b,d], T. Li[5], X. Li[106], Z. Li[159], Z. Li[14,114c], Z. Li[62], S. Liang[14,114c], Z. Liang[14], M. Liberatore[138], B. Liberti[76a], K. Lie[64c], J. Lieber Marin[83e], H. Lien[68], H. Lin[108], S. F. Lin[151], L. Linden[111], R. E. Lindley[7], J. H. Lindon[2], J. Ling[61], E. Lipeles[131], A. Lipniacka[17], A. Lister[170], J. D. Little[68], B. Liu[14], B. X. Liu[114b], D. Liu[144a,144b], E. H. L. Liu[21], J. K. K. Liu[33], K. Liu[144b], K. Liu[144a,144b], M. Liu[62], M. Y. Liu[62],

P. Liu[14], Q. Liu[142,144a,144b], X. Liu[62], X. Liu[143a], Y. Liu[114b,114c], Y. L. Liu[143a], Y. W. Liu[62], Z. Liu[66,m], S. L. Lloyd[96], E. M. Lobodzinska[48], P. Loch[7], E. Lodhi[161], T. Lohse[19], K. Lohwasser[145], E. Loiacono[48], J. D. Lomas[21], J. D. Long[42], I. Longarini[165], R. Longo[168], A. Lopez Solis[48], N. A. Lopez-canelas[7], N. Lorenzo Martinez[4], A. M. Lory[111], M. Losada[119a], G. Löschcke Centeno[152], X. Lou[47a,47b], X. Lou[14,114c], A. Lounis[66], P. A. Love[93], G. Lu[14,114c], M. Lu[66], S. Lu[131], Y. J. Lu[154], H. J. Lubatti[142], C. Luci[75a,75b], F. L. Lucio Alves[114a], F. Luehring[68], B. S. Lunday[131], O. Lundberg[150], J. Lunde[37], B. Lund-Jensen[150,*], N. A. Luongo[6], M. S. Lutz[37], A. B. Lux[26], D. Lynn[30], R. Lysak[134], V. Lysenko[135], E. Lytken[100], V. Lyubushkin[39], T. Lyubushkina[39], M. M. Lyukova[151], M. Firdaus M. Soberi[52], H. Ma[30], K. Ma[62], L. L. Ma[143a], W. Ma[62], Y. Ma[124], J. C. MacDonald[102], P. C. Machado De Abreu Farias[83e], R. Madar[41], T. Madula[98], J. Maeda[85], T. Maeno[30], P. T. Mafa[34c,l], H. Maguire[145], V. Maiboroda[66], A. Maio[133a,133b,133d], K. Maj[86a], O. Majersky[48], S. Majewski[126], R. Makhmanazarov[38], N. Makovec[66], V. Maksimovic[16], B. Malaescu[130], J. Malamant[128], Pa. Malecki[87], V. P. Maleev[38], F. Malek[60,r], M. Mali[95], D. Malito[97], U. Mallik[80,*], A. Maloizel[5], S. Maltezos[10], A. Malvezzi Lopes[83d], S. Malyukov[39], J. Mamuzic[13], G. Mancini[53], M. N. Mancini[27], G. Manco[73a,73b], J. P. Mandalia[96], S. S. Mandarry[152], I. Mandić[95], L. Manhaes de Andrade Filho[83a], I. M. Maniatis[175], J. Manjarres Ramos[91], D. C. Mankad[175], A. Mann[111], T. Manoussos[37], M. N. Mantinan[40], S. Manzoni[37], L. Mao[144a], X. Mapekula[34c], A. Marantis[158,w], R. R. Marcelo Gregorio[96], G. Marchiori[5], M. Marcisovsky[134], C. Marcon[71a], M. Marinescu[21], S. Marium[48], M. Marjanovic[123], A. Markhoos[54], M. Markovitch[66], M. K. Maroun[105], G. T. Marsden[103], E. J. Marshall[93], Z. Marshall[18a], S. Marti-Garcia[169], J. Martin[98], T. A. Martin[137], V. J. Martin[52], B. Martin dit Latour[17], L. Martinelli[75a,75b], M. Martinez[13,z], P. Martinez Agullo[169], V. I. Martinez Outschoorn[105], P. Martinez Suarez[13], S. Martin-Haugh[137], G. Martinovicova[136], V. S. Martoiu[28b], A. C. Martyniuk[98], A. Marzin[37], D. Mascione[78a,78b], L. Masetti[102], J. Masik[103], A. L. Maslennikov[39], S. L. Mason[42], P. Massarotti[72a,72b], P. Mastrandrea[74a,74b], A. Mastroberardino[44a,44b], T. Masubuchi[127], T. T. Mathew[126], J. Matousek[136], D. M. Mattern[49], J. Maurer[28b], T. Maurin[59], A. J. Maury[66], B. Maček[95], C. Mavungu Tsava[104], D. A. Maximov[38], A. E. May[103], E. Mayer[41], R. Mazini[34g], I. Maznas[118], M. Mazza[109], S. M. Mazza[139], E. Mazzeo[71a,71b], J. P. Mc Gowan[171], S. P. Mc Kee[108], C. A. Mc Lean[6], C. C. McCracken[170], E. F. McDonald[107], A. E. McDougall[117], L. F. Mcelhinney[93], J. A. Mcfayden[152], R. P. McGovern[131], R. P. Mckenzie[34g], T. C. Mclachlan[48], D. J. Mclaughlin[98], S. J. McMahon[137], C. M. Mcpartland[94], R. A. McPherson[171,ad], S. Mehlhase[111], A. Mehta[94], D. Melini[169], B. R. Mellado Garcia[34g], A. H. Melo[55], F. Meloni[48], A. M. Mendes Jacques Da Costa[103], H. Y. Meng[161], L. Meng[93], S. Menke[112], M. Mentink[37], E. Meoni[44a,44b], G. Mercado[118], S. Merianos[158], C. Merlassino[69a,69c], C. Meroni[71a,71b], J. Metcalfe[6], A. S. Mete[6], E. Meuser[102], C. Meyer[68], J-P. Meyer[138], R. P. Middleton[137], M. Mihovilovic[66], L. Mijović[52], G. Mikenberg[175], M. Mikestikova[134], M. Mikuž[95], H. Mildner[102], A. Milic[37], D. W. Miller[40], E. H. Miller[149], L. S. Miller[35], A. Milov[175], D. A. Milstead[47a,47b], T. Min[114a], A. A. Minaenko[38], I. A. Minashvili[155b], A. I. Mincer[120], B. Mindur[86a], M. Mineev[39], Y. Mino[89], L. M. Mir[13], M. Miralles Lopez[59], M. Mironova[18a], M. C. Missio[116], A. Mitra[173], V. A. Mitsou[169], Y. Mitsumori[113], O. Miu[161], P. S. Miyagawa[96], T. Mkrtchyan[63a], M. Mlinarevic[98], T. Mlinarevic[98], M. Mlynarikova[37], S. Mobius[20], P. Mogg[111], M. H. Mohamed Farook[115], A. F. Mohammed[14,114c], S. Mohapatra[42], S. Mohiuddin[124], G. Mokgatitswane[34g], L. Moleri[175], U. Molinatti[129], L. G. Mollier[20], B. Mondal[147], S. Mondal[135], K. Mönig[48], E. Monnier[104], L. Monsonis Romero[169], J. Montejo Berlingen[13], A. Montella[47a,47b], M. Montella[122], F. Montereali[77a,77b], F. Monticelli[92], S. Monzani[69a,69c], A. Morancho Tarda[43], N. Morange[66], A. L. Moreira De Carvalho[48], M. Moreno Llácer[169], C. Moreno Martinez[56], J. M. Moreno Perez[23b], P. Morettini[57b], S. Morgenstern[37], M. Morii[61], M. Morinaga[159], M. Moritsu[90], F. Morodei[75a,75b], P. Moschovakos[37], B. Moser[129], M. Mosidze[155b], T. Moskalets[45], P. Moskvitina[116], J. Moss[32,o], P. Moszkowicz[86a], A. Moussa[36d], Y. Moyal[175], H. Moyano Gomez[13], E. J. W. Moyse[105], O. Mtintsilana[34g], S. Muanza[104], J. Mueller[132], R. Müller[37], G. A. Mullier[167], A. J. Mullin[33], J. J. Mullin[51], A. E. Mulski[61], D. P. Mungo[161], D. Munoz Perez[169], F. J. Munoz Sanchez[103], M. Murin[103], W. J. Murray[137,173], M. Muškinja[95], C. Mwewa[48], A. G. Myagkov[38,a], A. J. Myers[8], G. Myers[108], M. Myska[135], B. P. Nachman[18a], K. Nagai[129], K. Nagano[84], R. Nagasaka[159], J. L. Nagle[30,am], E. Nagy[104], A. M. Nairz[37], Y. Nakahama[84], K. Nakamura[84], K. Nakkalil[5], H. Nanjo[127], E. A. Narayanan[45], Y. Narukawa[159], I. Naryshkin[38], L. Nasella[71a,71b], S. Nasri[119b], C. Nass[25], G. Navarro[23a], J. Navarro-Gonzalez[169], A. Nayaz[19], P. Y. Nechaeva[38], S. Nechaeva[24a,24b], F. Nechansky[134], L. Nedic[129], T. J. Neep[21], A. Negri[73a,73b], M. Negrini[24b], C. Nellist[117], C. Nelson[106], K. Nelson[108],

S. Nemecek[134], M. Nessi[37,i], M. S. Neubauer[168], J. Newell[94], P. R. Newman[21], Y. W. Y. Ng[168], B. Ngair[119a], H. D. N. Nguyen[110], J. D. Nichols[123], R. B. Nickerson[129], R. Nicolaidou[138], J. Nielsen[139], M. Niemeyer[55], J. Niermann[37], N. Nikiforou[37], V. Nikolaenko[38,a], I. Nikolic-Audit[130], P. Nilsson[30], I. Ninca[48], G. Ninio[157], A. Nisati[75a], N. Nishu[2], R. Nisius[112], N. Nitika[69a,69c], J-E. Nitschke[50], E. K. Nkadimeng[34g], T. Nobe[159], T. Nommensen[153], M. B. Norfolk[145], B. J. Norman[35], M. Noury[36a], J. Novak[95], T. Novak[95], R. Novotny[115], L. Nozka[125], K. Ntekas[165], N. M. J. Nunes De Moura Junior[83b], J. Ocariz[130], A. Ochi[85], I. Ochoa[133a], S. Oerdek[48,aa], J. T. Offermann[40], A. Ogrodnik[136], A. Oh[103], C. C. Ohm[150], H. Oide[84], R. Oishi[159], M. L. Ojeda[37], Y. Okumura[159], L. F. Oleiro Seabra[133a], I. Oleksiyuk[56], S. A. Olivares Pino[140d], G. Oliveira Correa[13], D. Oliveira Damazio[30], J. L. Oliver[165], Ö. O. Öncel[54], A. P. O'Neill[20], A. Onofre[133a,133e,f], P. U. E. Onyisi[11], M. J. Oreglia[40], D. Orestano[77a,77b], R. Orlandini[77a,77b], R. S. Orr[161], L. M. Osojnak[131], Y. Osumi[113], G. Otero y Garzon[31], H. Otono[90], G. J. Ottino[18a], M. Ouchrif[36d], F. Ould-Saada[128], T. Ovsiannikova[142], M. Owen[59], R. E. Owen[137], V. E. Ozcan[22a], F. Ozturk[87], N. Ozturk[8], S. Ozturk[82], H. A. Pacey[129], K. Pachal[162a], A. Pacheco Pages[13], C. Padilla Aranda[13], G. Padovano[75a,75b], S. Pagan Griso[18a], G. Palacino[68], A. Palazzo[70a,70b], J. Pampel[25], J. Pan[178], T. Pan[64a], D. K. Panchal[11], C. E. Pandini[117], J. G. Panduro Vazquez[137], H. D. Pandya[1], H. Pang[138], P. Pani[48], G. Panizzo[69a,69c], L. Panwar[130], L. Paolozzi[56], S. Parajuli[168], A. Paramonov[6], C. Paraskevopoulos[53], D. Paredes Hernandez[64b], A. Pareti[73a,73b], K. R. Park[42], T. H. Park[112], F. Parodi[57a,57b], J. A. Parsons[42], U. Parzefall[54], B. Pascual Dias[41], L. Pascual Dominguez[101], E. Pasqualucci[75a], S. Passaggio[57b], F. Pastore[97], P. Patel[87], U. M. Patel[51], J. R. Pater[103], T. Pauly[37], F. Pauwels[136], C. I. Pazos[164], M. Pedersen[128], R. Pedro[133a], S. V. Peleganchuk[38], O. Penc[37], E. A. Pender[52], S. Peng[15], G. D. Penn[178], K. E. Penski[111], M. Penzin[38], B. S. Peralva[83d], A. P. Pereira Peixoto[142], L. Pereira Sanchez[149], D. V. Perepelitsa[30,am], G. Perera[105], E. Perez Codina[162a], M. Perganti[10], H. Pernegger[37], S. Perrella[75a,75b], O. Perrin[41], K. Peters[48], R. F. Y. Peters[103], B. A. Petersen[37], T. C. Petersen[43], E. Petit[104], V. Petousis[135], A. R. Petri[71a,71b], C. Petridou[158,e], T. Petru[136], A. Petrukhin[147], M. Pettee[18a], A. Petukhov[82], K. Petukhova[37], R. Pezoa[140f], L. Pezzotti[24a,24b], G. Pezzullo[178], L. Pfaffenbichler[37], A. J. Pfleger[37], T. M. Pham[176], T. Pham[107], P. W. Phillips[137], G. Piacquadio[151], E. Pianori[18a], F. Piazza[126], R. Piegaia[31], D. Pietreanu[28b], A. D. Pilkington[103], M. Pinamonti[69a,69c], J. L. Pinfold[2], B. C. Pinheiro Pereira[133a], J. Pinol Bel[13], A. E. Pinto Pinoargote[130], L. Pintucci[69a,69c], K. M. Piper[152], A. Pirttikoski[56], D. A. Pizzi[35], L. Pizzimento[64b], A. Plebani[33], M.-A. Pleier[30], V. Pleskot[136], E. Plotnikova[39], G. Poddar[96], R. Poettgen[100], L. Poggioli[130], S. Polacek[136], G. Polesello[73a], A. Poley[148,162a], A. Polini[24b], C. S. Pollard[173], Z. B. Pollock[122], E. Pompa Pacchi[123], N. I. Pond[98], D. Ponomarenko[68], L. Pontecorvo[37], S. Popa[28a], G. A. Popeneciu[28d], A. Poreba[37], D. M. Portillo Quintero[162a], S. Pospisil[135], M. A. Postill[145], P. Postolache[28c], K. Potamianos[173], P. A. Potepa[86a], I. N. Potrap[39], C. J. Potter[33], H. Potti[153], J. Poveda[169], M. E. Pozo Astigarraga[37], A. Prades Ibanez[76a,76b], J. Pretel[171], D. Price[103], M. Primavera[70a], L. Primomo[69a,69c], M. A. Principe Martin[101], R. Privara[125], T. Procter[59], M. L. Proffitt[142], N. Proklova[131], K. Prokofiev[64c], G. Proto[112], J. Proudfoot[6], M. Przybycien[86a], W. W. Przygoda[86b], A. Psallidas[46], J. E. Puddefoot[145], D. Pudzha[53], D. Pyatiizbyantseva[116], J. Qian[108], R. Qian[109], D. Qichen[103], Y. Qin[13], T. Qiu[52], A. Quadt[55], M. Queitsch-Maitland[103], G. Quetant[56], R. P. Quinn[170], G. Rabanal Bolanos[61], D. Rafanoharana[54], F. Raffaeli[76a,76b], F. Ragusa[71a,71b], J. L. Rainbolt[40], J. A. Raine[56], S. Rajagopalan[30], E. Ramakoti[39], L. Rambelli[57a,57b], I. A. Ramirez-Berend[35], K. Ran[48,114c], D. S. Rankin[131], N. P. Rapheeha[34g], H. Rasheed[28b], V. Raskina[130], D. F. Rassloff[63a], A. Rastogi[18a], S. Rave[102], S. Ravera[57a,57b], B. Ravina[37], I. Ravinovich[175], M. Raymond[37], A. L. Read[128], N. P. Readioff[145], D. M. Rebuzzi[73a,73b], A. S. Reed[112], K. Reeves[27], J. A. Reidelsturz[177], D. Reikher[126], A. Rej[49], C. Rembser[37], H. Ren[62], M. Renda[28b], F. Renner[48], A. G. Rennie[59], A. L. Rescia[48], S. Resconi[71a], M. Ressegotti[57a,57b], S. Rettie[37], W. F. Rettie[35], J. G. Reyes Rivera[109], E. Reynolds[18a], O. L. Rezanova[39], P. Reznicek[136], H. Riani[36d], N. Ribaric[51], E. Ricci[78a,78b], R. Richter[112], S. Richter[47a,47b], E. Richter-Was[86b], M. Ridel[130], S. Ridouani[36d], P. Rieck[120], P. Riedler[37], E. M. Riefel[47a,47b], J. O. Rieger[117], M. Rijssenbeek[151], M. Rimoldi[37], L. Rinaldi[24a,24b], P. Rincke[55], G. Ripellino[167], I. Riu[13], J. C. Rivera Vergara[171], F. Rizatdinova[124], E. Rizvi[96], B. R. Roberts[18a], S. S. Roberts[139], D. Robinson[33], M. Robles Manzano[102], A. Robson[59], A. Rocchi[76a,76b], C. Roda[74a,74b], S. Rodriguez Bosca[37], Y. Rodriguez Garcia[23a], A. M. Rodríguez Vera[118], S. Roe[37], J. T. Roemer[37], O. Røhne[128], R. A. Rojas[37], C. P. A. Roland[130], J. Roloff[30], A. Romaniouk[79], E. Romano[73a,73b], M. Romano[24b], A. C. Romero Hernandez[168], N. Rompotis[94], L. Roos[130], S. Rosati[75a], B. J. Rosser[40], E. Rossi[129],

E. Rossi[72a,72b], L. P. Rossi[61], L. Rossini[54], R. Rosten[122], M. Rotaru[28b], B. Rottler[54], D. Rousseau[66], D. Rousso[48], S. Roy-Garand[161], A. Rozanov[104], Z. M. A. Rozario[59], Y. Rozen[156], A. Rubio Jimenez[169], V. H. Ruelas Rivera[19], T. A. Ruggeri[1], A. Ruggiero[129], A. Ruiz-Martinez[169], A. Rummler[37], Z. Rurikova[54], N. A. Rusakovich[39], H. L. Russell[171], G. Russo[75a,75b], J. P. Rutherfoord[7], S. Rutherford Colmenares[33], M. Rybar[136], P. Rybczynski[86a], E. B. Rye[128], A. Ryzhov[45], J. A. Sabater Iglesias[56], H. F.-W. Sadrozinski[139], F. Safai Tehrani[75a], S. Saha[1], M. Sahinsoy[82], B. Sahoo[175], A. Saibel[169], B. T. Saifuddin[123], M. Saimpert[138], M. Saito[159], T. Saito[159], A. Sala[71a,71b], D. Salamani[37], A. Salnikov[149], J. Salt[169], A. Salvador Salas[157], D. Salvatore[44a,44b], F. Salvatore[152], A. Salzburger[37], D. Sammel[54], E. Sampson[93], D. Sampsonidis[158,e], D. Sampsonidou[126], J. Sánchez[169], V. Sanchez Sebastian[169], H. Sandaker[128], C. O. Sander[48], J. A. Sandesara[176], M. Sandhoff[177], C. Sandoval[23b], L. Sanfilippo[63a], D. P. C. Sankey[137], T. Sano[89], A. Sansoni[53], L. Santi[37], C. Santoni[41], H. Santos[133a,133b], A. Santra[175], E. Sanzani[24a,24b], K. A. Saoucha[88b], J. G. Saraiva[133a,133d], J. Sardain[7], O. Sasaki[84], K. Sato[163], C. Sauer[37], E. Sauvan[4], P. Savard[161,ak], R. Sawada[159], C. Sawyer[137], L. Sawyer[99], C. Sbarra[24b], A. Sbrizzi[24a,24b], T. Scanlon[98], J. Schaarschmidt[142], U. Schäfer[102], A. C. Schaffer[45,66], D. Schaile[111], R. D. Schamberger[151], C. Scharf[19], M. M. Schefer[20], V. A. Schegelsky[38], D. Scheirich[136], M. Schernau[140e], C. Scheulen[56], C. Schiavi[57a,57b], M. Schioppa[44a,44b], B. Schlag[149], S. Schlenker[37], J. Schmeing[177], M. A. Schmidt[177], K. Schmieden[102], C. Schmitt[102], N. Schmitt[102], S. Schmitt[48], L. Schoeffel[138], A. Schoening[63b], P. G. Scholer[35], E. Schopf[147], M. Schott[25], S. Schramm[56], T. Schroer[56], H-C. Schultz-Coulon[63a], M. Schumacher[54], B. A. Schumm[139], Ph. Schune[138], H. R. Schwartz[139], A. Schwartzman[149], T. A. Schwarz[108], Ph. Schwemling[138], R. Schwienhorst[109], F. G. Sciacca[20], A. Sciandra[30], G. Sciolla[27], F. Scuri[74a], C. D. Sebastiani[37], K. Sedlaczek[118], S. C. Seidel[115], A. Seiden[139], B. D. Seidlitz[42], C. Seitz[48], J. M. Seixas[83b], G. Sekhniaidze[72a], L. Selem[60], N. Semprini-Cesari[24a,24b], A. Semushin[38,179], D. Sengupta[56], V. Senthilkumar[169], L. Serin[66], M. Sessa[76a,76b], H. Severini[123], F. Sforza[57a,57b], A. Sfyrla[56], Q. Sha[14], E. Shabalina[55], H. Shaddix[118], A. H. Shah[33], R. Shaheen[150], J. D. Shahinian[131], D. Shaked Renous[175], M. Shamim[37], L. Y. Shan[14], M. Shapiro[18a], A. Sharma[37], A. S. Sharma[170], P. Sharma[30], P. B. Shatalov[38], K. Shaw[152], S. M. Shaw[103], Q. Shen[144a], D. J. Sheppard[148], P. Sherwood[98], L. Shi[98], X. Shi[14], S. Shimizu[84], C. O. Shimmin[178], I. P. J. Shipsey[129,*], S. Shirabe[90], M. Shiyakova[39,ab], M. J. Shochet[40], D. R. Shope[128], B. Shrestha[123], S. Shrestha[122,ap], I. Shreyber[39], M. J. Shroff[171], P. Sicho[134], A. M. Sickles[168], E. Sideras Haddad[34g,166], A. C. Sidley[117], A. Sidoti[24b], F. Siegert[50], Dj. Sijacki[16], F. Sili[92], J. M. Silva[52], I. Silva Ferreira[83b], M. V. Silva Oliveira[30], S. B. Silverstein[47a], S. Simion[66], R. Simoniello[37], E. L. Simpson[103], H. Simpson[152], L. R. Simpson[108], S. Simsek[82], S. Sindhu[55], P. Sinervo[161], S. N. Singh[27], S. Singh[30], S. Sinha[48], S. Sinha[103], M. Sioli[24a,24b], K. Sioulas[9], I. Siral[37], E. Sitnikova[48], J. Sjölin[47a,47b], A. Skaf[55], E. Skorda[21], P. Skubic[123], M. Slawinska[87], I. Slazyk[17], V. Smakhtin[175], B. H. Smart[137], S.Yu. Smirnov[140b], Y. Smirnov[82], L. N. Smirnova[38,a], O. Smirnova[100], A. C. Smith[42], D. R. Smith[165], E. A. Smith[40], J. L. Smith[103], M. B. Smith[35], R. Smith[149], H. Smitmanns[102], M. Smizanska[93], K. Smolek[135], P. Smolyanskiy[135], A. A. Snesarev[39], H. L. Snoek[117], S. Snyder[30], R. Sobie[171,ad], A. Soffer[157], C. A. Solans Sanchez[37], E.Yu. Soldatov[39], U. Soldevila[169], A. A. Solodkov[34g], S. Solomon[27], A. Soloshenko[39], K. Solovieva[54], O. V. Solovyanov[41], P. Sommer[50], A. Sonay[13], W. Y. Song[162b], A. Sopczak[135], A. L. Sopio[52], F. Sopkova[29b], J. D. Sorenson[115], I. R. Sotarriva Alvarez[141], V. Sothilingam[63a], O. J. Soto Sandoval[140b,140c], S. Sottocornola[68], R. Soualah[88a], Z. Soumaimi[36e], D. South[48], N. Soybelman[175], S. Spagnolo[70a,70b], M. Spalla[112], D. Sperlich[54], B. Spisso[72a,72b], D. P. Spiteri[59], L. Splendori[104], M. Spousta[136], E. J. Staats[35], R. Stamen[63a], E. Stanecka[87], W. Stanek-Maslouska[48], M. V. Stange[50], B. Stanislaus[18a], M. M. Stanitzki[48], B. Stapf[48], E. A. Starchenko[38], G. H. Stark[139], J. Stark[91], P. Staroba[134], P. Starovoitov[88b], R. Staszewski[87], G. Stavropoulos[46], A. Stefl[37], P. Steinberg[30], B. Stelzer[148,162a], H. J. Stelzer[132], O. Stelzer-Chilton[162a], H. Stenzel[58], T. J. Stevenson[152], G. A. Stewart[37], J. R. Stewart[124], M. C. Stockton[37], G. Stoicea[28b], M. Stolarski[133a], S. Stonjek[112], A. Straessner[50], J. Strandberg[150], S. Strandberg[47a,47b], M. Stratmann[177], M. Strauss[123], T. Strebler[104], P. Strizenec[29b], R. Ströhmer[172], D. M. Strom[126], R. Stroynowski[45], A. Strubig[47a,47b], S. A. Stucci[30], B. Stugu[17], J. Stupak[123], N. A. Styles[48], D. Su[149], S. Su[62], W. Su[144b], X. Su[62], D. Suchy[29a], K. Sugizaki[131], V. V. Sulin[38], M. J. Sullivan[94], D. M. S. Sultan[129], L. Sultanaliyeva[38], S. Sultansoy[3b], S. Sun[176], W. Sun[14], O. Sunneborn Gudnadottir[167], N. Sur[100], M. R. Sutton[152], H. Suzuki[163], M. Svatos[134], P. N. Swallow[33], M. Swiatlowski[162a], T. Swirski[172], I. Sykora[29a], M. Sykora[136], T. Sykora[136], D. Ta[102], K. Tackmann[48,aa], A. Taffard[165], R. Tafirout[162a], Y. Takubo[84], M. Talby[104], A. A. Talyshev[38], K. C. Tam[64b], N. M. Tamir[157], A. Tanaka[159], J. Tanaka[159], R. Tanaka[66], M. Tanasini[151],

Z. Tao[170], S. Tapia Araya[140f], S. Tapprogge[102], A. Tarek Abouelfadl Mohamed[109], S. Tarem[156], K. Tariq[14], G. Tarna[28b], G. F. Tartarelli[71a], M. J. Tartarin[91], P. Tas[136], M. Tasevsky[134], E. Tassi[44a,44b], A. C. Tate[168], G. Tateno[159], Y. Tayalati[36e,ac], G. N. Taylor[107], W. Taylor[162b], A. S. Tegetmeier[91], P. Teixeira-Dias[97], J. J. Teoh[161], K. Terashi[159], J. Terron[101], S. Terzo[13], M. Testa[53], R. J. Teuscher[161,ad], A. Thaler[79], O. Theiner[56], T. Theveneaux-Pelzer[104], O. Thielmann[177], D. W. Thomas[97], J. P. Thomas[21], E. A. Thompson[18a], P. D. Thompson[21], E. Thomson[131], R. E. Thornberry[45], C. Tian[62], Y. Tian[56], V. Tikhomirov[82], Yu. A. Tikhonov[39], S. Timoshenko[38], D. Timoshyn[136], E. X. L. Ting[1], P. Tipton[178], A. Tishelman-Charny[30], S. H. Tlou[34g], K. Todome[141], S. Todorova-Nova[136], S. Todt[50], L. Toffolin[69a,69c], M. Togawa[84], J. Tojo[90], S. Tokár[29a], O. Toldaiev[68], G. Tolkachev[104], M. Tomoto[84,113], L. Tompkins[149,q], E. Torrence[126], H. Torres[91], E. Torró Pastor[169], M. Toscani[31], C. Tosciri[40], M. Tost[11], D. R. Tovey[145], T. Trefzger[172], P. M. Tricarico[13], A. Tricoli[30], I. M. Trigger[162a], S. Trincaz-Duvoid[130], D. A. Trischuk[27], A. Tropina[39], L. Truong[34c], M. Trzebinski[87], A. Trzupek[87], F. Tsai[151], M. Tsai[108], A. Tsiamis[158], P. V. Tsiareshka[39], S. Tsigaridas[162a], A. Tsirigotis[158,w], V. Tsiskaridze[161], E. G. Tskhadadze[155a], M. Tsopoulou[158], Y. Tsujikawa[89], I. I. Tsukerman[38], V. Tsulaia[18a], S. Tsuno[84], K. Tsuri[121], D. Tsybychev[151], Y. Tu[64b], A. Tudorache[28b], V. Tudorache[28b], S. Turchikhin[57a,57b], I. Turk Cakir[3a], R. Turra[71a], T. Turtuvshin[39,ae], P. M. Tuts[42], S. Tzamarias[158,e], E. Tzovara[102], Y. Uematsu[84], F. Ukegawa[163], P. A. Ulloa Poblete[140b,140c], E. N. Umaka[30], G. Unal[37], A. Undrus[30], G. Unel[165], J. Urban[29b], P. Urrejola[140a], G. Usai[8], R. Ushioda[160], M. Usman[110], F. Ustuner[52], Z. Uysal[82], V. Vacek[135], B. Vachon[106], T. Vafeiadis[37], A. Vaitkus[98], C. Valderanis[111], E. Valdes Santurio[47a,47b], M. Valente[162a], S. Valentinetti[24a,24b], A. Valero[169], E. Valiente Moreno[169], A. Vallier[91], J. A. Valls Ferrer[169], D. R. Van Arneman[117], T. R. Van Daalen[142], A. Van Der Graaf[49], H. Z. Van Der Schyf[34g], P. Van Gemmeren[6], M. Van Rijnbach[37], S. Van Stroud[98], I. Van Vulpen[117], P. Vana[136], M. Vanadia[76a,76b], U. M. Vande Voorde[150], W. Vandelli[37], E. R. Vandewall[124], D. Vannicola[157], L. Vannoli[53], R. Vari[75a], E. W. Varnes[7], C. Varni[18b], D. Varouchas[66], L. Varriale[169], K. E. Varvell[153], M. E. Vasile[28b], L. Vaslin[84], M. D. Vassilev[149], A. Vasyukov[39], L. M. Vaughan[124], R. Vavricka[136], T. Vazquez Schroeder[13], J. Veatch[32], V. Vecchio[103], M. J. Veen[105], I. Veliscek[30], I. Velkovska[95], L. M. Veloce[161], F. Veloso[133a,133c], S. Veneziano[75a], A. Ventura[70a,70b], S. Ventura Gonzalez[138], A. Verbytskyi[112], M. Verducci[74a,74b], C. Vergis[96], M. Verissimo De Araujo[83b], W. Verkerke[117], J. C. Vermeulen[117], C. Vernieri[149], M. Vessella[165], M. C. Vetterli[148,ak], A. Vgenopoulos[102], N. Viaux Maira[140f], T. Vickey[145], O. E. Vickey Boeriu[145], G. H. A. Viehhauser[129], L. Vigani[63b], M. Vigl[112], M. Villa[24a,24b], M. Villaplana Perez[169], E. M. Villhauer[52], E. Vilucchi[53], M. G. Vincter[35], A. Visibile[117], C. Vittori[37], I. Vivarelli[24a,24b], E. Voevodina[112], F. Vogel[111], J. C. Voigt[50], P. Vokac[135], Yu. Volkotrub[86b], E. Von Toerne[25], B. Vormwald[37], K. Vorobev[51], M. Vos[169], K. Voss[147], M. Vozak[37], L. Vozdecky[123], N. Vranjes[16], M. Vranjes Milosavljevic[16], M. Vreeswijk[117], N. K. Vu[144a,144b], R. Vuillermet[37], O. Vujinovic[102], I. Vukotic[40], I. K. Vyas[35], J. F. Wack[33], S. Wada[163], C. Wagner[149], J. M. Wagner[18a], W. Wagner[177], S. Wahdan[177], H. Wahlberg[92], C. H. Waits[123], J. Walder[137], R. Walker[111], W. Walkowiak[147], A. Wall[131], E. J. Wallin[100], T. Wamorkar[18a], A. Z. Wang[139], C. Wang[102], C. Wang[11], H. Wang[18a], J. Wang[64c], P. Wang[103], P. Wang[98], R. Wang[61], R. Wang[6], S. M. Wang[154], S. Wang[14], T. Wang[62], T. Wang[62], W. T. Wang[80], W. Wang[14], X. Wang[168], X. Wang[144a], X. Wang[48], Y. Wang[114a], Y. Wang[62], Z. Wang[108], Z. Wang[51,144a,144b], Z. Wang[108], C. Wanotayaroj[84], A. Warburton[106], A. L. Warnerbring[147], N. Warrack[59], S. Waterhouse[97], A. T. Watson[21], H. Watson[52], M. F. Watson[21], E. Watton[59], G. Watts[142], B. M. Waugh[98], J. M. Webb[54], C. Weber[30], H. A. Weber[19], M. S. Weber[20], S. M. Weber[63a], C. Wei[62], Y. Wei[54], A. R. Weidberg[129], E. J. Weik[120], J. Weingarten[49], C. Weiser[54], C. J. Wells[48], T. Wenaus[30], B. Wendland[49], T. Wengler[37], N. S. Wenke[112], N. Wermes[25], M. Wessels[63a], A. M. Wharton[93], A. S. White[61], A. White[8], M. J. White[1], D. Whiteson[165], L. Wickremasinghe[127], W. Wiedenmann[176], M. Wielers[137], R. Wierda[150], C. Wiglesworth[43], H. G. Wilkens[37], J. J. H. Wilkinson[33], D. M. Williams[42], H. H. Williams[131], S. Williams[33], S. Willocq[105], B. J. Wilson[103], D. J. Wilson[103], P. J. Windischhofer[40], F. I. Winkel[31], F. Winklmeier[126], B. T. Winter[54], M. Wittgen[149], M. Wobisch[99], T. Wojtkowski[60], Z. Wolffs[117], J. Wollrath[37], M. W. Wolter[87], H. Wolters[133a,133c], M. C. Wong[139], E. L. Woodward[42], S. D. Worm[48], B. K. Wosiek[87], K. W. Woźniak[87], S. Wozniewski[55], K. Wraight[59], C. Wu[161], C. Wu[21], M. Wu[114b], M. Wu[116], S. L. Wu[176], S. Wu[14], X. Wu[56], X. Wu[62], Y. Wu[62], Z. Wu[4], J. Wuerzinger[112,ai], T. R. Wyatt[103], B. M. Wynne[52], S. Xella[43], L. Xia[114a], M. Xia[15], M. Xie[62], A. Xiong[126], J. Xiong[18a], D. Xu[14], H. Xu[62], L. Xu[62], R. Xu[131], T. Xu[108], Y. Xu[142], Z. Xu[52], Z. Xu[114a], B. Yabsley[153], S. Yacoob[34a], Y. Yamaguchi[84], E. Yamashita[159], H. Yamauchi[163], T. Yamazaki[18a], Y. Yamazaki[85], S. Yan[59], Z. Yan[105],

H. J. Yang[144a,144b], H. T. Yang[62], S. Yang[62], T. Yang[64c], X. Yang[37], X. Yang[14], Y. Yang[159], Y. Yang[62], W-M. Yao[18a], C. L. Yardley[152], H. Ye[55], J. Ye[14], S. Ye[30], X. Ye[62], Y. Yeh[98], I. Yeletskikh[39], B. Yeo[18b], M. R. Yexley[98], T. P. Yildirim[129], P. Yin[42], K. Yorita[174], C. J. S. Young[37], C. Young[149], N. D. Young[126], Y. Yu[62], J. Yuan[14,114c], M. Yuan[108], R. Yuan[144a,144b], L. Yue[98], M. Zaazoua[62], B. Zabinski[87], I. Zahir[36a], A. Zaio[57a,57b], Z. K. Zak[87], T. Zakareishvili[169], S. Zambito[56], J. A. Zamora Saa[140d], J. Zang[159], D. Zanzi[54], R. Zanzottera[71a,71b], O. Zaplatilek[135], C. Zeitnitz[177], H. Zeng[14], J. C. Zeng[168], D. T. Zenger Jr[27], O. Zenin[38], T. Ženiš[29a], S. Zenz[96], D. Zerwas[66], M. Zhai[14,114c], D. F. Zhang[145], J. Zhang[143a], J. Zhang[6], K. Zhang[14,114c], L. Zhang[62], L. Zhang[114a], P. Zhang[14,114c], R. Zhang[176], S. Zhang[91], T. Zhang[159], X. Zhang[144a], Y. Zhang[142], Y. Zhang[98], Y. Zhang[62], Y. Zhang[114a], Z. Zhang[18a], Z. Zhang[143a], Z. Zhang[66], H. Zhao[142], T. Zhao[143a], Y. Zhao[35], Z. Zhao[62], Z. Zhao[62], A. Zhemchugov[39], J. Zheng[114a], K. Zheng[168], X. Zheng[62], Z. Zheng[149], D. Zhong[168], B. Zhou[108], H. Zhou[7], N. Zhou[144a], Y. Zhou[15], Y. Zhou[114a], Y. Zhou[7], C. G. Zhu[143a], J. Zhu[108], X. Zhu[144b], Y. Zhu[144a], Y. Zhu[62], X. Zhuang[14], K. Zhukov[68], N. I. Zimine[39], J. Zinsser[63b], M. Ziolkowski[147], L. Živković[16], A. Zoccoli[24a,24b], K. Zoch[61], T. G. Zorbas[145], O. Zormpa[46], W. Zou[42], L. Zwalinski[37]

1 Department of Physics, University of Adelaide, Adelaide, Australia
2 Department of Physics, University of Alberta, Edmonton, AB, Canada
3 (a)Department of Physics, Ankara University, Ankara, Türkiye; (b)Division of Physics, TOBB University of Economics and Technology, Ankara, Türkiye
4 LAPP, Université Savoie Mont Blanc, CNRS/IN2P3, Annecy, France
5 APC, Université Paris Cité, CNRS/IN2P3, Paris, France
6 High Energy Physics Division, Argonne National Laboratory, Argonne, IL, USA
7 Department of Physics, University of Arizona, Tucson, AZ, USA
8 Department of Physics, University of Texas at Arlington, Arlington, TX, USA
9 Physics Department, National and Kapodistrian University of Athens, Athens, Greece
10 Physics Department, National Technical University of Athens, Zografou, Greece
11 Department of Physics, University of Texas at Austin, Austin, TX, USA
12 Institute of Physics, Azerbaijan Academy of Sciences, Baku, Azerbaijan
13 Institut de Física d'Altes Energies (IFAE), Barcelona Institute of Science and Technology, Barcelona, Spain
14 Institute of High Energy Physics, Chinese Academy of Sciences, Beijing, China
15 Physics Department, Tsinghua University, Beijing, China
16 Institute of Physics, University of Belgrade, Belgrade, Serbia
17 Department for Physics and Technology, University of Bergen, Bergen, Norway
18 (a)Physics Division, Lawrence Berkeley National Laboratory, Berkeley, CA, USA; (b)University of California, Berkeley, CA, USA
19 Institut für Physik, Humboldt Universität zu Berlin, Berlin, Germany
20 Albert Einstein Center for Fundamental Physics and Laboratory for High Energy Physics, University of Bern, Bern, Switzerland
21 School of Physics and Astronomy, University of Birmingham, Birmingham, UK
22 (a)Department of Physics, Bogazici University, Istanbul, Türkiye; (b)Department of Physics Engineering, Gaziantep University, Gaziantep, Türkiye; (c)Department of Physics, Istanbul University, Istanbul, Türkiye
23 (a)Facultad de Ciencias y Centro de Investigaciónes, Universidad Antonio Nariño, Bogotá, Colombia; (b)Departamento de Física, Universidad Nacional de Colombia, Bogotá, Colombia
24 (a)Dipartimento di Fisica e Astronomia A. Righi, Università di Bologna, Bologna, Italy; (b)INFN Sezione di Bologna, Bologna, Italy
25 Physikalisches Institut, Universität Bonn, Bonn, Germany
26 Department of Physics, Boston University, Boston, MA, USA
27 Department of Physics, Brandeis University, Waltham, MA, USA
28 (a)Transilvania University of Brasov, Brasov, Romania; (b)Horia Hulubei National Institute of Physics and Nuclear Engineering, Bucharest, Romania; (c)Department of Physics, Alexandru Ioan Cuza University of Iasi, Iasi, Romania; (d)National Institute for Research and Development of Isotopic and Molecular Technologies, Physics Department, Cluj-Napoca, Romania; (e)National University of Science and Technology Politechnica, Bucharest,

Romania; [f] West University in Timisoara, Timisoara, Romania; [g] Faculty of Physics, University of Bucharest, Bucharest, Romania
[29] [a] Faculty of Mathematics, Physics and Informatics, Comenius University, Bratislava, Slovak Republic; [b] Department of Subnuclear Physics, Institute of Experimental Physics of the Slovak Academy of Sciences, Kosice, Slovak Republic
[30] Physics Department, Brookhaven National Laboratory, Upton, NY, USA
[31] Universidad de Buenos Aires, Facultad de Ciencias Exactas y Naturales, Departamento de Física, y CONICET, Instituto de Física de Buenos Aires (IFIBA), Buenos Aires, Argentina
[32] California State University, CA, United States of America
[33] Cavendish Laboratory, University of Cambridge, Cambridge, UK
[34] [a] Department of Physics, University of Cape Town, Cape Town, South Africa; [b] iThemba Labs, Western Cape, South Africa; [c] Department of Mechanical Engineering Science, University of Johannesburg, Johannesburg, South Africa; [d] National Institute of Physics, University of the Philippines Diliman (Philippines), Quezon City, Philippines; [e] University of South Africa, Department of Physics, Pretoria, South Africa; [f] University of Zululand, KwaDlangezwa, Ongoye, South Africa; [g] School of Physics, University of the Witwatersrand, Johannesburg, South Africa
[35] Department of Physics, Carleton University, Ottawa, ON, Canada
[36] [a] Faculté des Sciences Ain Chock, Université Hassan II de Casablanca, Casablanca, Morocco; [b] Faculté des Sciences, Université Ibn-Tofail, Kénitra, Morocco; [c] Faculté des Sciences Semlalia, LPHEA-Marrakech, Université Cadi Ayyad, Marrakech, Morocco; [d] LPMR, Faculté des Sciences, Université Mohamed Premier, Oujda, Morocco; [e] Faculté des sciences, Université Mohammed V, Rabat, Morocco; [f] Institute of Applied Physics, Mohammed VI Polytechnic University, Ben Guerir, Morocco
[37] CERN, Geneva, Switzerland
[38] Affiliated with an Institute Formerly Covered by a Cooperation Agreement with CERN, Geneva, Switzerland
[39] Affiliated with an International Laboratory Covered by a Cooperation Agreement with CERN, Geneva, Switzerland
[40] Enrico Fermi Institute, University of Chicago, Chicago, IL, USA
[41] LPC, CNRS/IN2P3, Université Clermont Auvergne, Clermont-Ferrand, France
[42] Nevis Laboratory, Columbia University, Irvington, NY, USA
[43] Niels Bohr Institute, University of Copenhagen, Copenhagen, Denmark
[44] [a] Dipartimento di Fisica, Università della Calabria, Rende, Italy; [b] Laboratori Nazionali di Frascati, INFN Gruppo Collegato di Cosenza, Cosenza, Italy
[45] Physics Department, Southern Methodist University, Dallas, TX, USA
[46] National Centre for Scientific Research "Demokritos", Agia Paraskevi, Greece
[47] [a] Department of Physics, Stockholm University, Stockholm, Sweden; [b] Oskar Klein Centre, Stockholm, Sweden
[48] Deutsches Elektronen-Synchrotron DESY, Hamburg and Zeuthen, Germany
[49] Fakultät Physik , Technische Universität Dortmund, Dortmund, Germany
[50] Institut für Kern- und Teilchenphysik, Technische Universität Dresden, Dresden, Germany
[51] Department of Physics, Duke University, Durham, NC, USA
[52] SUPA-School of Physics and Astronomy, University of Edinburgh, Edinburgh, UK
[53] INFN e Laboratori Nazionali di Frascati, Frascati, Italy
[54] Physikalisches Institut, Albert-Ludwigs-Universität Freiburg, Freiburg, Germany
[55] II. Physikalisches Institut, Georg-August-Universität Göttingen, Göttingen, Germany
[56] Département de Physique Nucléaire et Corpusculaire, Université de Genève, Geneva, Switzerland
[57] [a] Dipartimento di Fisica, Università di Genova, Genoa, Italy; [b] INFN Sezione di Genova, Genoa, Italy
[58] II. Physikalisches Institut, Justus-Liebig-Universität Giessen, Giessen, Germany
[59] SUPA-School of Physics and Astronomy, University of Glasgow, Glasgow, UK
[60] LPSC, CNRS/IN2P3, Grenoble INP, Université Grenoble Alpes, Grenoble, France
[61] Laboratory for Particle Physics and Cosmology, Harvard University, Cambridge, MA, USA
[62] Department of Modern Physics and State Key Laboratory of Particle Detection and Electronics, University of Science and Technology of China, Hefei, China
[63] [a] Kirchhoff-Institut für Physik, Ruprecht-Karls-Universität Heidelberg, Heidelberg, Germany; [b] Physikalisches Institut, Ruprecht-Karls-Universität Heidelberg, Heidelberg, Germany

[64] [(a)]Department of Physics, Chinese University of Hong Kong, Shatin, N.T., Hong Kong; [(b)]Department of Physics, University of Hong Kong, Hong Kong, China; [(c)]Department of Physics and Institute for Advanced Study, Hong Kong University of Science and Technology, Clear Water Bay, Kowloon, Hong Kong, China
[65] Department of Physics, National Tsing Hua University, Hsinchu, Taiwan
[66] IJCLab, CNRS/IN2P3, Université Paris-Saclay, 91405 Orsay, France
[67] Centro Nacional de Microelectrónica (IMB-CNM-CSIC), Barcelona, Spain
[68] Department of Physics, Indiana University, Bloomington, IN, USA
[69] [(a)]INFN Gruppo Collegato di Udine, Sezione di Trieste, Udine, Italy; [(b)]ICTP, Trieste, Italy; [(c)]Dipartimento Politecnico di Ingegneria e Architettura, Università di Udine, Udine, Italy
[70] [(a)]INFN Sezione di Lecce, Lecce, Italy; [(b)]Dipartimento di Matematica e Fisica, Università del Salento, Lecce, Italy
[71] [(a)]INFN Sezione di Milano, Milan, Italy; [(b)]Dipartimento di Fisica, Università di Milano, Milan, Italy
[72] [(a)]INFN Sezione di Napoli, Naples, Italy; [(b)]Dipartimento di Fisica, Università di Napoli, Naples, Italy
[73] [(a)]INFN Sezione di Pavia, Pavia, Italy; [(b)]Dipartimento di Fisica, Università di Pavia, Pavia, Italy
[74] [(a)]INFN Sezione di Pisa, Pisa, Italy; [(b)]Dipartimento di Fisica E. Fermi, Università di Pisa, Pisa, Italy
[75] [(a)]INFN Sezione di Roma, Rome, Italy; [(b)]Dipartimento di Fisica, Sapienza Università di Roma, Rome, Italy
[76] [(a)]INFN Sezione di Roma Tor Vergata, Rome, Italy; [(b)]Dipartimento di Fisica, Università di Roma Tor Vergata, Rome, Italy
[77] [(a)]INFN Sezione di Roma Tre, Rome, Italy; [(b)]Dipartimento di Matematica e Fisica, Università Roma Tre, Rome, Italy
[78] [(a)]INFN-TIFPA, Povo, Italy; [(b)]Università degli Studi di Trento, Trento, Italy
[79] Universität Innsbruck, Department of Astro and Particle Physics, Innsbruck, Austria
[80] University of Iowa, Iowa City, IA, USA
[81] Department of Physics and Astronomy, Iowa State University, Ames, IA, USA
[82] Istinye University, Sariyer, Istanbul, Türkiye
[83] [(a)]Departamento de Engenharia Elétrica, Universidade Federal de Juiz de Fora (UFJF), Juiz de Fora, Brazil; [(b)]Universidade Federal do Rio De Janeiro COPPE/EE/IF, Rio de Janeiro, Brazil; [(c)]Instituto de Física, Universidade de São Paulo, São Paulo, Brazil; [(d)]Rio de Janeiro State University, Rio de Janeiro, Brazil; [(e)]Federal University of Bahia, Bahia, Brazil
[84] KEK, High Energy Accelerator Research Organization, Tsukuba, Japan
[85] Graduate School of Science, Kobe University, Kobe, Japan
[86] [(a)]AGH University of Krakow, Faculty of Physics and Applied Computer Science, Kraków, Poland; [(b)]Marian Smoluchowski Institute of Physics, Jagiellonian University, Kraków, Poland
[87] Institute of Nuclear Physics Polish Academy of Sciences, Kraków, Poland
[88] [(a)]Khalifa University of Science and Technology, Abu Dhabi, United Arab Emirates; [(b)]University of Sharjah, Sharjah, United Arab Emirates
[89] Faculty of Science, Kyoto University, Kyoto, Japan
[90] Research Center for Advanced Particle Physics and Department of Physics, Kyushu University, Fukuoka , Japan
[91] L2IT, CNRS/IN2P3, UPS, Université de Toulouse, Toulouse, France
[92] Instituto de Física La Plata, Universidad Nacional de La Plata and CONICET, La Plata, Argentina
[93] Physics Department, Lancaster University, Lancaster, UK
[94] Oliver Lodge Laboratory, University of Liverpool, Liverpool, UK
[95] Department of Experimental Particle Physics, Jožef Stefan Institute and Department of Physics, University of Ljubljana, Ljubljana, Slovenia
[96] Department of Physics and Astronomy, Queen Mary University of London, London, UK
[97] Department of Physics, Royal Holloway University of London, Egham, UK
[98] Department of Physics and Astronomy, University College London, London, UK
[99] Louisiana Tech University, Ruston, LA, USA
[100] Fysiska institutionen, Lunds universitet, Lund, Sweden
[101] Departamento de Física Teorica C-15 and CIAFF, Universidad Autónoma de Madrid, Madrid, Spain
[102] Institut für Physik, Universität Mainz, Mainz, Germany
[103] School of Physics and Astronomy, University of Manchester, Manchester, UK
[104] CPPM, Aix-Marseille Université, CNRS/IN2P3, Marseille, France
[105] Department of Physics, University of Massachusetts, Amherst, MA, USA
[106] Department of Physics, McGill University, Montreal, QC, Canada

[107] School of Physics, University of Melbourne, Victoria, Australia
[108] Department of Physics, University of Michigan, Ann Arbor, MI, USA
[109] Department of Physics and Astronomy, Michigan State University, East Lansing, MI, USA
[110] Group of Particle Physics, University of Montreal, Montreal, QC, Canada
[111] Fakultät für Physik, Ludwig-Maximilians-Universität München, Munich, Germany
[112] Max-Planck-Institut für Physik (Werner-Heisenberg-Institut), Munich, Germany
[113] Graduate School of Science and Kobayashi-Maskawa Institute, Nagoya University, Nagoya, Japan
[114] [(a)]Department of Physics, Nanjing University, Nanjing, China; [(b)]School of Science, Shenzhen Campus of Sun Yat-sen University, Shenzhen, China; [(c)]University of Chinese Academy of Science (UCAS), Beijing, China
[115] Department of Physics and Astronomy, University of New Mexico, Albuquerque, NM, USA
[116] Institute for Mathematics, Astrophysics and Particle Physics, Radboud University/Nikhef, Nijmegen, Netherlands
[117] Nikhef National Institute for Subatomic Physics and University of Amsterdam, Amsterdam, Netherlands
[118] Department of Physics, Northern Illinois University, DeKalb, IL, USA
[119] [(a)]New York University Abu Dhabi, Abu Dhabi, United Arab Emirates; [(b)]United Arab Emirates University, Al Ain, United Arab Emirates
[120] Department of Physics, New York University, New York, NY, USA
[121] Ochanomizu University, Otsuka, Bunkyo-ku, Tokyo, Japan
[122] Ohio State University, Columbus, OH, USA
[123] Homer L. Dodge Department of Physics and Astronomy, University of Oklahoma, Norman, OK, USA
[124] Department of Physics, Oklahoma State University, Stillwater, OK, USA
[125] Joint Laboratory of Optics, Palacký University, Olomouc, Czech Republic
[126] Institute for Fundamental Science, University of Oregon, Eugene, OR, USA
[127] Graduate School of Science, Osaka University, Osaka, Japan
[128] Department of Physics, University of Oslo, Oslo, Norway
[129] Department of Physics, Oxford University, Oxford, UK
[130] LPNHE, CNRS/IN2P3, Sorbonne Université, Université Paris Cité, Paris, France
[131] Department of Physics, University of Pennsylvania, Philadelphia, PA, USA
[132] Department of Physics and Astronomy, University of Pittsburgh, Pittsburgh, PA, USA
[133] [(a)]Laboratório de Instrumentação e Física Experimental de Partículas-LIP, Lisbon, Portugal; [(b)]Departamento de Física, Faculdade de Ciências, Universidade de Lisboa, Lisbon, Portugal; [(c)]Departamento de Física, Universidade de Coimbra, Coimbra, Portugal; [(d)]Centro de Física Nuclear da Universidade de Lisboa, Lisbon, Portugal; [(e)]Departamento de Física, Escola de Ciências, Universidade do Minho, Braga, Portugal; [(f)]Departamento de Física Teórica y del Cosmos, Universidad de Granada, Granada, Spain; [(g)]Departamento de Física, Instituto Superior Técnico, Universidade de Lisboa, Lisbon, Portugal
[134] Institute of Physics of the Czech Academy of Sciences, Prague, Czech Republic
[135] Czech Technical University in Prague, Prague, Czech Republic
[136] Charles University, Faculty of Mathematics and Physics, Prague, Czech Republic
[137] Particle Physics Department, Rutherford Appleton Laboratory, Didcot, UK
[138] IRFU, CEA, Université Paris-Saclay, Gif-sur-Yvette, France
[139] Santa Cruz Institute for Particle Physics, University of California Santa Cruz, Santa Cruz, CA, USA
[140] [(a)]Departamento de Física, Pontificia Universidad Católica de Chile, Santiago, Chile; [(b)]Millennium Institute for Subatomic Physics at High Energy Frontier (SAPHIR), Santiago, Chile; [(c)]Instituto de Investigación Multidisciplinario en Ciencia y Tecnología y Departamento de Física, Universidad de La Serena, La Serena, Chile; [(d)]Universidad Andres Bello, Department of Physics, Santiago, Chile; [(e)]Instituto de Alta Investigación, Universidad de Tarapacá, Arica, Chile; [(f)]Departamento de Física, Universidad Técnica Federico Santa María, Valparaíso, Chile
[141] Department of Physics, Institute of Science, Tokyo, Japan
[142] Department of Physics, University of Washington, Seattle, WA, USA
[143] [(a)]Institute of Frontier and Interdisciplinary Science and Key Laboratory of Particle Physics and Particle Irradiation (MOE), Shandong University, Qingdao, China; [(b)]School of Physics, Zhengzhou University, China
[144] [(a)]State Key Laboratory of Dark Matter Physics, School of Physics and Astronomy, Shanghai Jiao Tong University, Key Laboratory for Particle Astrophysics and Cosmology (MOE), SKLPPC, Shanghai, China; [(b)]State Key Laboratory of Dark Matter Physics, Tsung-Dao Lee Institute, Shanghai Jiao Tong University, Shanghai, China
[145] Department of Physics and Astronomy, University of Sheffield, Sheffield, UK

[146] Department of Physics, Shinshu University, Nagano, Japan
[147] Department Physik, Universität Siegen, Siegen, Germany
[148] Department of Physics, Simon Fraser University, Burnaby, BC, Canada
[149] SLAC National Accelerator Laboratory, Stanford, CA, USA
[150] Department of Physics, Royal Institute of Technology, Stockholm, Sweden
[151] Departments of Physics and Astronomy, Stony Brook University, Stony Brook, NY, USA
[152] Department of Physics and Astronomy, University of Sussex, Brighton, UK
[153] School of Physics, University of Sydney, Sydney, Australia
[154] Institute of Physics, Academia Sinica, Taipei, Taiwan
[155] [(a)]E. Andronikashvili Institute of Physics, Iv. Javakhishvili Tbilisi State University, Tbilisi, Georgia; [(b)]High Energy Physics Institute, Tbilisi State University, Tbilisi, Georgia; [(c)]University of Georgia, Tbilisi, Georgia
[156] Department of Physics, Technion, Israel Institute of Technology, Haifa, Israel
[157] Raymond and Beverly Sackler School of Physics and Astronomy, Tel Aviv University, Tel Aviv, Israel
[158] Department of Physics, Aristotle University of Thessaloniki, Thessaloniki, Greece
[159] International Center for Elementary Particle Physics and Department of Physics, University of Tokyo, Tokyo, Japan
[160] Graduate School of Science and Technology, Tokyo Metropolitan University, Tokyo, Japan
[161] Department of Physics, University of Toronto, Toronto, ON, Canada
[162] [(a)]TRIUMF, Vancouver, BC, Canada; [(b)]Department of Physics and Astronomy, York University, Toronto, ON, Canada
[163] Division of Physics and Tomonaga Center for the History of the Universe, Faculty of Pure and Applied Sciences, University of Tsukuba, Tsukuba, Japan
[164] Department of Physics and Astronomy, Tufts University, Medford, MA, USA
[165] Department of Physics and Astronomy, University of California Irvine, Irvine, CA, USA
[166] University of West Attica, Athens, Greece
[167] Department of Physics and Astronomy, University of Uppsala, Uppsala, Sweden
[168] Department of Physics, University of Illinois, Urbana, IL, USA
[169] Instituto de Física Corpuscular (IFIC), Centro Mixto Universidad de Valencia-CSIC, Valencia, Spain
[170] Department of Physics, University of British Columbia, Vancouver, BC, Canada
[171] Department of Physics and Astronomy, University of Victoria, Victoria, BC, Canada
[172] Fakultät für Physik und Astronomie, Julius-Maximilians-Universität Würzburg, Würzburg, Germany
[173] Department of Physics, University of Warwick, Coventry, UK
[174] Waseda University, Tokyo, Japan
[175] Department of Particle Physics and Astrophysics, Weizmann Institute of Science, Rehovot, Israel
[176] Department of Physics, University of Wisconsin, Madison, WI, USA
[177] Fakultät für Mathematik und Naturwissenschaften, Fachgruppe Physik, Bergische Universität Wuppertal, Wuppertal, Germany
[178] Department of Physics, Yale University, New Haven, CT, USA
[179] Yerevan Physics Institute, Yerevan, Armenia

[a] Also at Affiliated with an Institute Formerly Covered by a Cooperation Agreement with CERN, Geneva, Switzerland
[b] Also at An-Najah National University, Nablus, Palestine
[c] Also at Borough of Manhattan Community College, City University of New York, New York, NY, USA
[d] Also at Center for High Energy Physics, Peking University, China
[e] Also at Center for Interdisciplinary Research and Innovation (CIRI-AUTH), Thessaloniki, Greece
[f] Also at Centre of Physics of the Universities of Minho and Porto (CF-UM-UP), Porto, Portugal
[g] Also at CERN, Geneva, Switzerland
[h] Also at CMD-AC UNEC Research Center, Azerbaijan State University of Economics (UNEC), Baku, Azerbaijan
[i] Also at Département de Physique Nucléaire et Corpusculaire, Université de Genève, Geneva, Switzerland
[j] Also at Departament de Fisica de la Universitat Autonoma de Barcelona, Barcelona, Spain
[k] Also at Department of Financial and Management Engineering, University of the Aegean, Chios, Greece
[l] Also at Department of Mathematical Sciences, University of South Africa, Johannesburg, South Africa
[m] Also at Department of Modern Physics and State Key Laboratory of Particle Detection and Electronics, University of Science and Technology of China, Hefei, China
[n] Also at Department of Physics, Bolu Abant Izzet Baysal University, Bolu, Türkiye

[o] Also at Department of Physics, California State University, Sacramento, USA
[p] Also at Department of Physics, King's College London, London, UK
[q] Also at Department of Physics, Stanford University, Stanford, CA, USA
[r] Also at Department of Physics, Stellenbosch University, South Africa
[s] Also at Department of Physics, University of Fribourg, Fribourg, Switzerland
[t] Also at Department of Physics, University of Thessaly, Volos, Greece
[u] Also at Department of Physics, Westmont College, Santa Barbara, USA
[v] Also at Faculty of Physics, Sofia University, 'St. Kliment Ohridski', Sofia, Bulgaria
[w] Also at Hellenic Open University, Patras, Greece
[x] Also at Henan University, Kaifeng, China
[y] Also at Imam Mohammad Ibn Saud Islamic University, Riyadh, Saudi Arabia
[z] Also at Institucio Catalana de Recerca i Estudis Avancats, ICREA, Barcelona, Spain
[aa] Also at Institut für Experimentalphysik, Universität Hamburg, Hamburg, Germany
[ab] Also at Institute for Nuclear Research and Nuclear Energy (INRNE) of the Bulgarian Academy of Sciences, Sofia, Bulgaria
[ac] Also at Institute of Applied Physics, Mohammed VI Polytechnic University, Ben Guerir, Morocco
[ad] Also at Institute of Particle Physics (IPP), Toronto, Canada
[ae] Also at Institute of Physics and Technology, Mongolian Academy of Sciences, Ulaanbaatar, Mongolia
[af] Also at Institute of Physics, Azerbaijan Academy of Sciences, Baku, Azerbaijan
[ag] Also at Institute of Theoretical Physics, Ilia State University, Tbilisi, Georgia
[ah] Also at National Institute of Physics, University of the Philippines Diliman (Philippines), Quezon City, Philippines
[ai] Also at Technical University of Munich, Munich, Germany
[aj] Also at The Collaborative Innovation Center of Quantum Matter (CICQM), Beijing, China
[ak] Also at TRIUMF, Vancouver, BC, Canada
[al] Also at Università di Napoli Parthenope, Naples, Italy
[am] Also at Department of Physics, University of Colorado, Boulder, CO, USA
[an] Also at University of Sienna, Sienna, Italy
[ao] Also at University of the Western Cape, Cape Town, South Africa
[ap] Also at Washington College, Chestertown, MD, USA
[aq] Also at Yeditepe University, Physics Department, Istanbul, Türkiye
*Deceased